

**THERMOMECHANICAL BEHAVIOR AND CHEMICAL SENSING
CATIONIC POLY(DIALLYLDIMETHYLAMMONIUM CHLORIDE) AND
ANIONIC POLY(SODIUM 4-STYRENE SULFONATE) ASSEMBLED INTO
COMPOSITE POLYELECTROLYTE MULTILAYER THIN FILMS
AND COMPLEX MEMBRANES**

Rateeya Saikaew

A Dissertation Submitted in Partial Fulfilment of the Requirements
for the Degree of Doctor of Philosophy
The Petroleum and Petrochemical College, Chulalongkorn University
in Academic Partnership with
The University of Michigan, The University of Oklahoma,
and Case Western Reserve University
2018

บทคัดย่อและแฟ้มข้อมูลฉบับเต็มของวิทยานิพนธ์ตั้งแต่ปีการศึกษา 2554 ที่ให้บริการในคลังปัญญาจุฬาฯ (CUIR)
เป็นแฟ้มข้อมูลของนิสิตเจ้าของวิทยานิพนธ์ที่ส่งผ่านทางบัณฑิตวิทยาลัย

The abstract and full text of theses from the academic year 2011 in Chulalongkorn University Intellectual Repository (CUIR)
are the thesis authors' files submitted through the Graduate School.

Thesis Title: Thermomechanical Behavior and Chemical Sensing of Cationic Poly(Diallyldimethyl Ammonium Chloride) and Anionic Poly(Sodium 4-Styrene Sulfonate) Assembled into Composite Polyelectrolyte Multilayer Thin Films and Complex Membranes

By: Rateeya Saikaew

Program: Polymer Science

Thesis Advisor: Asst. Prof. Stephan Thierry Dubas

Accepted by The Petroleum and Petrochemical College, Chulalongkorn University, in partial fulfilment of the requirements for the Degree of Doctor of Philosophy.

..... College Dean
(Prof. Suwabun Chirachanchai)

Thesis Committee:

.....
(Asst. Prof. Stephan Thierry Dubas)

.....
(Prof. Christoph Weder)

.....
(Prof. Suwabun Chirachanchai)

.....
(Prof. Sujitra Wongkasemjit)

.....
(Assoc. Prof. Thanyalak Chaisuwan)

ABSTRACT

5792002063: Polymer Science Program

Rateeya Saikaew: Thermomechanical Behavior and Chemical Sensing of Cationic Poly(Diallyldimethyl Ammonium Chloride) and Anionic Poly(Sodium 4-Styrene Sulfonate) Assembled into Composite Polyelectrolyte Multilayer Thin Films and Complex Membranes.

Thesis Advisor: Asst. Prof. Stephan Thierry Dubas 149 pp.

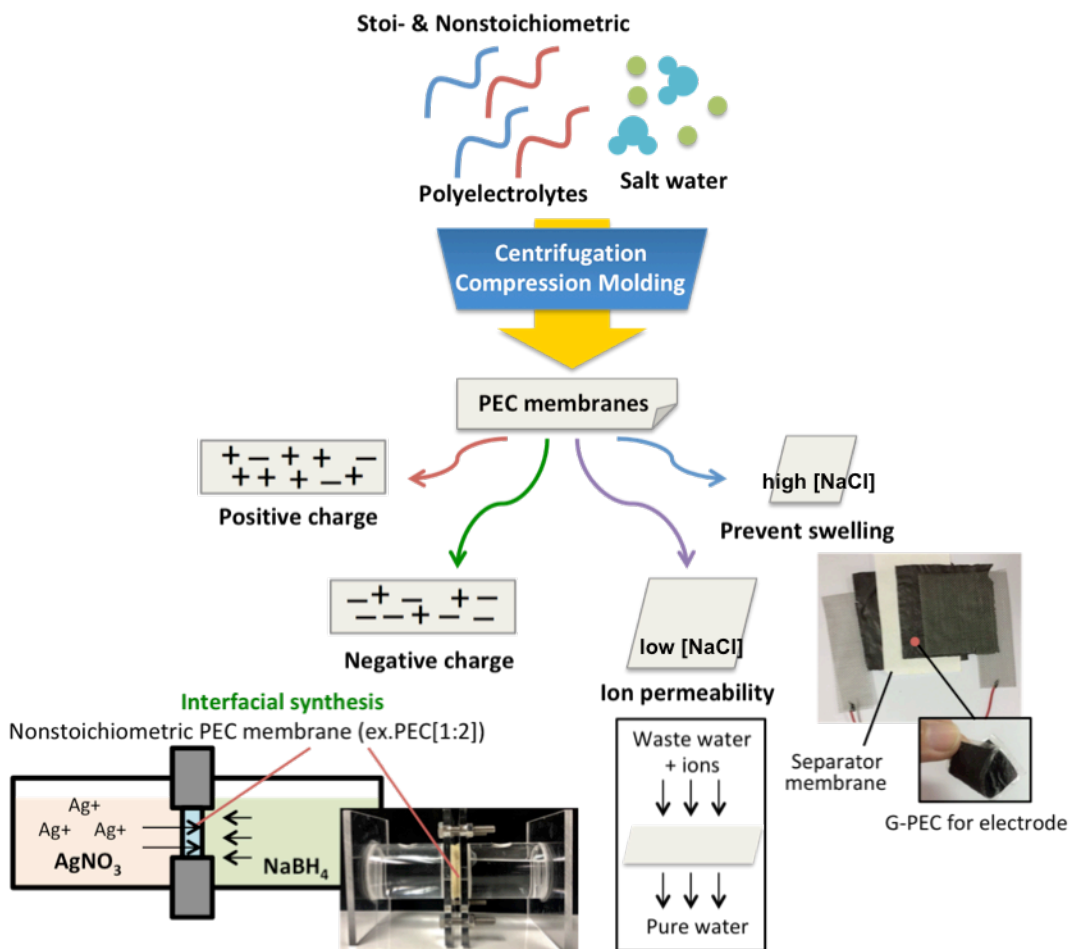
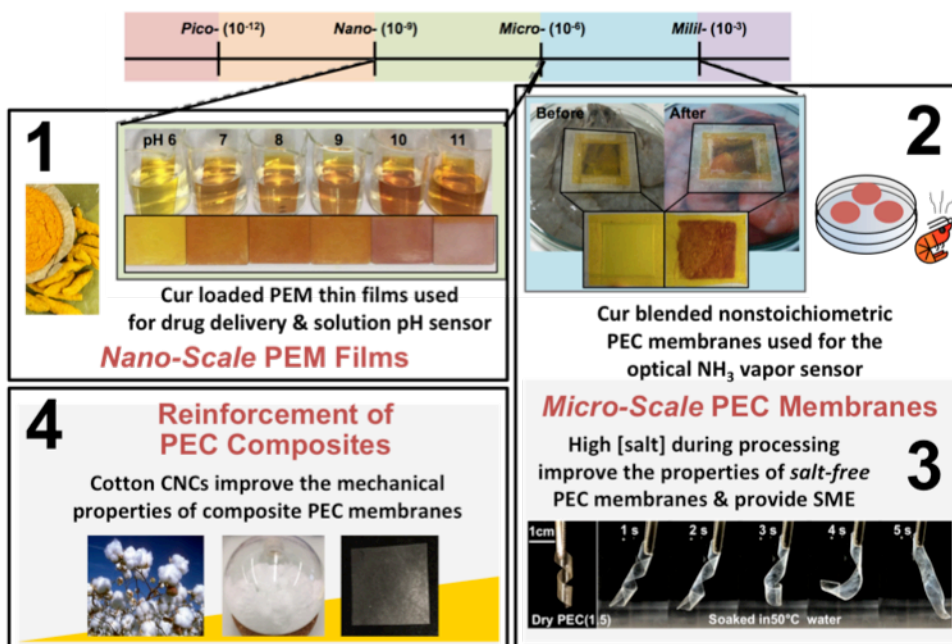
Keywords: Polyelectrolyte Multilayers/ Layer-by-Layer/ Polyelectrolyte Complexes/ Solution-Mixing/ Curcumin/ Cellulose Nanocrystals/ Thermomechanical/ Sensing

Polyelectrolyte composite membranes of cationic PDADMAC and anionic PSS assembled into polyelectrolyte multilayer (PEM) thin film and polyelectrolyte complex (PEC) membranes were used as matrix embedded with several additive molecules. Nano-scale PEM films fabricated using the layer-by-layer deposition method and the loading and release of a hydrophobic model drug curcumin (Cur) was studied for drug delivery and sensing applications. Interestingly, it was found that the loading and release of Cur could be triggered by solvent composition and temperature. In a parallel study, the alternative to the nanoscale PEM was studied in the form of PEC, which were used as stand-alone film with a thickness in micro-scale. PECs prepared by solution-mixing using NaCl as a plasticizer followed by centrifugation and compression molding were investigated. Remarkably, not only the tuning of [NaCl] used during mixing could affect the thermomechanical behavior of salt-free films but also the changes in polyelectrolytes stoichiometry. Cur blended into non-stoichiometric PEC membranes were tested as optical NH₃ vapor sensor and it was found that the excess positive stoichiometry gave the best results. To further improve the mechanical properties of both the free-standing PEM and PEC films, cellulose nanocrystals (CNCs) were used as fillers to reinforce the polymer matrix.

บทคัดย่อ

รศ.ดร.ทราญแก้ว : คุณสมบัติเชิงกลทางความร้อน และการตรวจวัดทางเคมีของพอลิไดอัลลิลไดเมทิลแอมโมเนียมคลอไรด์ประจุบวก และพอลิโซเดียมโฟร์สไตรีนซัลโฟเนตประจุลบ ในรูปแบบคอมโพสิตฟิล์มบางพอลิอิเล็กโทรไลต์มัลติเลเยอร์ และเมมเบรนพอลิอิเล็กโทรไลต์คอมเพล็กซ์ (Thermomechanical Behavior and Chemical Sensing of Cationic Poly(Diallyldimethyl Ammonium Chloride) and Anionic Poly(Sodium 4-Styrene Sulfonate) Assembled into Composite Polyelectrolyte Multilayer Thin Films and Complex Membranes) อ. ที่ปรึกษา : รศ.ดร.สตีฟาน เทียร์ ดูบาส์ 149 หน้า

ฟิล์มคอมโพสิตของพอลิอิเล็กโทรไลต์ประจุบวก พีดีเอดีเอ็มเอซี (poly(diallyldimethyl ammonium chloride), PDADMAC) และประจุลบ พีเอสเอส (poly(sodium 4-styrene sulfonate), PSS) ต่อกันด้วยแรงอิเล็กโตรสแตติก สามารถใช้ในการสร้างฟิล์มบางระดับนาโนเมตร พีอีเอ็ม (พอลิอิเล็กโทรไลต์มัลติเลเยอร์) โดยเทคนิคการสร้างฟิล์มบางหลายชั้นบนพื้นผิวของวัสดุโดยตรง การศึกษาการบรรจุโมเลกุลเคอคูมิน (ขมิ้น) ลงในฟิล์มพีอีเอ็มพบว่า สามารถบรรจุและปลดปล่อยได้ด้วยการควบคุมอุณหภูมิและการปรับค่าของสารละลาย ฟิล์มชนิดนี้สร้างขึ้นเพื่อประยุกต์ใช้ในระบบการส่งยา และใช้เป็นตัวตรวจวัดความเป็นกรดเบสของสารละลายได้ โดยฟิล์มเคอคูมินจะเปลี่ยนจากสีเหลืองเป็นสีแดงในสภาวะความเป็นเบส นอกจากนี้พีดีเอ็มเอซีและพีเอสเอส ยังสามารถสร้างเมมเบรนระดับไมโครเมตร พีอีซี (พอลิอิเล็กโทรไลต์คอมเพล็กซ์) โดยเทคนิคการผสมสารละลายภายใต้การเติมเกลือโซเดียมคลอไรด์เพื่อเป็นพลาสติกไซเซอร์ ตามด้วยการปั่นเหวี่ยงและขึ้นรูปโดยการบีบอัดเป็นแผ่นที่อุณหภูมิ 40 – 60 องศาเซลเซียส ผลการทดลองชี้ให้เห็นว่าการปรับปริมาณเกลือที่ใช้ระหว่างการเตรียมตัวอย่างนั้น ส่งผลต่อคุณสมบัติเชิงกลทางความร้อนของฟิล์ม เนื่องจากเกลือส่งผลต่อการจัดเรียงตัวของสายโซ่พอลิเมอร์ แม้ว่าจะทำการล้างเกลือออกในภายหลังก็ตาม อีกทั้งการปรับเปลี่ยนอัตราส่วนระหว่างพอลิเมอร์ประจุบวกและประจุลบ ยังสามารถเป็นวิธีเพื่อบังคับให้เมมเบรน แสดงความเป็นพวกหรือลบมากกว่าได้ เรียกว่าวัสดุชนิดนี้ว่านอนสตอยซิโอเมตริกพีอีซี ซึ่งจากการศึกษาด้วยการบรรจุเคอคูมินลงในฟิล์มที่มีสัดส่วนของพอลิเมอร์ประจุบวกมากกว่า พบว่าฟิล์มชนิดนี้สามารถตรวจวัดปริมาณแก๊สแอมโมเนียได้ดีขึ้น การศึกษาเกี่ยวกับวัสดุคอมโพสิตพอลิอิเล็กโทรไลต์เมมเบรนนี้ ยังรวมไปถึงการเติมเซลล์ลูโลสนาโนคริสทอลล์ เพื่อช่วยในการเสริมแรงของฟิล์มอีกด้วย จากผลการศึกษาจะเห็นได้ว่าฟิล์มนี้สามารถประยุกต์ใช้ได้อย่างกว้างขวาง ขึ้นอยู่กับการประกอบต่างๆ ที่บรรจุลงไปเนื้อฟิล์ม



ACKNOWLEDGEMENTS

The author would like to express the deepest appreciation to her supportive supervisor, Asst. Prof. Stephan Thierry Dubas, for his understanding, encouragement, inspiration, knowledge and many life skills. Without his valuable guidance this dissertation would not have been possible.

She would like to thank the Development and Promotion of Science and Technology Talents (DPST) Project under the Institute for the Promotion of Teaching Science and Technology (IPST), Ministry of Education, Thailand for providing the full scholarship, the potential development activities, and the supports since 2005. Unforgettable thanks go to the Petroleum and Petrochemical College, Grant for International Research Integration: Chula-Research Scholar, Ratchadaphiseksompot Endowment Fund and the Center of Excellence on Petrochemical and Materials Technology, Chulalongkorn University.

The author wishes to extend her gratitude to Prof. Christoph Weder for his well taken-care throughout her stay as an exchange student at Adolphe Merkle Institute (AMI), University of Fribourg, Fribourg, Switzerland for a year. She has learned many things not only academic but also the living with different cultures.

The author would like to express her appreciation to Prof. Suwabun Chirachanchai, Prof. Sujitra Wongkasemjit and Assoc. Prof. Thanyalak Chaisuwan for their suggestions, comments and participation as thesis committees for her study.

Without the education from her former schools and teachers from Yupparaj Wittayalai School, Chiang Mai University, and the PPC, Chulalongkorn University, she cannot have this day.

Last but not least, she gratefully appreciates her beloved parents and her family for their unconditionally love, sacrifices, encouragement and moral support throughout my life. The completed thesis cannot be done without the SD group members and all of her friends, who always support her both academic and social life.

TABLE OF CONTENTS

	PAGE
Title Page	i
Abstract (in English)	iii
Abstract (in Thai)	iv
Acknowledgements	vi
Table of Contents	vii
List of Tables	xi
List of Figures	xii
 CHAPTER	
I INTRODUCTION	1
 II LITERATURE REVIEW	 3
2.1 Polyelectrolytes (PEs)	3
2.2 Polyelectrolyte Multilayers (PEMs)	5
2.2.1 Parameters Controlling the Growth of PEM Thin Films	6
2.2.2 Free-Standing PEM Thin Films	7
2.2.3 Potential Applications of Composite PEM Thin Films	8
2.3 Polyelectrolyte Complexes (PECs)	9
2.3.1 Parameters Controlling the Properties of PECs	10
2.3.2 Potential Applications of Composite PECs	14
2.4 Curcumin (Cur)	15
2.4.1 Loading of Cur Based Polyelectrolyte Systems for Drug Delivery	15
2.4.2 pH Solution and Ammonia Vapor Sensing of Cur Based Polyelectrolyte Systems	16
2.5 Mechanical Properties of PEMs and PECs	17
2.6 Cellulose Nanocrystals (CNCs)	20

CHAPTER	PAGE
III CURCUMIN LOADED POLYELECTROLYTE MULTILAYERS THIN FILMS	22
3.1 Proposed Research	22
3.2 Experimental	24
3.3 Results and Discussion	25
3.3.1 Fabrication and Characterization of PEM Thin Films	25
3.3.2 Temperature Controlled Loading and Release of Cur in PEMs Thin Films	28
3.3.3 Improved pH Sensing of Cur Loaded PEMs Thin Films	42
3.4 Conclusion	50
3.5 Acknowledgements	51
3.6 References	51
IV CURCUMIN BLENDED NONSTOICHIOMETRIC POLYELECTROLYTE COMPLEX MEMBRANES FOR THE OPTICAL AMMONIA VAPOR SENSOR	54
4.1 Proposed Research	55
4.2 Experimental	55
4.3 Results and Discussion	58
4.3.1 Hydrophilic Dyes Absorption on the Salt-Free Stoi- and Nonstoichiometric PEC Membranes	58
4.3.2 Fabrication of Salt-Free Cur-PEC Films	62
4.3.3 pH Sensing of Salt-Free Cur-PEC Films	63
4.3.4 The Effect of [NaCl] used during Complexation on the Moisture Content and the NH ₃ Vapor Sensing of Cur-PEC Films	67
4.3.5 Enhanced the NH ₃ Vapor Sensing of Cur-PEC Films Based on Nonstoichiometric Ratio	71
4.3.6 Cur-PEC Film for Optical Detection of Shrimp Spoilage	75
4.3.7 Cur-PEC Film Prepared with Different Types of Salt	77

CHAPTER	PAGE
4.4 Conclusion	78
4.5 Acknowledgements	79
4.6 References	79
V INFLUENCE OF THE SALT CONCENTRATION DURING PROCESSING ON THE PROPERTIES OF SALT-FREE POLYELECTROLYTE COMPLEX MEMBRANES	83
5.1 Proposed Research	83
5.2 Experimental	83
5.3 Results and Discussion	86
5.3.1 Fabrication of Salt-Free PEC Films	86
5.3.2 Effect of [NaCl] during Processing on the T_g of Hydrated PEC Films	91
5.3.3 Effect of Polymer Molar Ratio on the Thermo- Mechanical Properties of Salt-Free PEC Films	99
5.3.4 Shape Memory Effect of PEC Membranes	104
5.4 Conclusion	107
5.5 Acknowledgements	108
5.6 References	108
VI IMPROVING THE MECHANICAL PROPERTIES OF COMPOSITE POLYELECTROLYTE MULTILAYER THIN FILMS AND COMPLEX MEMBRANES BY REINFORCEMENT WITH CELLULOSE NANOCRYSTALS	110
6.1 Proposed Research	110
6.2 Experimental	112

CHAPTER	PAGE
6.3 Results and Discussion	114
6.3.1 Improving the Mechanical Properties of Composite PEC Membranes by Reinforcement with CNCs	114
6.3.2 Improving the Mechanical Properties of LbL Assembled Free-Standing PEM Thin Films by Reinforcement with CNCs	123
6.4 Conclusion	133
6.5 Acknowledgements	134
6.6 References	134
VII CONCLUSION AND RECOMMENDATIONS	137
REFERENCES	139
APPENDICES	147
CURRICULUM VITAE	149

LIST OF TABLES

TABLE		PAGE
3.1	DLS measurement of 1 mg/ml Cur in different solution	47
5.1	The storage modulus of PEC films in the dry, salt-containing (rate 5°C/min, tension clamp) and hydrated, salt-free (rate 0.5°C/min, submersion clamp) state	94
5.2	The storage modulus of hydrated salt-free PEC at different molar ratio	100
6.1	The storage modulus of CNC-PEC films at different the order of mixing	116
6.2	The storage modulus of CNC-PEC films at different CNC content	118
6.3	Peak assignments for PDADMAC/PSS multilayer on the CA-coated glass slide	127
6.4	Root mean square (rms) roughness and the thickness of PDADMAC/PSS multilayer film measure from AFM analysis and ellipsometry calculation	130

LIST OF FIGURES

FIGURE	PAGE	
2.1	Examples of polyelectrolytes.	3
2.2	Polyelectrolyte assembly techniques.	4
2.3	The layer-by-layer (LbL) assemble technique (Decher, 1997).	6
2.4	Effect of added KBr on the microstructures of PEC (Wang, 2014).	10
2.5	Water plasticizing effect of PEC (Hariri, 2012).	13
2.6	Rhizome of <i>Curcumin longa</i> Linn (left), curcumin extract powder (middle) and chemical structure of curcumin (right).	15
2.7	(a) DSC thermograms of dried samples of Aldrich; A PDADMAC, B PSS and C extrude PEC after soaked in 1.0 M NaCl and (b) The storage modulus (u), loss modulus (n) and loss tangent (Δ) of extruded PECs soaked in A 0.1 M, B 0.5 M and C 1.0 M NaCl (Shamoun <i>et al.</i> , 2012).	19
2.8	Cellulose structure and its nanomaterial types (Trache, 2017).	21
3.1	Schematic representation of Cur loaded into PEM thin films for the study of temperature controlled loading and release of Cur and the improved pH sensing of Cur loaded PEMs thin films.	23
3.2	Procedure of PDADMAC/PSS fabrication on pre-treated glass slide.	26
3.3	UV-Vis spectra (a) with absorbance at 230 nm on quartz slide and the thickness measured by ellipsometry on a silicon wafer (b) of PDADMAC/PSS film when increasing the number of layers.	27

FIGURE	PAGE
3.4 Plot of contact angle measurement of PDADMAC/PSS on glass slide with increasing the number of layers.	28
3.5 Fabrication of PEM thin films loaded with Cur at different temperature and solvent compositions.	29
3.6 (a) UV-Vis spectra and (b) plot of the absorbance at 440 nm of Cur loaded into a 13-layer PDADMAC/PSS films as a function of the water:solvent mixture at room temperature (25°C).	30
3.7 The absorbance at 440 nm of Cur PEM films as a function of loading temperature and water:solvent fraction for (a) methanol (b) ethanol and (c) isopropanol.	32
3.7 (Cont.) The absorbance at 440 nm of Cur PEM films as a function of loading temperature and water:solvent fraction for (a) methanol (b) ethanol and (c) isopropanol.	33
3.8 Kinetic property and absorbance spectra with images of Cur-loaded PEM thin films using 90:10 water:ethanol after 3 h.	34
3.9 (a) AFM images and (b) the thickness and the absorbance as a function of loading time of 13-layer PEM film on glass slide before A and after B loading.	35
3.10 Absorbance of Cur loading into PEM in 5% w/v Cur in 90:10 water:ethanol solvent.	36
3.11 Absorbance of Cur releasing from PEM to water at various temperatures.	37
3.12 (a) Absorbance spectra, (b) photographic images under UV light and (c) schematic representation of Cur released on 7%w/v agar with different loading and release temperature; A loaded at 5°C and released at 25°C, B loaded at 25°C and released at 25°C, C and D loaded at 5 and 25°C then released at 5°C.	38

FIGURE	PAGE
3.13 The quantitation of Cur released from PEM film on agar as a function of releasing time.	39
3.14 The absorbance of Cur loaded PEM when attached on agar as a function of time and a required number of PEM layer.	41
3.15 The absorbance of Cur loaded PEM when increased the deposition layer of PDADMAC/PSS.	42
3.16 Schematic representation of Cur loaded PEM thin film.	43
3.17 Fabrication of Cur loaded PEM thin films for pH solution testing.	43
3.18 (a) UV-Vis spectra and (b) absorbance of Cur loaded in PDADMAC/PSS thin film with different layers.	45
3.19 Cur (0.1 %w/v) mixed with various solutions.	46
3.20 Radius of Cur particles in different solution observed by DLS measurement.	46
3.21 Keto-enol tautomerization of Cur.	47
3.22 The UV spectra of Cur loaded on PEM with PDADMAC on top (a) and PSS on top (a) film dipped at different phosphate buffer pH. The absorbance at 540 nm of Cur loaded PEM film with different polymer on top of layers (c).	49
3.23 Cur loaded 13-layer PEM exposed in air (a) and ammonia vapor (b).	50
4.1 The concept of Cur loaded PEM film with different polymer charge on top and Cur blended PEC membrane with various polymer ratio.	54
4.2 The fabrication of compressed stoi- and nonstoichiometric PEC membrane of PDADMAC/PSS.	58
4.3 UV-Vis spectrum (a) and absorbance (b) of mixed dye solution of MO and MB after dye absorption for 150 min of salt-free PEC(1.5) with various mol% of PDADMAC/PSS.	59

FIGURE	PAGE
4.4 Kinetic properties of mixed dye absorption of salt-free PEC film various polymer molar ratio; (a) MO and (b) MB absorption (A is absorbance at 465 and 665 nm, respectively, and A_0 is absorbance of initial mixed dye).	61
4.5 Photographic images and dye absorption of salt-free PEC film various polymer molar ratio after 8 h.	62
4.6 Schematic illustrates the fabrication of compressed Cur-PDADMAC/PSS film for NH_3 vapor sensing.	63
4.7 (a) UV-Vis spectrum of stoichiometric 1:1 PDADMAC:PSS of salt-free Cur-PEC(1.5) films immersed to solution pH 11 and (b) absorbance at 535 nm and the color change of the films immersed to various pH solutions as a function of time.	64
4.8 Absorbance at 535 nm and the color change of the salt-free stoi- and nonstoichiometric Cur-PEC(1.5) films immersed to various pH solutions after 1 h.	65
4.9 The reversible color change of the salt-free stoi- and nonstoichiometric Cur-PEC(1.5) films immersed to pH 11 and pH 2.34 solutions.	66
4.10 Absorbance at 470 and 535 nm represent the yellow and orange-red color of Cur solution dissolve in different polymer and pH solution.	67
4.11 Absorbance at λ_{max} of Cur-PEC films exposed to vapor of various $[\text{NH}_3]$ as a function of $[\text{NaCl}]$ during processing.	68
4.12 The moisture content of PEC films as a function of % RH at various $[\text{NaCl}]$ during processing.	68
4.13 (a) UV-Vis spectrum of moisted Cur-PEC(1.5) film and (b) kinetic properties the films stored in various % RHs exposed to vapor of 15 ppm $[\text{NH}_3]$.	70

FIGURE	PAGE
4.14 Schematic representation of the color change of moisted Cur-PEC films when exposed to NH ₃ vapor.	71
4.15 Response time of moisted Cur-PEC(1.5) films fabricated from stoi- and nonstoichiometric PDADMAC/PSS exposed to vapor of 15 ppm [NH ₃].	72
4.16 The moisture content of the Cur-PEC films as a function of RHs.	73
4.17 The ATR-FTIR spectra of PEC and Cur-PEC films with different polymer ratio.	74
4.18 The reversible color change cycling of nonstoichiometric PEC films when exposed to NH ₃ vapor and air condition.	75
4.19 Sensing properties for shrimp spoilage of Cur-PEC film of excess PDADMAC composition. (a) The color change of film was observed from (b) UV-Vis spectroscopy and (c) colorimeter (the table shows the color parameters of film).	76
4.20 Response time of moisted Cur-PEC(1.5) films of PEC67/33 at different types of salt used during fabrication exposed to vapour of 15 ppm [NH ₃].	77
4.21 The moisture content of Cur-PEC(1.5) films of PEC67/33 with different types of salt at 97% RH.	78
5.1 Photographic images of tension (a) and submersion (b) clamps for dynamic mechanical analysis (DMA).	84
5.2 Photographic image of the manual stretching device (model) and schematic procedure for shape memory experiment.	85
5.3 PECs formation of PDADMAC and PSS prepared at various [NaCl].	87
5.4 (a) PEC(0.25) after annealing for 24 h in different [NaCl] solutions for 24 h and (b) PEC coacervate soaked in 3 M NaCl and became solid in water.	88

FIGURE	PAGE
5.5 Schematic representation of the fabrication process used to create PDADMAC/PSS based PEC films and PEC films with different [NaCl] during complexation.	89
5.6 The PEC films when compression molding at different temperature.	90
5.7 TGA thermogram of dry, PEC(0) and PEC(1.5) films before and after rinsed with water for 24 h and then dried at 60°C for 48 h (heating rate 10°C/min).	90
5.8 DSC thermogram (second heating scan with rate 10°C/min, exotherm up) of dry, salt-containing PDADMAC/PSS films.	91
5.9 Storage modulus at room temperature with heating rate 5°C/min using tension clamp of dry, salt-containing PDADMAC/PSS films.	92
5.10 DMA traces of hydrated PDADMAC/PSS PEC films measured in water. (a) Storage modulus E' and (b) normalized $\tan(\delta)$.	93
5.11 E' at 5°C extracted from the graphs shown in (a) and glass transition temperature (T_g) established from the maxima of the $\tan(\delta)$ peaks shown in (b) as a function of [NaCl] used during processing.	94
5.12 Equilibrium water uptake and moisture content of salt containing and salt-free PDADMAC/PSS films at 25°C as a function of [NaCl] used during processing.	95
5.13 (a) Stress-strain curves (strain rate of 20%/min) and (b) Young's modulus and toughness of hydrated PDADMAC/PSS films as a function of [NaCl] used during processing.	97

FIGURE		PAGE
5.14	Schematic representation of salt influence PE chain conformation with (a) no add salt and (b) 1.5 M NaCl during complexation.	98
5.15	Storage modulus E' (rate 0.5°C/min, submersion clamp) with photographic images of PEC(1.5) films with different molar ratio after soaked in DI water overnight.	100
5.16	Water uptake at room temperature of PDADMAC/PSS films with various molar ratio of polymer.	101
5.17	(a) Stress-strain curves (strain rate of 20%/min) and (b) Young's modulus and toughness of hydrated PEC(1.5) films with various the molar ratio of PDADMAC/PSS.	102
5.18	Ionic conductivities of hydrated PEC films prepared at different molar ratio of polymer after soaked in DI water.	139
5.19	(a) Strain as a function of step during shape memory programming and release of compressed PDADMAC/PSS films and (b) a series of photographs illustrating the shape recovery of twisted PEC(1.5) film in 50°C water.	109
5.20	Storage modulus of PEC(1.5) film soaked in water measured during three cycles in which the temperature was increase to 55°C, decreased to 5°C, and increased again to 55°C (heating rate 0.5°C/min) as a function of time (a) and temperature (b).	106
6.1	Schematic representation of CNC reinforced (a) PEC membrane and (b) free-standing PEM thin film.	111
6.2	The fabrication of CNC-PDADMAC/PSS films prepared using a compression molding.	115

FIGURE	PAGE	
6.3	<i>E'</i> of hydrated PDADMAC/PSS films reinforced with 10% CNC at different conditions and the order of mixing (Rate 0.5°C/min); (A) CNC-PDADMAC mixed with PSS, (B) CNC-PDADMAC mixed with PSS-NaCl, (C) CNC-PDADMAC-NaCl mixed with PSS-NaCl, (D) PDADMAC-NaCl mixed with CNC-PSS, and (E) PDADMAC-NaCl mixed with CNC-PSS-NaCl ([NaCl] in each solution is 1.5 M).	117
6.4	DMA measurement of hydrated PDADMAC/PSS films reinforced with different CNCs content. (a) Storage modulus <i>E'</i> and (b) normalized tan(δ) (rate 0.5°C/min).	119
6.5	<i>E'</i> at 5°C from the graphs shown in Figure 6.3(a) and <i>T_g</i> extracted from the maxima of the tan(δ) peaks shown in Figure 6.3(b) for the hydrated PDADMAC/PSS films as a function of CNCs content.	120
6.6	Water uptake for the hydrated PDADMAC/PSS films reinforcing with different CNCs content.	121
6.7	TGA thermogram of salt-free CNC-PEC films after soaked in water overnight (Dried at 60°C for 2 days) with heating rate 10°C/min.	122
6.8	Thermal transitions of hydrated films of PDADMAC/PSS and CNC-PDADMAC/PSS from DMA with submersion clamp (Rate 0.5°C/min).	123
6.9	Procedure for fabrication of PDADMAC/PSS (a) and PDADMAC/CNC (b) free-standing nanofilm.	124
6.10	ATR-IR spectra 10 mM PDADMAC/PSS with 1M NaCl on CA-modified glass slide.	126

FIGURE	PAGE
6.11 The absorbance for CA (1738 cm^{-1}), PSS (1125 cm^{-1}) and PDADMAC (1650 cm^{-1}) as a function of the number of PEM layers.	128
6.12 (a) The thickness of free-standing films with various number of bilayers measured from ellipsometry; AFM images of (b) 10-bilayer (c) 15-bilayer (d) 20-bilayer free-standing film on mica substrate.	129
6.13 Photographic images for a 20-bilayer of free-standing PDADMAC/PSS film on glass slide ($1.9\times 2.5\text{ cm}$) (a) and film released from substrate in acetone (b).	131
6.14 CA-coated on glass slide, LbL of 5-layer PDADMAC/PSS primer and PDADMAC/CNC film with increasing the number of layer from 5 to 30.	132
6.15 Free-standing film of 20-layer CNC/PDADMAC with 1 M NaCl after soaked in acetone. The film is easy to manipulate compare to 40-layer PDADMAC/PSS free-standing film.	133

CHAPTER I

INTRODUCTION

The utilization of polyelectrolytes, cationic poly(diallyldimethylammonium chloride) (PDADMAC) and anionic poly(sodium 4-styrene-sulfonate) (PSS), has gathered remarkable interest based on the interaction between cationic and anionic functional group. Interestingly, when these oppositely charged electrolytes are assembled into nano-thin films using the layer-by-layer (LbL) deposition or solution mixing into precipitated complexes, they are stable and remain insoluble in water or any organic solvents. These films can indeed be doped with numbers of organic or inorganic molecules due to the interaction between oppositely charged components. Nevertheless, the direct incorporation of non-ionic or hydrophobic molecules in the polar surface or within the film matrix remains a challenge due to the lack of interactions between the components. The LbL assembly of PDADMAC and PSS onto a substrate can provide nanostructured layers with tunable thickness and composition. In this work, the attempt to load hydrophobic 1,7-bis-(4-hydroxy-3-methoxyphenyl)-1,6-heptadiene-2,5-dione (curcumin, Cur) in polyelectrolyte multilayer (PEM) is presented in Chapter 3. The study of the loading and release behaviors of Cur from the PEM thin films led to the finding that both solvent and temperature can affect the loading and release of these hydrophobic model drugs. The application of Cur in PEM as pH indicator for sensor applications is described.

Although the PEMs produce very thin, smooth, and homogenous films, their limitation is the time-consuming in the fabrication process. To accelerate the assembly of polyelectrolyte films, PDADMAC and PSS can be used to prepare micro-scale membranes of polyelectrolyte complexes (PECs) by solution-mixing (Michaels, 1965) using NaCl as plasticizer followed by centrifugation and compression molding into 100 μm sheet. In Chapter 4 mainly discusses the concept of an excess electrolyte, nonstoichiometric PEC, membranes blended with oppositely charged and non-charged molecules. The PECs were prepared using various $[\text{P}^+]:[\text{P}^-]$ polymer ratio ranging from [2:1] to [1:2]. These Cur-PEC films were demonstrated here as visual detectors for aqueous pH solution and ammonia (NH_3) vapor phase.

The PECs formation is thermodynamically driven by the entropy gain associated with the release of the salt counter-ions. Because PECs cannot be directly melted with temperature and are non-soluble in water, they are known to be hardly processable in the solid state and brittle when dry. It is known that water and salt are two important parameters that allow the softening of the PECs by modifying the chains interactions, enhancing chain mobility, and creating free volume in the ionic network (Hariri *et al.*, 2012). Depending on the ionic strength of the solution, PECs are obtained in the form of tough complexes, elastic liquid coacervates, or liquid-like solutions (Shamoun, 2012, Wang, 2014). The effect of NaCl concentration on the mechanical properties and the glass transition temperature (T_g) of compressed PEC membranes have been reported in Chapter 5. Unlike the several previous studies on PECs (Zhang, 2015, Shamoun, 2012), the work presented here focused on the influence of salt addition *during* mixing and complex formation on the thermo-mechanical and shape memory effect of PEC membranes *after* the salt was rinsed out.

The improvement of the mechanical properties of PEC membranes and also free-standing PEM films by reinforcement with cotton cellulose nanocrystals (CNCs) isolated from sulfuric hydrolysis was studied in Chapter 6. There are several possible applications of these composite membranes depending on the additive molecules combined with polymer matrix.

CHAPTER II

LITERATURE REVIEW

2.1 Polyelectrolytes (PEs)

Polyelectrolytes (PEs) are polymer systems consisting of positively and negatively charged groups interacted together with electrostatic force and balanced the charge by small molecule counterions, which were electroneutrality. The PEs are become more interesting materials because of the both characteristics that shows the charge possibilities of electrolytes and the practically useful properties of polymers. Their properties are being used in a wide range of technological, industrial, biology, and also chemistry fields. The commercial PEs were synthesized by polymerization, polycondensation, or polyaddition process. Moreover, there can be obtained from natural sources including gelatin, pectin, or from chemical modification of nonionic polymers such as cellulose, starch, etc. The examples of PEs are show in Figure 2.1.

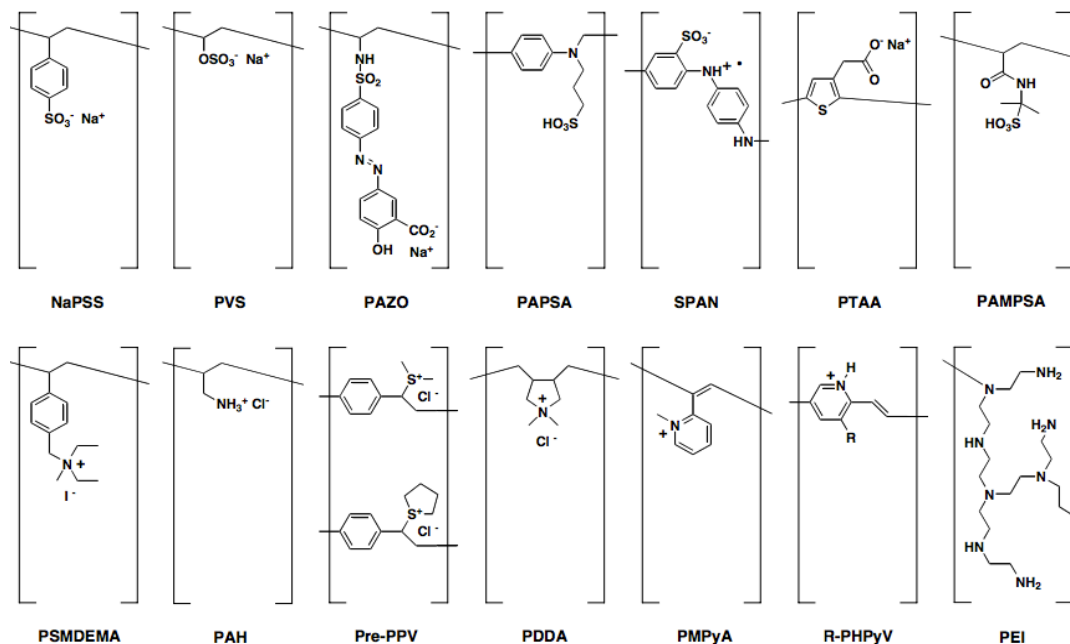


Figure 2.1 Examples of polyelectrolytes.

The strong PEs, cationic poly(diallyldimethylammonium chloride) (PDADMAC) and anionic poly(sodium 4-styrene sulfonate) (PSS) are macroions and counterions on aqueous solution, remain as dissociated polyacid and polybase in all range of pH and show high chemical stability under wide a range of conditions (Dubas, 1999).

Early development focused on achieving fundamental understanding of nano-scale polyelectrolyte multilayer (PEM) films, due to the practically used of thin layer formation, and controlling the properties of materials at a molecular level by layer-by-layer (LbL) deposition using spinning, spraying, immersion, fluidic or electromagnetic. The different types of layer and substrates can provide widely applications. After that, the assembly focused on applying two or more building blocks to accelerate the process for prepare polyelectrolyte complex (PEC) driven by sedimentation, spray dry of particles, electrochemical assembly, and simultaneous spray (Richardson, 2016). The electrolytes assembly techniques for PEM and PEC formations are shown in Figure 2.2.

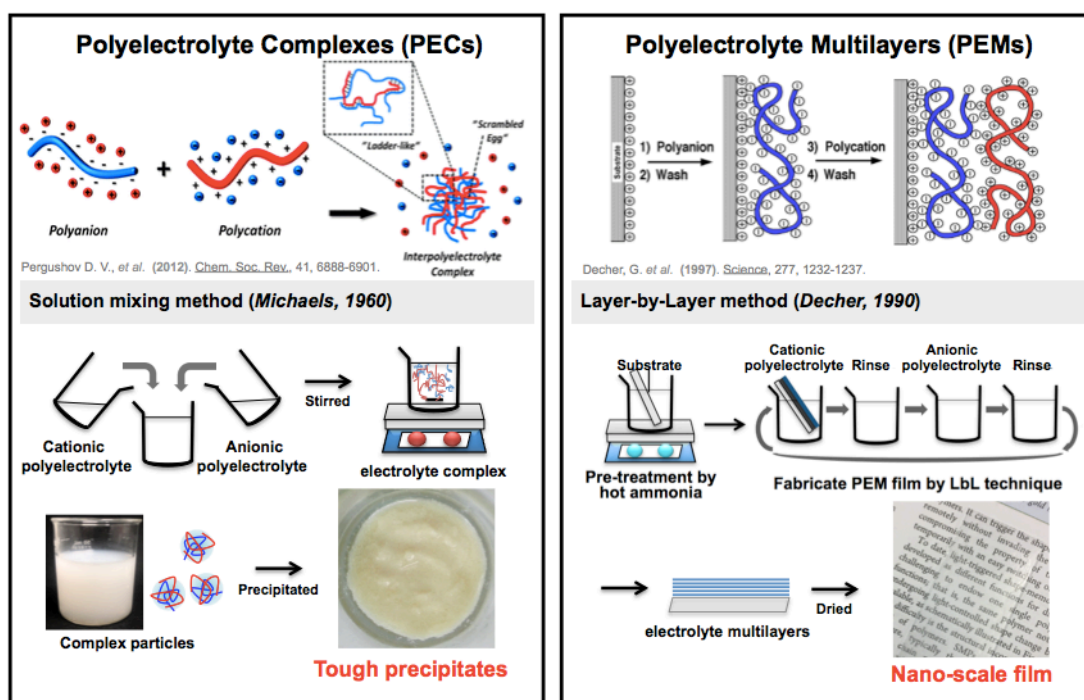


Figure 2.2 Polyelectrolyte assembly techniques.

2.2 Polyelectrolyte Multilayers (PEMs)

The development of ultrathin films for application in biomedical such as drug and gene delivery is an interesting technology. The number of publications about thin films for biomedical fields is strongly expanding. The layer-by-layer (LbL) self-assembly has been widely used for prepare the nanostructure ultrathin films, the so-called polyelectrolyte multilayer (PEM), achieved in a directly on surface with any shapes and sizes, low-cost manner, simplicity of process, and preformed under mild conditions, which is suitable for preserving activity of drugs or biomolecules (Villiers, 2011, Bertrand, 1999). This method was introduced in the early 1990s by Decher and co-workers. The adsorption in alternative multilayers is governed by electrostatic interactions between the polyelectrolyte in solution and the polyelectrolyte of opposite charge on the top of layer (Rechert, 2004). A substrate with the negative charge on surface is immersed in the positive charge polyelectrolyte solution and a monolayer of the polycation is built. After rinsing in DI water to get out of residues polyion on the surface, the substrate is immersed in the negative charge polyelectrolyte solution. The buildup of the PEM was obtained by repeating in a cyclic step until the desired number of layers was achieved (Decher, 1992). The layers can be preformed in different ways such as dipping, spinning (Jiang, 2004), spraying (Schlenoff, 2000), and flow base technique. Even when the combination of anionic and cationic PEs is the same, the different coating technique can lead to the difference in material properties (Mertz, 2013). After deposition of each layer, the rinsing with the washing solution is required to remove the excess PE chains that are not tightly adsorbed on the surface of substrate (Dobrynin, 2008) and then dried under air or nitrogen. The experimental parameters that can affect the roughness, thickness and porosity of multilayers are pH of solution, ionic strength, polyelectrolyte type and concentration, molecular weight, salt type and salt concentration ([salt]), solvent quality, and deposition time (Dubas, 1999). The LbL assemble technique procedure is showed in Figure 2.3.

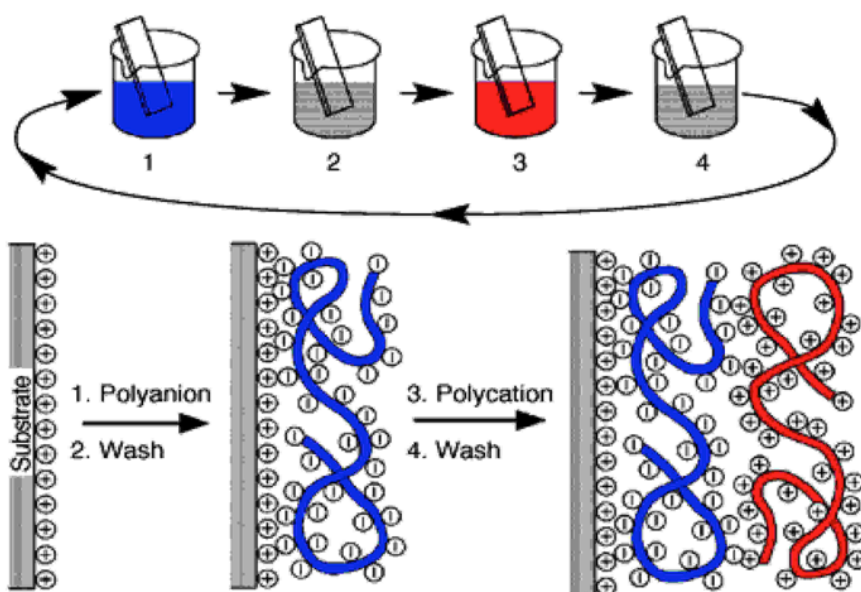


Figure 2.3 The layer-by-layer (LbL) assemble technique (Decher, 1997).

The LbL has become practical strategy for the fabrication of nanostructured devices for several fields in sensing, electrochemical, electroresponsive and energy devices applications because its can control the molecular level of layer such as charge transport mechanisms or can be induced the formation of LbL films by active trigger, covalent coupling, to use for supercapacitor, biosensors, or swelling/shrinking films in drug delivery systems (Crespiho, 2006, Rydzek, 2015). They are also use for biomedical fields that can preserve the bioactivity of biomolecules because these films are used in dry state. Additionally, there are the several advantages of LbL technique including extremely simple and low-cost manufacturing, environmental friendly, wide range of material that can be used of materials such as polyions, metals, ceramics, NPs, and biological molecules, obtainment of homogeneous film, and easy to control the thickness (Gentile, 2015).

2.2.1 Parameters Controlling the Growth of PEM Thin Films

The growth of PEM can be controlled by type of PEs that affected the total thickness, polymer charge density required for neutralized charge of the chemical structure, the ratio of cationic and anionic charged PEs during the buildup of PE pair fabrication, and influence of ionic strength since the total multilayer

thickness can be controlled by adding salt to the polyions solution. Salt plays a significant role to the multilayer structure not only collapse the pores that crated inside the PEM but also anneal the surface of PEM by decrease the surface roughness at high [salt] solution (Ghoshine, 2013, Dubas, 2001). The surface structure of films and PEMs formation significantly dominated by the NaCl concentration (Ge, 2016, Steitz, 2001). The film thickness increase dramatically with increasing [salt] due to the strongly screening of charges along the PE chain, which induces an increasing coiling of chains. The type of salt is influence the growth of PEM films refers to the Hofmeister series. The solvent of solution medium affects the interaction between salt counterions and oppositely charged PEs. The thickness of PEM film was increase when increasing ethanol composition. Because of the poor solvation effect on the ions, strong PE-ion association and strong coiling chain occur lead to the increasing in the film thickness (Volodkin, 2014).

2.2.2 Free-Standing PEM Thin Films

The powerful of obtain the ultrathin films with out substrates is estimated to broaden the field of sensors, separation membranes, micromechanical devices, and wound dressing (Estillore, 2011). The fabrication of the stand-alone film, which is called free-standing polyelectrolyte films or self-sustaining polymer films (Fujie, 2009), trough the LbL self-assembled is a challenging technology. Because the limitation of the films is not ability to maintain their shape after released form the substrate because they have a huge aspect ratio in the air (Fujie, 2007). There are several methods are being to fabricate LbL assembled free-standing films while can maintain the shape of film after releasing from substrate. The most frequently used method is using a preliminarily covered sacrificial layer (Ma, 2007). The sacrificial layer is deposited between the film and its substrate in order to facilitate removal of the free-standing thin film from the substrate (Baxamusa, 2014). The fabrication of sacrificial layer was based on the spin coating method that is appropriate for preparing an ultrathin film directly on a substrate. Then, the LbL film was built on the sacrificial layer-coated substrate. The dissolution of the sacrificial layer in a suitable solvent yields a free-standing LbL film within a several minutes (Hasan, 2009, Fujie, 2009). Cellulose acetate (CA) was selected as the sacrificial

layer polymer because it is dissolved by acetone that do not dissolve the LbL film. Moreover, CA would not dissolve in the aqueous polyelectrolyte solution (Hasan, 2010).

2.2.3 Potential Applications of Composite PEM Thin Films

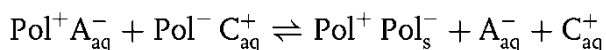
The PEM thin films fabricated through LbL method can control thickness, surface and bulk properties by a build up conditions as well as post-treatments. Especially, they provide very wide range of applications that can be innovated by embedded with the variety of added component. The nanocoating LbL technology provided surface modification that can be maintained the interaction between the substrate and the environment. The fabrication of PEM thin film permitting multimaterial fabrication includes proteins and colloids, which can be used for anticorrosion, antireflective coating, biocompatibilisation, sensors and biosensors, water filtration (Ng, 2014), enzyme immobilization, separation membrane, fuel cell, implants, optical waveguides, electroluminescent devices, microreactors, batteries, supercapacitors, and cancer therap (Ariga, 2014). The practical advantage of these materials is can be preserved the activity of biomolecules such as enzymes due to the low temperatures and aqueous environment (Lyngge, 2013). The PEM films can be reinforce with metal or inorganic NPs for photoelectronics, sensing, magnetism, and catalysis applications. The in-situ synthesis of metal NPs such as silver (AgNPs) (Limsavarn, 2007, Gong, 2011), gold (Au) (Li, 2011) in PEMs is significant affected by the functional groups content in the multilayers. The AgNPs loaded PEM films can be used in sensing applications (Detsri, 2015), antibacterial and electrical devices (Huang, 2014).

The important advantage of PEMs is they can load with biomolecules under mild conditions, which is suitable for preserving their bioactivity properties. The biomolecules can be divided into two groups. First, hydrophilic molecules that can soluble in water. Previous works suggest that the hydrophilic molecules can diffuse into PEMs because of their hydrophilicity and the PEM films could be a promising drug delivery system (Wong, 2010, Jian, 2013). Second, hydrophobic molecules that cannot soluble in water, so, it is hard to be immobilized onto the

hydrophilic materials. The idea of Cur, as a hydrophobic molecule, loaded into PEM thin film was reported by Kittitheeranum *et al.* in 2010.

2.3 Polyelectrolyte Complexes (PECs)

The study of polyelectrolyte complexes (PECs) was introduced by Michaels and co-workers in the 1960s. PECs are solution-precipitated of highly charged PEs or polysalt structures that show homogeneous, transparent, extremely hard and brittle when dry but either leathery or rubbery when wet (Michaels, 1965). There are properties of PECs including insoluble in water and common solvents, infusibility, amorphous structure, can blend with constituents in a molecular level, almost no salt or counterions inside the complex, high dielectric constant when wet, highly permeable to water and electrolytes, permeable to water and electrolytes but resistant to macrosolutes, and swelling or plastizing by salts water, which is so called “Saloplastics” (Schlenoff, 2012, Schaaf, 2015). PECs formed by exposing positively and negatively charge PE solutions together. The strong Coulombic interaction between oppositely charged electrolytes generated the self-aggregation, which is not only strong but also very fast due to the PECs formation governed by thermodynamic and kinetic factors (Dautzenberg, 1997, Thunemann, 2004). There are PE ion-pairing and entropic releasing of small molecule counterions, with considered as polyion coupling reaction. The strength of the Pol^+Pol^- ion pairs is directly related to the amount of water released, driven by greater dehydration.



The primary PECs formation is governed through secondary binding sources such as Coulombic forces follow by the formation process within intracomplexes to create the new bonds and the adjustment of the PE chain distortion. Finally, the secondary PECs were aggregated that mainly hydrophobic interaction (Gubbala, 2012). These aggregated complexes can be separated out as a concentrated PE phase, so called “Coacervated”.

However, the reported study of PECs was very low because they are hard to process in solid-state formation due to their brittleness and infusible when dry. The

PECs are become an attractive topic after Michael *et al.* (1961) investigated the way to process the water insoluble complexes by dissolving the precipitated polysalts with sodium bromide (NaBr)-acetone-water mixtures. The processing of dense PECs in several formations was performed by Shamoun *et al.* in 2012. They successful prepare the salt-plasticized PECs using a laboratory extruder into fibers, rods, tubes and tapes shape with homogeneous and low pore volume content (less than 10%). Although, permanently chemical crosslink PECs are difficult to extrude but physically crosslinked, that can be broken and reformed, is adequate to allowed the permanently crosslinked to reform during the process with sufficient temperature and salt water.

2.3.1 Parameters Controlling the Properties of PECs

2.3.1.1 Effect of Salt and Ionic Strength

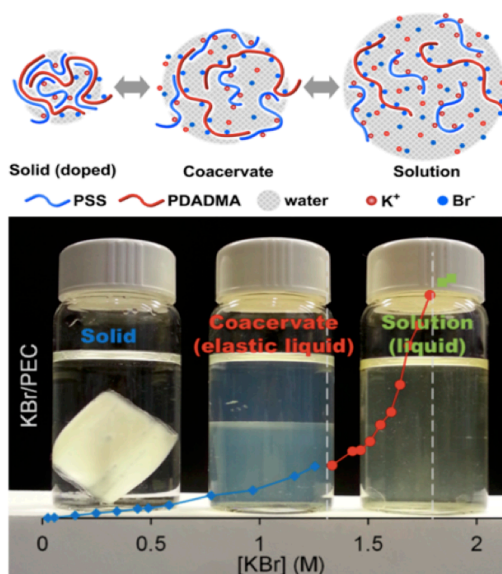


Figure 2.4 Effect of added KBr on the microstructures of PEC (Wang, 2014).

Namely saloplastic is from the main property of PECs that can soften by salt. Salt weakens the physical crosslink of complex by breaking the ionic network between oppositely charged monomers, which created the free volume that allow the PE chains to deformation and reorganization. PECs are plasticized with salt

water and could be compacted into a tough, transparent, hydrated, macroscopic complexes using a high centrifugal field. This complex contains porous but actually fulfill with excess PSS contracts with salt (Porcel, 2009). The charged balances of PEs are governed by intrinsic and extrinsic compensation, which created from oppositely charged electrolytes and counterions, respectively. The salt counterion can controls the physical and mechanical properties of PECs. In 2014, Wang *et al.* built a stoichiometric PEC of PDADMAC and PSS and then dissolved in aqueous KBr solution. When increasing the [salt], the solid state PECs spanning to coacervate and finally completely dissolve in solution as illustrated in Figure 2.4. The term of PEC coacervate can describe as a liquid-like, mobile and reversible structure, which can change to solid-like depending on their salt content. When adding small amount of salts, complexes can rearrange and then aggregate into larger insoluble PECs. Otherwise, when high amount of salt was added, the complexes completely dissociate and dissolve in salt solution (Gucht, 2011). The [salt] also affects the properties of complex by induce the water amount into extruded PECs (Ghostine, 2013). The PDADMAC/PSS complexes have 37 – 41 wt % water with the NaCl concentration in the range of 0.10 – 1.0 M (Shamoun, 2012). Due to the annealing of PECs in proper [salt] solution, which is high enough to penetrate into the complex and increased the mobility of PE chains, the complexes show mending and self-healing properties lead to the recovery of their initial mechanical properties (Reisch, 2014).

2.3.1.2 Effect of Molar Ratio and Order of Mixing

PECs are supposed to be equimolar as negatively equal to positively charged at equilibrium but it can be difficult to reach because the diffusion rates of PE chains in complexes is much slower than in solution. The mixing order during complex formation step also affects their composition. Equimolarity of PECS can be achieved by increasing the speed of addition, decreasing the PE concentration, or pouring both PE solutions together during complex formation (Schaaf, 2015). To achieve the maximum modulus of PEC, it should be stoichiometric with no pores inside. Nonstoichiometric complexes were dominated by the order of mixing and the kinetic control in PE association. The molar ratio between the concentration of non-absorbing species PDADMAC and free PSS provides the stoichiometry factors in the

PECs. The deviation from 1:1 stoichiometry reduces the crosslink density result in the decreasing of modulus. It can be confirmed by nuclear magnetic resonance (NMR) spectroscopy, the nearly stoichiometric PEC was obtained with the lowest ionic strength solution during the process. The porosity also decreases the modulus owing to additional PE stain in these pores, creating a nonuniform distribution of complex (Karibyants, 1997, Shamoun, 2012). It displays the maximum water stability with an excess PDADMAC film due to more hydrophobicity of PDADMAC than PSS and could be stated that PDADMAC act as a hydrophobization agent for PECs (Gai, 2016).

2.3.1.3 Effect of Temperature

The temperature is the major parameter in PEC processing step. Above the T_g , the polymer chains have high mobility and allow them to reptate out from entanglements during the process lead to decrease in modulus and increase in mobility (Shamoun, 2012). Temperature can enhance the relaxation and mobility of PSS chains due to its weakened hydrogen-bonded supramolecular network through water affects the dynamics of the whole PECs (Yildirim, 2015). The PE miscibility with water decreases with temperature, which is related to the low critical solution temperature (LCST) transitions.

2.3.1.4 Effect of Water Content

Water is an important factor for PECs by known to plasticized the complexes and required for the thermal transition of PECs. Increasing the amount of water in complexes cause the decreasing in T_g , elastic modulus, and tensile strength decrease but increasing in percent elongation. The water act as a plasticizer by creating free volume that allows the chain mobility, disrupting chain interactions, and softening the complex, which affect the properties of PECs as increasing temperature. Hydrated PECs are flexibly, rugged and have the modulus about 1 kPa – 10 MPa, which is similar to many living tissues. For proper condition for extrusion, PDADMAC/PSS need about 3.7 molecules of water for each ion pair doped with NaCl (Shamoun, 2012). The strain stored in PECs may be released with salt water or hot water, which have been considered as shape memory behavior. Likewise, a lack of salt doping could be compensated by high temperature or the complex remained fully hydrated (Wang, 2014). The PDADMAC/PSS complex swells about 20% upon

exposed to water vapor with 60% relative humidity or immersed in water according to the Flory-Huggins theory, which describes a phase separation in PE network when increase water contents. This makes the PEC suitable for the used in stimuli responsive materials (Köhler, 2009). The PDADMAC/PSS complex dehydrated under defined osmotic stress using poly(ethylene glycol) (PEG) and became transparent with much stiffer at the lowest osmotic stress due to the decreasing in water content. The exponential relationship between the elastic modulus and water/polymer ratio, known as the plasticizing efficiency, is 177 MPa at about 10 water molecules per PDADMAC/PSS ion pair and show strongly decrease with increasing water contents (Hariri, 2012). Water plasticizing effect of PEC shown in Figure 2.5.

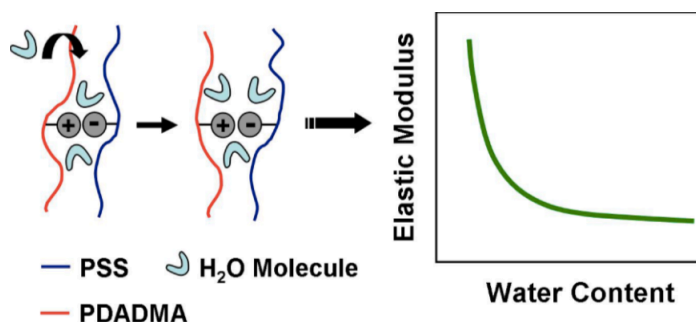


Figure 2.5 Water plasticizing effect of PEC (Hariri, 2012).

2.3.1.5 Effect of Processing Method

The processing methods affect the mechanical properties of PECs, which is related to the composition and porosity within the complex (Hariri, 2012). There are many techniques used to fabricate PECs such as extrusion, injection, compression, and centrifugation. The properties of PDADMAC/PSS complex by different process were described in the researches of Lankalapalli *et al.* (2009), Hariri *et al.* (2010) and Shamoun *et al.* (2012). The PECs fabricated through solution mixing process has the advantages that it is easy to synthesis and the precipitated can be collected immediately after formation but the drawback is some of the PEs and incorporated molecules are lost in supernatant solution during synthesis. The PECs precipitated at high [salt] by ultracentrifugation were

nonstoichiometric, high porosity and fully hydrate, which lead to low modulus value in kPa. In contrast, the PDADMAC/PSS complexes prepared from extrusion at low amount of salt were stoichiometric, homogeneous, compact and have low water content, which generate high stiffness within MPa.

2.3.2 Potential Applications of Composite PECs

PECs become much consideration in the past few years due to their practical applications such as membranes for control permeability, separator membranes for pervaporation and nanofiltration, battery and fuel cell separator membranes, dialysis and ultrafiltration membranes, conductive coatings, medical implants, contact lenses, and sensor applications (Zhao, 2011, Wang, 2014). Many of potential applications are based on the functional group along PE chains and can be classified by the interaction between PEC and additive molecules such as counter ions for ions filtration supporting membranes or ion exchange in analytical procedures, surfactants for insoluble polyion complex for low energy surface modification, charged low molar mass molecules for drug complexes, charged particles for waste water treatment, charged surfaces for displacement chromatography, additive in cosmetics or detergent (Lankalapalli, 2009) and supported membranes for separations, cell growth substrates, coatings (Kelly, 2015).

The benefits of PECs in pharmaceuticals field are the ability to maintain the individual properties of both PEs that combined together and can control the site-specific delivery of drugs by their swelling capability in gastrointestinal fluid or their pH dependent degradation as well (Siyawamwaya, 2015). The mechanism of drug release in PEC matrix is governed by the degradation of complex leads to swelling as free charges and then the drug molecules can release out from the PEC (Fu, 2015).

PEC nanocomposites can be prepared for use as a conductive membrane. There are use for applications such as thermal switches, EMI shielding, sensors, and fuel cell. The advantages of these composite films are low density compare to metals or ceramics, good chemical resistance, easily to form a complex shape and their barrier properties (Motlagh, 2008). The nano- (NPs) or micro-sized particles, such as graphite (G) and silver (AgNPs), can be embedded in many polymer matrixes (Gelves, 2006, Lonjon, 2013), which are interesting for the flexible electrodes, energy storage applications and electromagnetic shielding (Pothukuchi,

2004) because of the improvement of the electrical properties due to the high surface area of the filler particles when homogeneously mixed and uniformly dispersed with polymer matrix were achieved.

2.4 Curcumin (Cur)

Curcumin (Cur), 1,7-bis-(4-hydroxy-3-methoxyphenyl)-1,6-heptadiene-2,5-dione], is a yellow powder extracted from rhizomes of turmeric (*Curcuma longa* Linn.) which is a therapeutic compound in medical applications. The remedial properties of Cur were found to antioxidant property, anti-inflammatory, Alzheimer disease, anticancer, antimicrobial, and wound healing (Pandey, 2011, Patel, 2009). The effect of Cur on enhancing cutaneous wound healing depicted a huge number of infiltrating cells such as fibroblasts, myfibroblasts, macrophage, and neutrophils as compared to untreated wound (Joe, 2004, Maheshwari, 2006, Sidhu, 1998). Kittitheeranun recently reported that the Cur dispersed in an 80:20 water:EtOH solution can be loaded into PDADMAC/PSS film (Kittitheranun, 2010). Cur can change color from yellow to red at the first pK_a in the pH range of 7.5 – 8.5. When pH increases, the water solubility of Cur was increased and also when temperature increases due to the breaking of the intramolecular hydrogen bonding of Cur (Jagannathan, 2012). The Cur structure is shown in Figure 2.6.

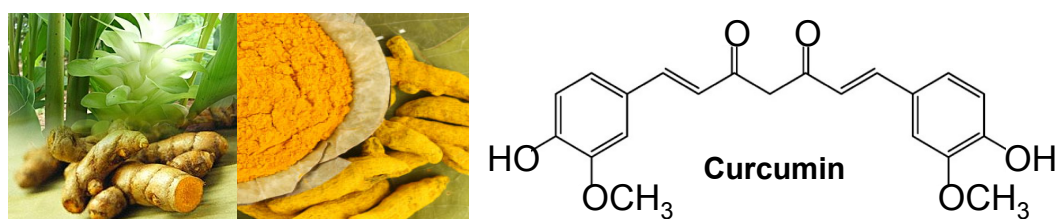


Figure 2.6 Rhizome of *Curcumin longa* Linn (left), Cur extract powder (middle) and chemical structure of Cur (right).

2.4.1 Loading of Cur Based Polyelectrolyte Systems for Drug Delivery

Cur is a natural component of the rhizome of turmeric (*Curcuma*

longa), which has been studied for its biological effects ranging from antioxidant, anti-inflammatory to inhibition of angiogenesis and is also studied for its antitumoral activity (Lee, 2013, Mahmood, 2015, Lin, 2008). Cur is used in transdermal applications for dermal treatment to kill bacteria or reducing acne (Shehzad, 2012). Cur has a poor solubility in water and the β -diketone moiety present in the center of the molecule induces an intramolecular keto-enol tautomerism, which is responsible for its solubility in either alkaline solution or non-polar solvent. However, being nearly insoluble in water limits its bioavailability and transfers from the gastrointestinal track to the bloodstream (Hazra, 2014). Although Cur solubility can be enhanced by the addition of polymers, surfactants or cyclodextrins, its loading and release from polymeric membranes remains a challenge (Potter, 2014, Carvalho, 2015). In 2010, Kittitheeranun *et al.* reported the utilisation of PEM thin films as a matrix for the loading of Cur. In the field of drug delivery, the LbL technique is used to coat nanoparticles or modify the surface of biomedical implants. In the case of transdermal drug delivery, LbL films can be used for the loading and release of hydrophilic molecules such as dyes and drugs (Wang, 2008, Gentile, 2015, Tang, 2006). Recently, interesting dispersed system based on the microencapsulation of hydrophilic molecules salts in PEM structured have been reported (Gau, 2017, Donath, 1998). The ionic character of the PEM allows the diffusion and immobilization of ionic species. It was demonstrated that hydrophobic Cur could be loaded in the PEM. The loading was found to be tuned by the solvent quality (water:ethanol) based on a liquid-solid partitioning mechanism and the release of Cur was triggered by a rinse step in ethanol, which is not practical to use in transdermal drug delivery applications (Kittitheeranun, 2010, Saikaew, 2016).

2.4.2 pH Solution and Ammonia Vapor Sensing of Cur Based Polyelectrolyte Systems

The development of colorimetric freshness indicators used in food packages has received great attention and various technologies have been developed to this end. Although some systems can be quite sophisticated such as in RFID tag equipped with chemical sensors or gold nanoparticles used in lab-on-chip solutions, the devices must be inexpensive, accurate and food safe. Food spoilage can be monitored through indicators that are mostly based on pH changes and gas emissions

(Ajaykumar, 2014, Pourreza, 2015, Correa, 2014, Kuswandi, 2012). For example the decrease in pH observed in sour milk as a result of bacterial activity can be monitored by colorimetric dyes that have color change in the corresponding pH range (Kuswandi, 2012). Besides, colorimetric dyes can be monitored the changes in gas composition due to CO₂ or ammonia released in spoil meat and fish products (Kwon, 2012). Among the available sensing molecules, Cur, a natural poly-phenolic compound found in turmeric, is of great interest. Cur has astonishing properties ranging from anti-fungi, anti-inflammatory, anticancer and also has the interesting property to change color from yellow (in acid) to orange red (in base) at pH value above 8.5 (Prasad, 2014, Sim, 2003). The color change is due to the protonation of the Cur structure from its keto form (yellow) to the enol form (red). For these reasons, Cur patches have been proposed as optical sensors for seafood spoilage by monitoring the color changes upon bacterial proliferation (Goel, 2008). Kuswandi *et al.* (2012) have reported a good correlation between Cur color change and the proliferation of bacteria.

2.5 Mechanical Properties of Polyelectrolyte Multilayers (PEMs) and Complexes (PECs)

The mechanical properties of PEMs and PECs are dominated by the glass transition temperature (T_g), which is limit the range of operation temperature of materials and considered for the curing and processing. The mechanical testing of PEMs, which depends on the chemical of electrolyte and the degree of electrostatic crosslink, was observed by quartz crystal microbalance, capillary wave techniques, point-load nanodeflection and nanoindentation using atomic force microscope (AFM). The elastic modulus of PDADMAC/PSS multilayers soaked in NaCl solution decrease with increasing [salt] with a value of 17 ± 2 and 1 ± 0.2 MPa at 0 and 1.0 M NaCl, respectively. At low [salt], PEMs have high crosslink density, which connected by short and stiff segments without many degree of freedom providing high modulus value while at the present of salt, the crosslinks are broken, PEMs swell and absorb more water and salt ions (Jaber, 2006). The polymer charge density also affects the elasticity of PEM films, which exhibited a high elastic

modulus at high charge density. Moreover, high ionic crosslink density presents high adhesion values between each layer (Mermut, 2003)

The commonly techniques for determine the T_g of PECs are differential scanning calorimetry (DSC) and dynamic mechanical thermal analysis (DMTA). Many researchers have been studied the T_g of polyelectrolyte system and they were implied that the T_g of hydrated PDADMAC/PSS complex was about 35 – 40°C. Below the T_g PECs exhibited more rigid while above the T_g they were swollen due to the polyelectrolyte chains movement (Köhler, 2005). It was reported that the T_g for dry PDADMAC is 68°C and 180°C for dry PSS but the T_g s were increased to 166 and 211 °C for homopolymer PDADMAC and PSS, respectively, due to the presence of water content. Figure 2.7(a), Shamoun *et al.* (2012) showed DSC thermograms for extruded PDADMAC/PSS complex with no T_g for dry extruded PEC, whether it contained salt or not. However, they were observed a faint transition at about 30 and 10°C for the PECs soaked in water and 1 M NaCl, respectively.

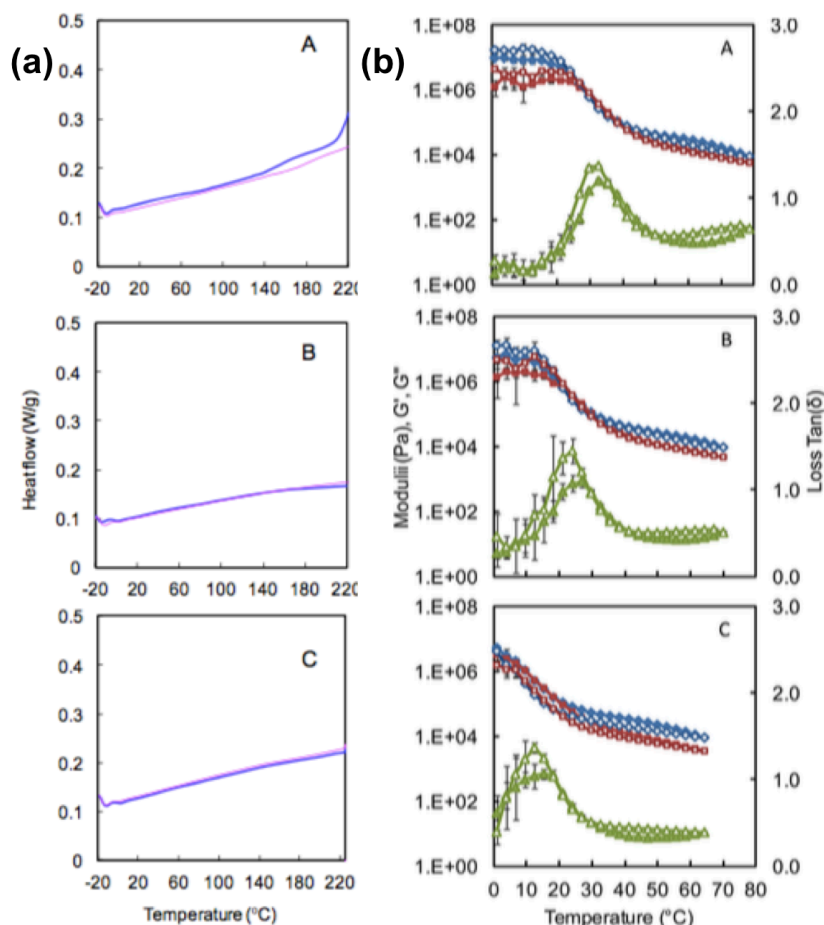


Figure 2.7 (a) DSC thermograms of dried samples of Aldrich, **A** PDADMAC, **B** PSS and **C** extrude PEC after soaked in 1.0 M NaCl and (b) The storage modulus (u), loss modulus (n) and loss tangent (Δ) of extruded PECs soaked in **A** 0.1 M, **B** 0.5 M and **C** 1.0 M NaCl (Shamoun, 2012).

However, the T_g can observe by DSC but they depict more clearly transition from glassy to rubbery state by using DMTA. For DMTA measurement, the viscoelastic response of material, either the storage modulus, loss modulus or loss tangent, is observed as a function of time or temperature. Storage modulus is the elastic or recoverable energy during polymer deformation and loss modulus is the viscous or net energy dissipated while loss tangent represents the ratio of loss to storage modulus. The T_g is located where a significant drop of storage modulus or the maximum loss tangent or loss modulus is occurred. The DMTA detects the relaxation of viscoelastic polymer by applying a small oscillating force on the sample

and measure the strain lags from the stress (Li, 2000). It observes the drop of storage modulus value from 10^6 to 10^4 Pa, which depicts the strong transition in mechanical properties near room temperature. Time or frequency, temperature, and [salt] in term of doping are significant factors for the PECs transition, which called time/temperature/salt (TTS) superposition. Temperature putting more energy into the PE chains motion in backbone level and can be accelerated by doping with salt. The TTS plots were fit with the empirical equation $T_g = 38 + 2.3 \ln f - 20[\text{NaCl}]^{6/5}$ whereas 38 is a reference temperature. The T_g s were shift to lower temperature when increase [salt] or decrease frequency (Shamoun, 2012). The hydrated PECs were soften with increased temperature and the addition of salts according to the TTS superposition leading to the T_g shift to lower temperature when materials are more soften. The moduli of PEC soaked in different [salt] measured by DMTA are show in Figure 2.7(b). The location of this T_g depends on the concentration of salt doping and the deformation rate. Hydrated PEC shows the T_g represents by a thermal transition appears when the complexes are hydrated in water but not in the presence of alcohols, which supports that water is required for this transition. It can be state that PDADMAC/PSS are thermoresponsive polymer, which the transition is driven by the (de)hydration of molecular level in aqueous environments (Yildirim, 2015). At the transition temperature the polyelectrolyte miscibility with water decrease with temperature, which similar to a lower critical solution temperature (LCST)-type transitions during dehydration step (Fu, 2017).

2.6 Cellulose Nanocrystals (CNCs)

Nanoscale cellulose can be divided into nanostructured materials and nanofibers depend on the natural sources as well as the use of various isolation processes (Trache, 2017). Their structures and nanomaterial types are shown in Figure 2.8. Cellulose nanocrystals (CNCs) were isolated from plant-, animal- and bacteria-based materials. The typical process for the isolation of CNCs is acid hydrolysis such as sulfuric acid, phosphoric acid, or hydrochloric acid (Espinosa, 2013), which provides the differences in shape, size or properties. This process provides CNCs with typical diameters of 5-50 nm, lengths of 100-3000 nm and

elastic moduli about 105-168 GPa depend on the sources. CNCs consist of rigid rod-like or needle-like particles possess low cost, potentially low toxicity, high-aspect-ratio, high crystallinity and high specific surface area that can be renewable reinforced in polymer nanocomposite (Xu, 2013, Lee, 2014). There are many potential applications of CNCs reinforced polymer matrix including oilfield applications, membranes for water purification, coatings, packaging applications (Azeredo, 2016), gas or water barrier (Hubbe, 2017), sensing and biosensing, opto/electronic devices, textiles, cosmetics (Golmohammadi, 2017), biomedical fields (Lin, 2014), or can be functionalized for advanced applications such as controlled delivery systems, emulsion stabilizers, sustainable catalysts and anti-microbial agents (Tang, 2017).

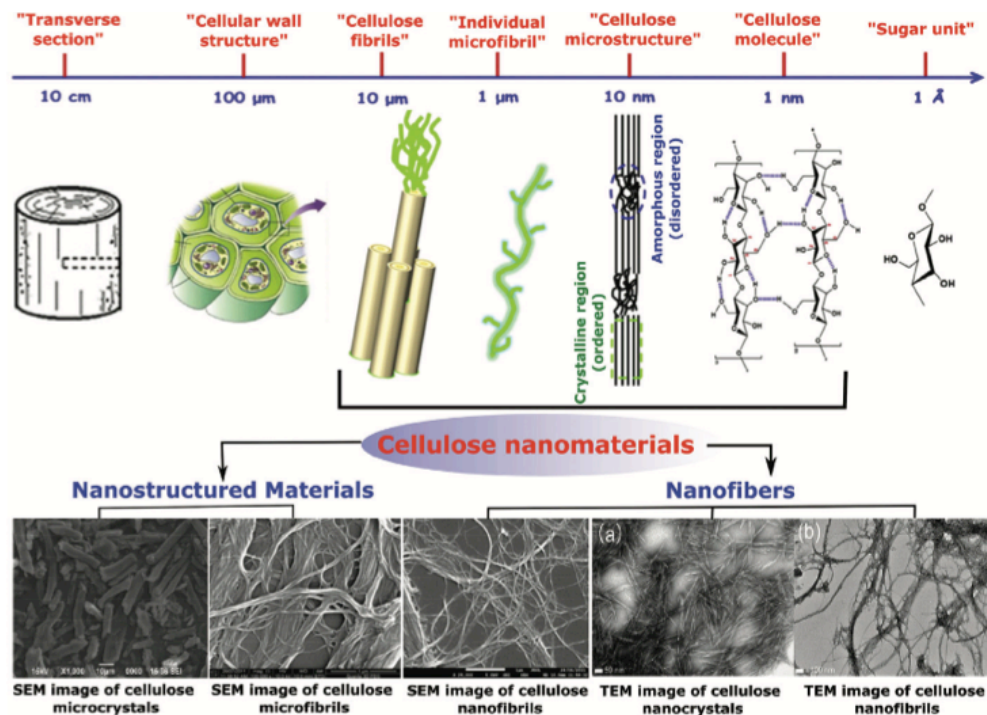


Figure 2.8 Cellulose structure and its nanomaterial types (Trache, 2017).

CHAPTER III

CURCUMIN LOADED POLYELECTROLYTE MULTILAYERS THIN FILMS

To fabricate the polyelectrolyte multilayer (PEM) film, strong polyelectrolyte (PE) pair: anionic poly(sodium 4-styrene-sulfonate) (PSS) and cationic poly(diallyldimethyl ammonium chloride) (PDADMAC) were used. These electrolytes display interesting properties such as pH-dependence, chemical stability under a wide range of conditions and a fast growth rate under high ionic strength. PDADMAC and PSS are used in the biomedical field as wound dressings and artificial skin because of their biocompatibility and used as pH detector application as food packaging stickers. Each PE was prepared in an aqueous solution containing 1 M NaCl, thereby screening the electrostatic interaction between opposite charge PEs in order to get a smooth surface film (Villiers, 2011).

3.1 Proposed Research

Our group reported the utilization of polyelectrolyte multilayer (PEM) thin films as a matrix for the loading of Cur (Kittitheeranun, 2010). The PEM thin films were fabricated by the well-known layer-by-layer (LbL) self-assembly method (Richardson *et al.*, 2016), which was introduced in the early 1990s by Decher and co-workers (Decher, 1992). The growth and structure of these PEM thin films can be finely tuned by the type of PE and the number of deposited layers (Dubas, 1999, Dubas, 2001). The LbL approach is a combination of self-assembly and dip-coating based on attractive Coulombic force between the oppositely charged species from each electrolytes (Ariga, 2014). The LbL deposition of PEM is a very mature technology, which has been the subject of numbers of review articles and books. In the field of drug delivery, the LbL technique is used to coat nanoparticles or modify the surface of biomedical implants. In the case of transdermal drug delivery, LbL films can be used for the loading and release of hydrophilic molecules such as dyes and drugs (Wang, 2008, Gentile, 2015, Tang, 2006). Recently, interesting dispersed system based on the microencapsulation of hydrophilic molecules salts in PEM

structured have been reported (Gai, 2017, Donath, 1998). The ionic characters of the PEM allow the diffusion and immobilization of ionic species. The work presented here focuses on the immobilization of hydrophobic drugs because it was previously demonstrated that hydrophobic Cur could be loaded in the PEM. The loading was found to be tuned by the solvent quality (water:ethanol) (Kittitheeranun, 2010) based on a liquid-solid partitioning mechanism. Nevertheless in previous work, the release of Cur was triggered by a rinse step in ethanol, which is not practical to use in transdermal drug delivery applications.

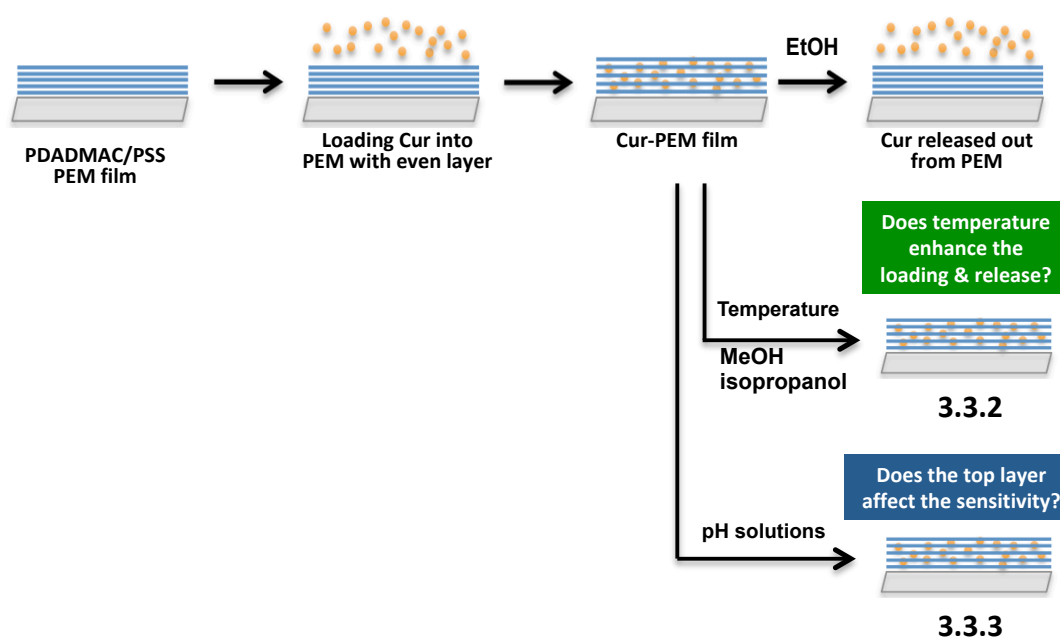


Figure 3.1 Schematic representation of Cur loaded into PEM thin films for the study of temperature controlled loading and release of Cur and the improved pH sensing of Cur loaded PEMs thin films.

In this work, as seen in Figure 3.1 the effect of other solvents (methanol, ethanol and isopropanol) was studied as well as the effect of the loading and release temperature. Using UV-Vis spectroscopy it was demonstrated that when Cur was loaded at 5°C in the PEM film, it could spontaneously be released at body temperature (37°C). Interestingly, a wide variety of active compounds can be loaded in the PEM films either directly during the deposition process or post assembly.

These include organic (Kong, 2011), inorganic (Podsiadlo, 2009) or metallic nanoparticles (Zhang, 2010) as well as proteins or drugs that can be loaded in the PEM films which then act as a host matrix (Kittiheeranun, 2010). Anionic or cationic species are easier to immobilize in the film by taking advantage of the electrostatic interactions with the matrix. However hydrophobic drugs or essential oils are more challenging to incorporate due to the lack of interactions. Nevertheless, we recently reported the loading of Cur in PEM thin films by tuning the solvent quality with different water:ethanol ratios. Cur molecules are thermodynamically driven from the poor solvent into the PEM matrix resulting in the formation of a yellow colored film. Because Cur is known to present a color change at pH above 8.5, it could be potentially used as an optical sensor for ammonia in meat packages to detect spoiled food.

3.2 Experimental

3.2.1 Chemicals and Materials

Poly(diallyldimethylammonium chloride) (PDADMAC, medium molecular weight, 20 wt.% in water, typical $M_w = 200,000\text{--}350,000$), Poly(sodium 4-styrene-sulfonate) (PSS, typical $M_w = 70,000$), and 1,7-bis-(4-hydroxy-3-methoxyphenyl)-1,6-heptadiene-2,5-dione (Curcumin, Cur) were purchased from Sigma-Aldrich. Sodium chloride (NaCl), A.R. grade, phosphate buffer, methanol, ethanol, and isopropanol were purchased from Labscan Asia Co., Ltd. All chemicals and solvents were used as received without any further purification. Double distilled water was used in all experiments.

3.2.2 Temperature Controlled Loading and Release of Cur in PEMs Thin Films

Chemically clean glass slides were dipped in 10 mM PDADMAC or PSS solutions with 1 M NaCl until 13 layers were deposited. After each PE solution steps the film was rinsed with DI for 1 min before the next PE solution. The Cur powder was dissolved in ethanol with the concentration of 0.01% w/v (100 PPM). Cur was loaded by immersing the film into a dilute solution of Cur dispersed in solvents having different ratio of water:methanol, water:ethanol or water:isopropanol

at a fixed temperature. The ratio of water and organic solvent in each mixture was varied from 60:40, 70:30, 80:20, 90:10 and 95:5. The total amount of Cur in the PEM film was characterized with a UV–Vis spectrophotometer (Specord S600, analytikJenna).

3.2.3 Improved pH Sensing of Cur Loaded PEMs Thin Films

Before coating the substrates with PEM films, the glass slides were cleaned in piranha solution (70% H₂SO₄/30% H₂O₂) followed by a 20 min dip in a 60°C solution of 30% ammonia/30% H₂O₂/water (1:1:5) and rinsed in DI. The dipping method has been described in numbers of papers (Goel *et al.*, 2008) and could be summarized as follow. The clean slides were coated by 2 min dipping into a 10 mM PE solution of PDADMAC or PSS layers with 1 M NaCl, followed by 3 rinses of 1 min each in DI. The loading of Cur in PEM thin films has also been previously described (Iler, 1966). The coated slides were dipped for 2 h into a 0.1 %w/v Cur solution having 90:10 %v/v of water:ethanol as solvent. To investigate the pH sensing of Cur loaded PEM films, phosphate buffers (10 mM) adjusted to pH 6-10 (pH 6, 7, 8, 8.5, 9, 9.5 and 10) were used to induce the color change of the Cur loaded films as a function of pH. UV–Vis spectrophotometer (Avantes, AvaSpec-2048) was used to record the spectra of the solutions and coated thin films.

3.3 Results and Discussion

This chapter is divided into two parts. Begin with the study of temperature controlled loading and release of Cur in PEMs thin films for drug delivery applications and follow by improved pH sensing of Cur loaded PEMs thin films for potential use as a chemical sensor.

3.3.1 Fabrication and Characterization of PEM Thin Films

The parameters controlling the growth of PEM thin films were studied. The PDADMAC/PSS multilayers were prepared as Figure 3.2 with a concentration of each polymer equal to 10 mM containing 1 M NaCl and the dipping time is 1 min.

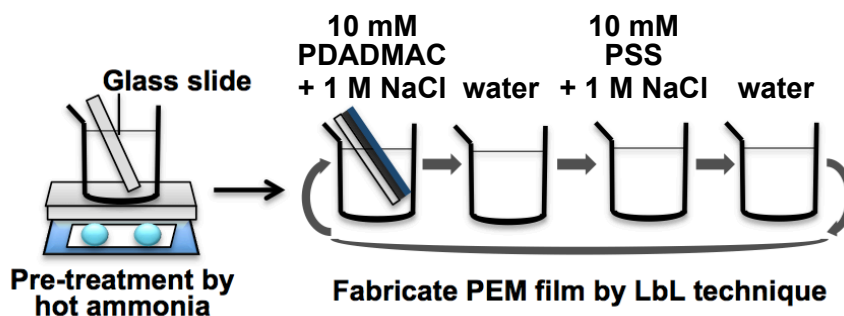


Figure 3.2 Procedure of PDADMAC/PSS fabrication on pre-treated glass slide.

The PEM fabricated by increasing the layers of 10 mM PDADMAC/PSS containing 1 M NaCl on quartz slide. The deposition time of each layer was 1 min and then rinsed with water for 1 min. The growth of PEM thin films was characterized by UV-Vis spectroscopy. As seen in Figure 3.3, the absorbance at 230 nm increase with increasing number of even layers, that are PSS on top, represents the increase of sulfonate ($-\text{SO}_4^{2-}$) peak in the absorbance. Figure 3.3(b) depicts the thickness of PEM film on silicon wafer after pre-treatment by piranha and hot ammonia solution measured by ellipsometry at an angle of incidence 60° (Delta: 174-178 and Psi: ~ 23 for bare silicon wafer) and air-dried every 4 layers. The thickness was found to increase with increasing number of layers in a linear relationship after 8 layers and observed that the average thickness of a single bilayer is 19.71 nm, which similar to the previous studied by Dubas in 1999 (~ 20 nm per layer pair with 1 M NaCl).

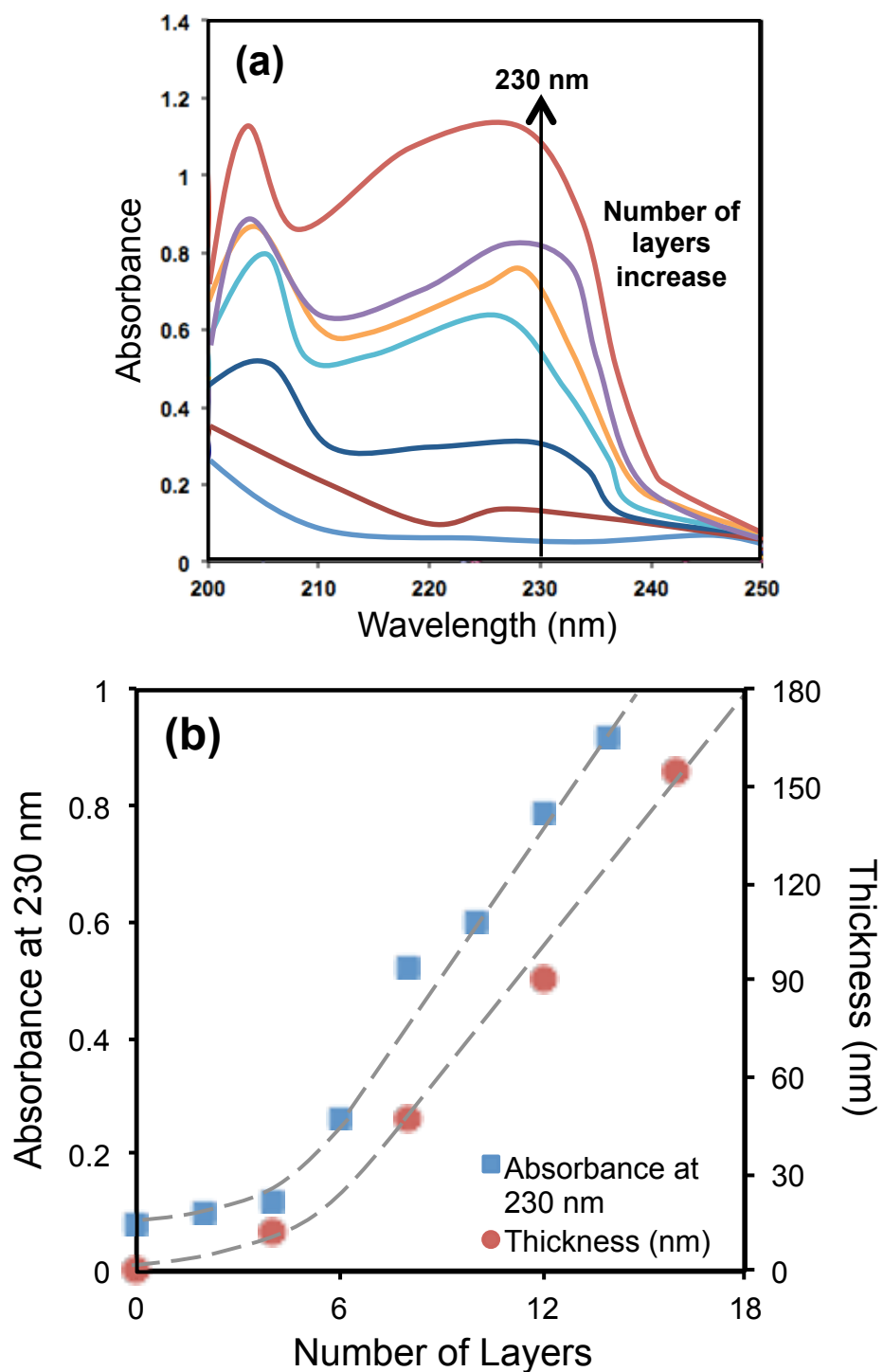


Figure 3.3 UV-Vis spectra (a) with absorbance at 230 nm on quartz slide and the thickness measured by ellipsometry on a silicon wafer (b) of PDADMAC/PSS film when increasing the number of layers.

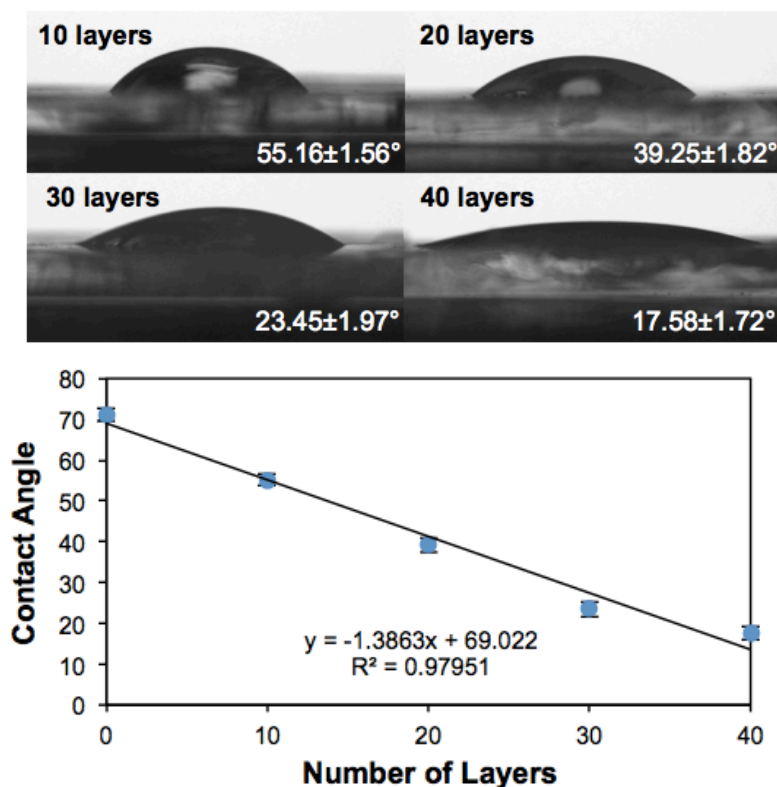


Figure 3.4 Plot of contact angle measurement of PDADMAC/PSS on glass slide with increasing the number of layers.

In Figure 3.4, the contact angle of PEM thin film can be seen to decrease with increasing deposited layers due to the film becoming more hydrophilic. The results confirm that the PEMs provide a more hydrophilic surface which can be used as a matrix for loaded with water-soluble or hydrophilic molecules achieved directly on the surface of substrate.

3.3.2 Temperature Controlled Loading and Release of Cur in PEMs Thin Films

The temperature triggered loading and release of hydrophobic model drug Cur from PEM thin films was demonstrated. Thin films built from the LbL deposition of PDADMAC and PSS were dipped in Cur and studied as patches that could be used in temperature controlled drug delivery applications. Three different solvents (methanol, ethanol and isopropanol) were mixed with different fractions of water (from 60:40% to 95:5% aqueous:organic solvent) and fixed amount of Cur

(100 ppm). The effect of other solvents was studied as well as the effect of the loading and release temperature using UV-Vis spectroscopy. Using this method a new type of transdermal patch for the release of hydrophobic drugs from PEM membrane would be possible. The procedure of PEM thin films loaded with Cur by various temperatures and solvent compositions shown in Figure 3.5

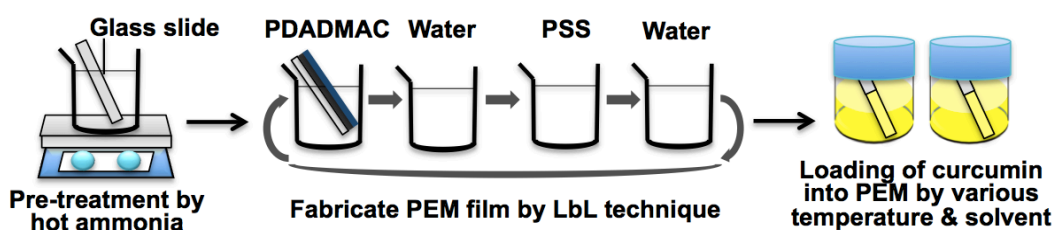


Figure 3.5 Fabrication of PEM thin films loaded with Cur at different temperature and solvent compositions.

3.3.2.1 Solvent Driven Loading of Cur

The PE pair chosen in this study was the commonly used PDADMAC and PSS because these PEs are both fully ionized in a wide range of pH (pH 1 to pH 14). The quantitative study of Cur loading as a function of water:solvent ratio for the three organic solvents (methanol, ethanol and isopropanol) was observed by UV-Vis spectroscopy at 440 nm, which corresponds to the maximum absorbance wavelength (λ_{max}) of Cur as Beer's law equation:

$$\text{Absorbance at 440 nm} = \epsilon lc$$

where ϵ is the extinction coefficient value for Cur presented in databases (Kittitheeranun, 2010), l is the thickness of PEM film and c is the amount of Cur in PEM film.

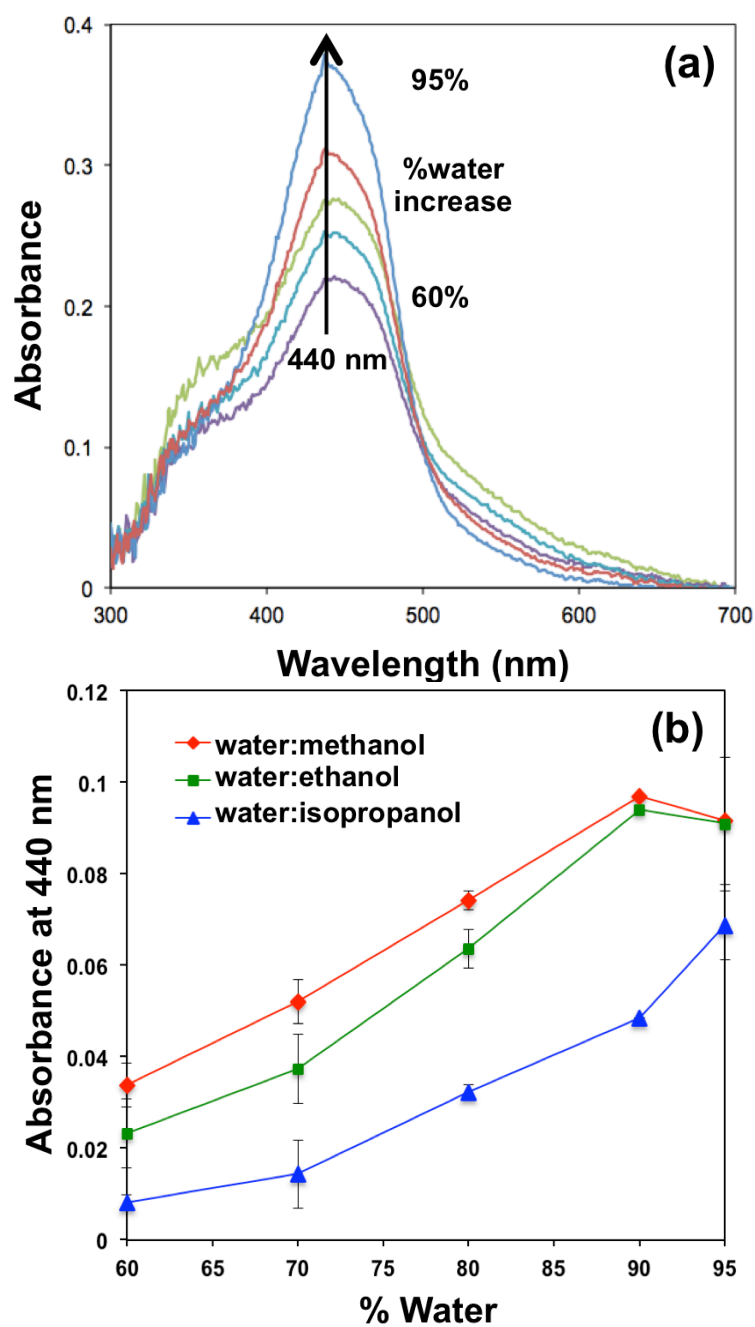


Figure 3.6 (a) UV-Vis spectra and (b) plot of the absorbance at 440 nm of Cur loaded into a 13-layer PDADMAC/PSS films as a function of the water:solvent mixture at room temperature (25°C).

In Figure 3.6 is plotted the UV-Vis spectra and absorbance at 440 nm of the 13-layer PEM thin films soaked for 2 h in the three different solvents

mixtures (methanol:water, ethanol:water and isopropanol:water) with various water content. Each curve corresponds to the variation of the water:solvent fraction from 60:40% to 95:5% and the X-axis representing the water fraction. The prepared 13 layers PEM films without Cur were used as blank in all spectroscopy measurements and automatically subtracted from all spectra. The absorption spectrum of Cur in PEM film was observed at λ_{\max} 440 nm, which is the result of the π - π^* electronic transition of the conjugated segment in Cur (Priyadarsini, 2009). The absorption intensity of the film can be seen to increase for all three solvent systems when the water content was increased from 60 to 90%. The absorbance was also highest for the more polar solvent, methanol, followed by ethanol and isopropanol, which have a dielectric constant of 33, 24 and 18, respectively, and 80 for water. This partitioning of the Cur from the solvent into the solid PEM is partly due to the increase in solvation energy of Cur in the more polar solvent making the PEM membrane appear a more hydrophobic media making the diffusion of Cur a thermodynamically driven process. The solubility of Cur is the lowest in water, but increase in methanol, ethanol and isopropanol to more than 10 mg/ml (Anjomshoa *et al.*, 2016). The loading of Cur with the water:methanol and water:ethanol solvent mixture can be seen to decrease above 90% water because Cur started to precipitate out of the solutions. It did not appear to decrease in the isopropanol mixture due to a better solubility.

3.3.2.2 Effect of Loading and Release Temperature

The effect of the temperature on the loading of Cur in PEM thin films was investigated at 5, 15, 25 and 50°C and solvent compositions as shown in Figure 3.7. Regarding the loading behavior, it can be seen that the amount of Cur diffusing in the PEM decreased with increasing temperature for all solvent systems. The partitioning phenomenon is the most efficient at loading Cur at 5°C while it is the lowest at 50°C. The mechanism by which Cur loading is lowest at 50°C can be explained by both thermodynamic and structural considerations. From a thermodynamic point of view, the increase in temperature does not change the dielectric interaction with the solvent, nevertheless, it is clear that the partitioning process is spontaneous and leads to a decrease in energy of the molecules through an exothermic reaction (Jagannathan, 2012). The amount of heat released by the system

is proportional to the decrease in solvation energy of Cur when considering the two Cur/solvent and Cur/PEM environments. Therefore by taking Lechatelier principle into consideration, the increase in solvent temperature will slow down the exothermic adsorption process. On a structural point of view, previous work has been published by Möhwald and Sukhorukov regarding the study of the glass transition temperature (T_g) of PEM systems. Several publications suggested that the T_g of PEM was located at room temperature in the range of 25 to 30°C (Köhler, 2005). Below the T_g temperature the PEM is expected to be more rigid and hydrophobic while above T_g a more swollen and solvent-like structure is expected. It is thought that a more solvent like structure would not promote liquid-solid partitioning thus explaining the decrease in absorbance at higher temperature.

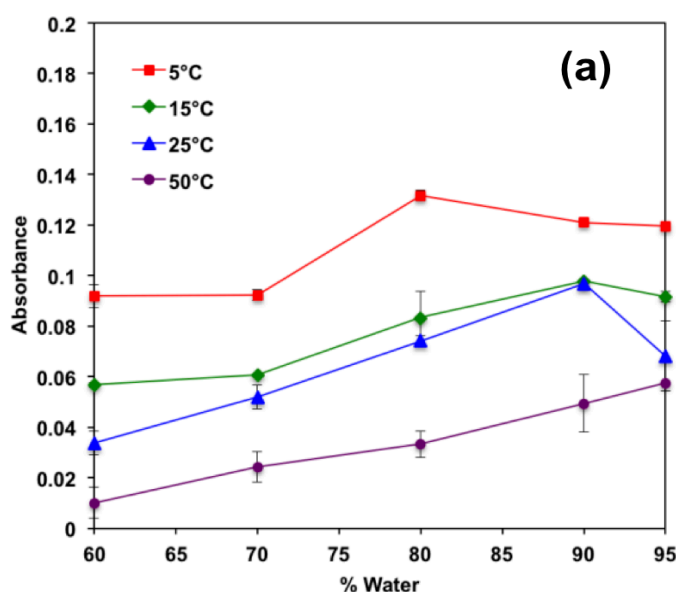


Figure 3.7 The absorbance at 440 nm of Cur PEM films as a function of loading temperature and water:solvent fraction for (a) methanol (b) ethanol and (c) isopropanol.

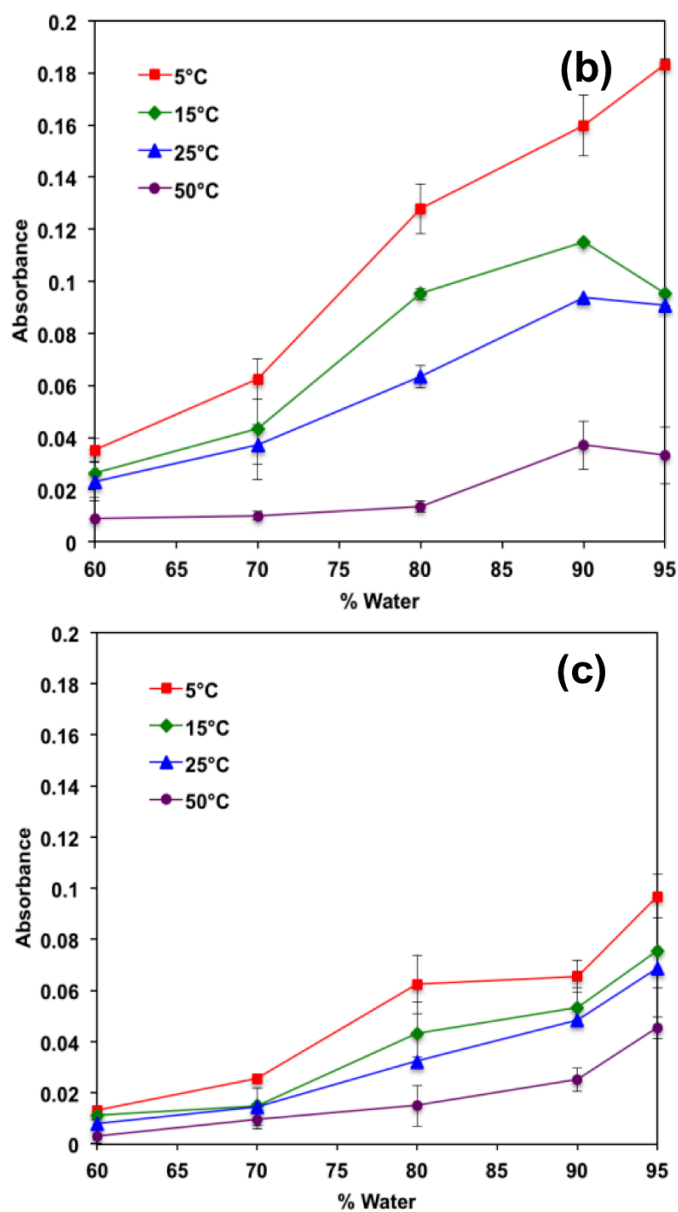


Figure 3.7 (Cont.) The absorbance at 440 nm of Cur PEM films as a function of loading temperature and water:solvent fraction for (a) methanol (b) ethanol and (c) isopropanol.

Although, the using of the water:methanol as a loading solvent exhibits the highest amount of Cur loaded into the film but methanol is toxic for humans, therefore, we prefer using water:ethanol as a loading solvent to prepare the Cur loaded PEM. The temperature plays an important role for the behaviour of Cur

in ethanol because of the high solvent polarity. The loading of Cur in the 90% volume fraction of water in ethanol at low temperature present the highest absorbance as show in Figure 3.8. The loading was found to saturated in each condition after 3 h and the kinetic of the loading depict a sharp growth at low temperature. When the temperature of loading solvent was increased, the absorbance intensity of Cur in PEM film was decreased because the Cur solubility was enhanced in each solvent. High solvent temperature can cause the breakdown of the intramolecular H-bonding in Cur molecules which depict the polar property and then formed intermolecular bonding with solvent resulting in the dispersion of Cur in the loading solvent (Barik, 2013). It can be seen that the amount of Cur loaded in the PEM thin film can be enhanced by loading at low temperature.

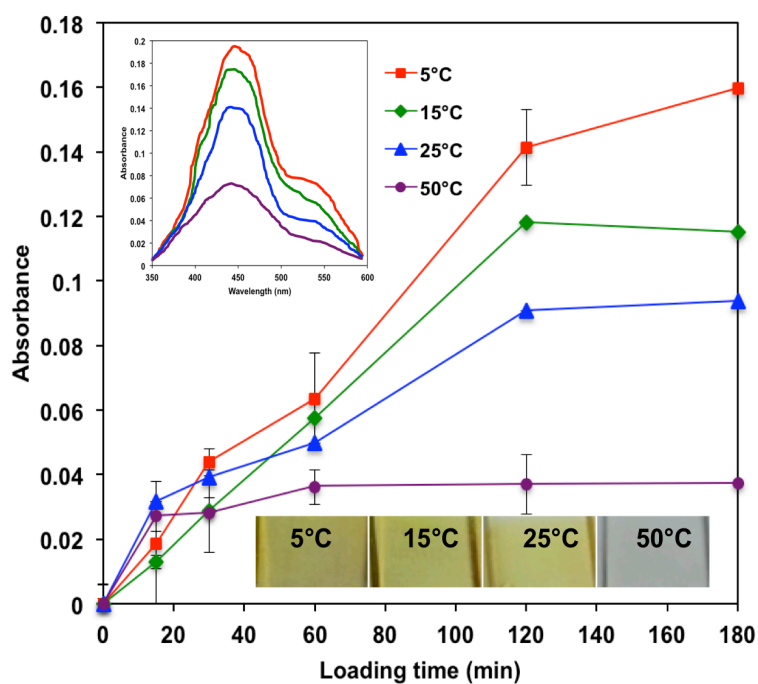


Figure 3.8 Kinetic property and absorbance spectra with images of Cur-loaded PEM thin films using 90:10 water:ethanol after 3 h.

3.3.2.3 Effect of Cur Loading on the Thickness of PEM Thin Films

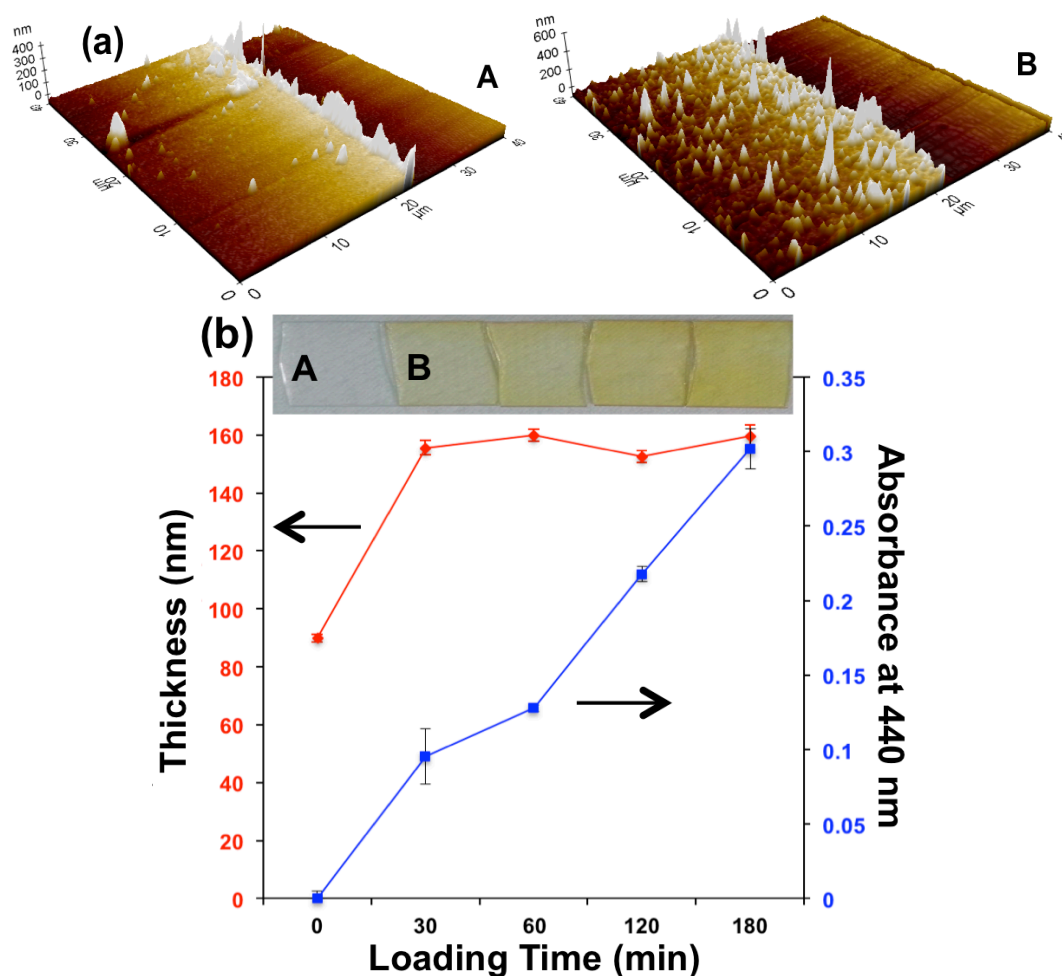


Figure 3.9 (a) AFM images and (b) the thickness and the absorbance as a function of loading time of 13-layer PEM film on glass slide before **A** and after **B** loading.

Atomic force microscopy (AFM) in contact mode was used to measure the thickness of PEM film by making a scratch on the film with a sharp needle and measuring the step height. The alternative 13-layer PEM film was fabricated by 10 mM PDADMAC and PSS through LbL technique on glass slide and then loading with Cur using 90:10 water:ethanol at room temperature. The AFM images of film before and after loaded with Cur into PEM are shown in Figure 3.9(a). The thickness of film was increased from 90 nm to 155.67 nm after loading with Cur for 30 min and remain constant after that as Figure 3.9(b). It is apparent

from that the PEM film was swelled with the solvent and then Cur diffused into the bulk of the PEM film through the mixing zone immediately after immersing the film in Cur solution, which can confirm by the yellow color appear on the film after loading. Likewise, the UV-Vis absorbance spectra of Cur loading were shown linearly increased as a function of time while the thickness is constant.

3.3.2.4 Temperature controlled release of Cur from PEM Thin Films

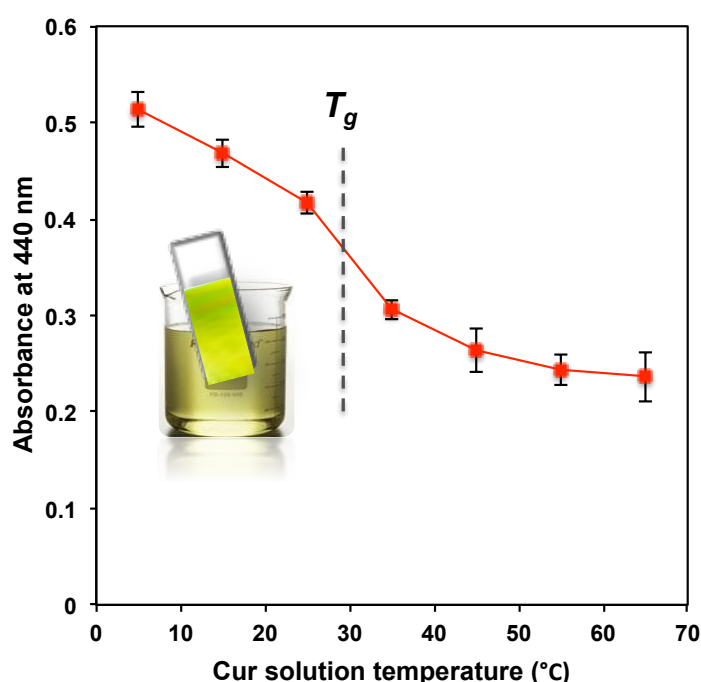


Figure 3.10 Absorbance of Cur loading into PEM in 5% w/v Cur in 90:10 water:ethanol solvent.

In order to elucidate the possible effect of the glass transition effect, the loading of Cur in a 90:10% water:ethanol mixture was studied as function of temperature. From the final data plotted in Figure 3.10, it is clear that an increase in temperature leads to a decrease in Cur loading in the PEM. Cur mobility can be taken into consideration since at high temperature the vibrational energy of the molecules increase leading to an increase in conformation vibration, which tends to decrease the solvent interface penalty and increase the solubility of hydrophobic molecules at high temperatures. But interestingly, it can also be observed a T_g like curve with a sharp decrease in

adsorption around the previously reported T_g (25 – 30°C). It can be hypothesized that as stated above, the crossing of the T_g lead to a swelling of the membrane as suggested in literature for PEM having a cationic top layers.

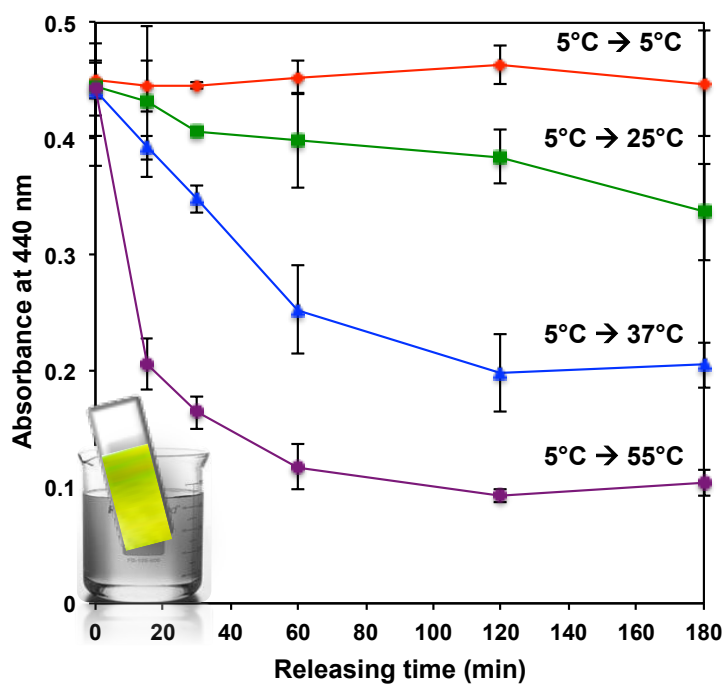


Figure 3.11 Absorbance of Cur releasing from PEM to water at various temperatures.

Because the loading of Cur appears to be temperature dependent, it was hypothesized that the release might also be thermo-activated. To test this hypothesis, PEM films were loaded with Cur from solvent mixture of 90:10% water:ethanol and soaked in water solution of various temperatures (5, 25, 37 and 55°C). It can be seen from the results in Figure 3.11 that the release of Cur from the PEM patch depends strongly on the temperature of solution. When the film was exposed to a 5°C solution, the absorbance of the film remain constant for more than 3 h. Cur cannot be released from the film because it corresponds to the thermodynamic equilibrium of the system from the loading condition. On the other hand, when the patch is exposed to a higher temperature (25, 37 and 55°C), Cur is released as a result of increased diffusion kinetic with temperature. Interestingly it

can be seen that in the case of the 37°C release solution which correspond to the body temperature, Cur can be release spontaneously. Within 1 h, 60% of the Cur dose can be release, which is interesting for transdermal drug delivery triggered by temperature.

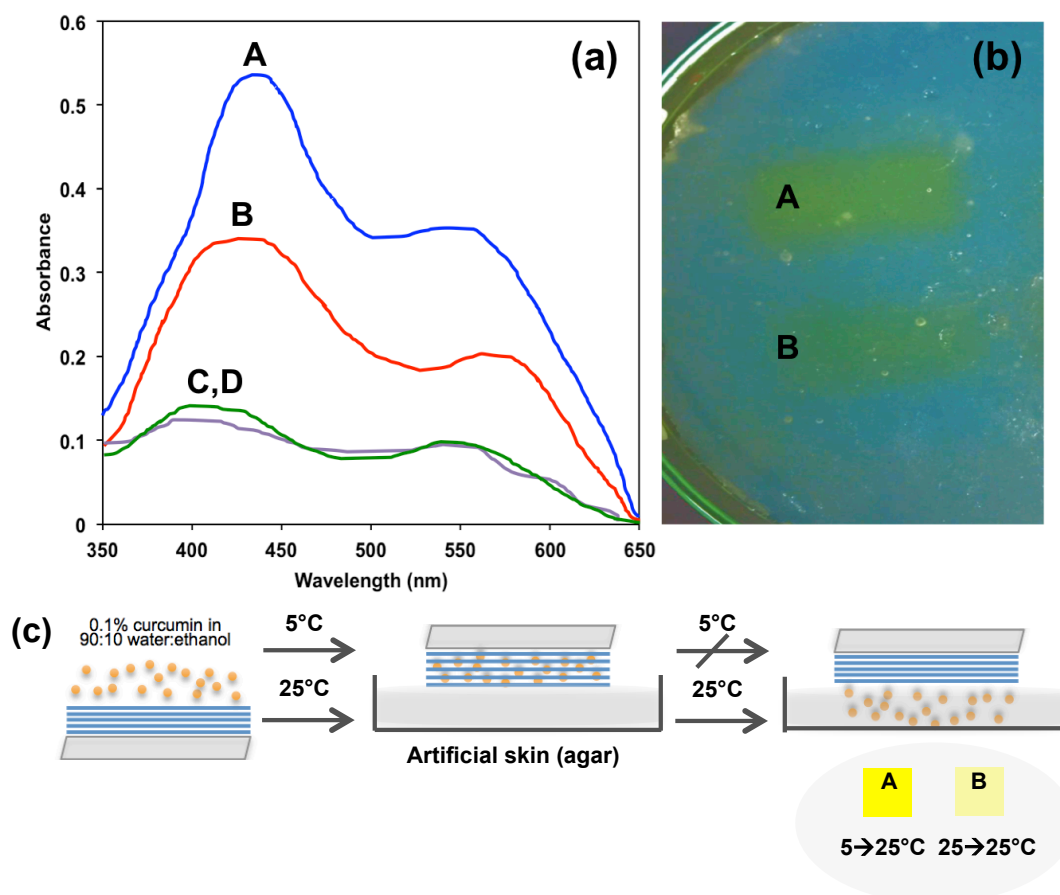


Figure 3.12 (a) Absorbance spectra, (b) photographic images under UV light and (c) schematic representation of Cur released on 7%w/v agar with different loading and release temperature, **A** loaded at 5°C and released at 25°C, **B** loaded at 25°C and released at 25°C, **C** and **D** loaded at 5 and 25°C then released at 5°C.

For testing a practical application of Cur loaded in PEM thin films as a transdermal patch, the loading and release of Cur from the films tuning by temperature were observed by UV-Vis spectrophotometer in reflection mode. The films fabricated from LbL approach of 10 mM PDADMAC/PSS were loaded with

0.1%w/v Cur using 90:10 water:ethanol as a solvent at 5°C and 25°C. Then, the film was attached to 7%w/v agar, represented an artificial skin, and the yellow color appeared on agar after 3 h indicated that the Cur can release from PEM onto the skin at room temperature (25°C). The absorbance spectra of Cur after released on the artificial skin are shown in Figure 3.12(a). The strong absorbance at λ_{\max} about 430-450 nm represent the amount of Cur released on the skin. It was confirmed from absorbance spectrum **A** that the Cur film loaded at low temperature (5°C) can release a high amount of Cur at room temperature (25°C) and was depicted the strongest yellow color under UV light (Figure 3.12(b)**A**). Nevertheless, the release of Cur at 5°C is very low and cannot observe with neglect eyes (**C** and **D**), which relates to the thermodynamic equilibrium of the system between the loading and release condition (Figure 3.12(c))

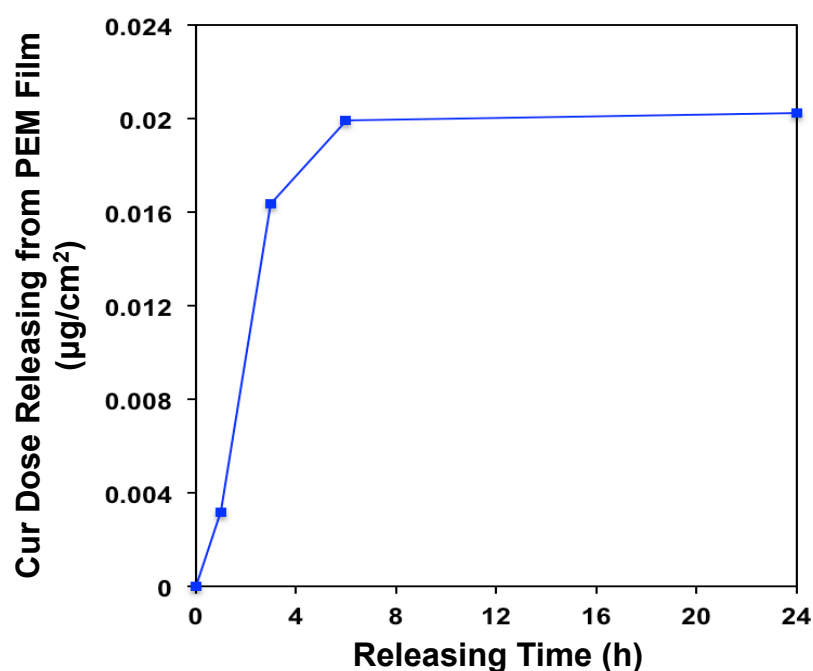


Figure 3.13 The quantitation of Cur released from PEM film on agar as a function of releasing time.

The kinetic release of Cur on the artificial skin was studied by using the PEM film loaded with Cur at 5°C in 90:10 water:ethanol solvent, which

achieves the highest amount of Cur loaded in the film, to release on agar at 25°C. The absorbance of Cur on agar was measured by UV-Vis spectrophotometer in reflection mode as a function of time (Figure 3.13). The results show that the releasing property of Cur could be enhanced by applied on the skin for a longer time and it can be used as a facial mask that did not causes the skin irritation after application for 6 h (Nawanopparatsakul, 2005). Conclusively, the results denoted that the Cur loaded in thin films based on PEM can be used as a patch for skin healing with non-toxic and can be applied on any substrate materials. Since the purpose of this work is to utilize the PEM film loaded with Cur for a transdermal patch, it is important to quantify the amount of Cur released out from the film. Although, the extinction coefficient (ϵ) value for Cur is presented in databases, it depends on the solvent and surrounding matrix. In 2010, Kittitheeranun *et al.* have reported the ϵ of Cur diffused in PDADMAC/PSS multilayer film (ϵ_{pem}), which is calculated from the absorbance measurement of Cur loaded into the film according to Beer's law. The final ϵ_{pem} value of Cur in PEM with a thickness in nanoscale range (157 nm) is 64,000 M⁻¹cm⁻¹. The absorbance of Cur film loaded at 5°C converted into the amount of Cur release on the artificial skin depict maximum Cur dose of 0.020 µg/cm². Moreover, the loading of Cur with the amount of 0.201 µg/cm² can be released to the half of original value, 54% releasing, after 6 h. It can also be seen that there is a rising of Cur dose released when loading Cur at low temperature. Nevertheless, the temperature is not the major determinant in the release of Cur on the surface of artificial skin. The PEM films could be a good potential matrix for loading with a hydrophobic molecule for drug delivery systems, which can control the loading and release of those molecules by adjusting the loading solvent composition and especially altering the temperature.

3.3.2.5 Improvement the Loading and Release of Cur by increasing thickness of PEM Thin Films

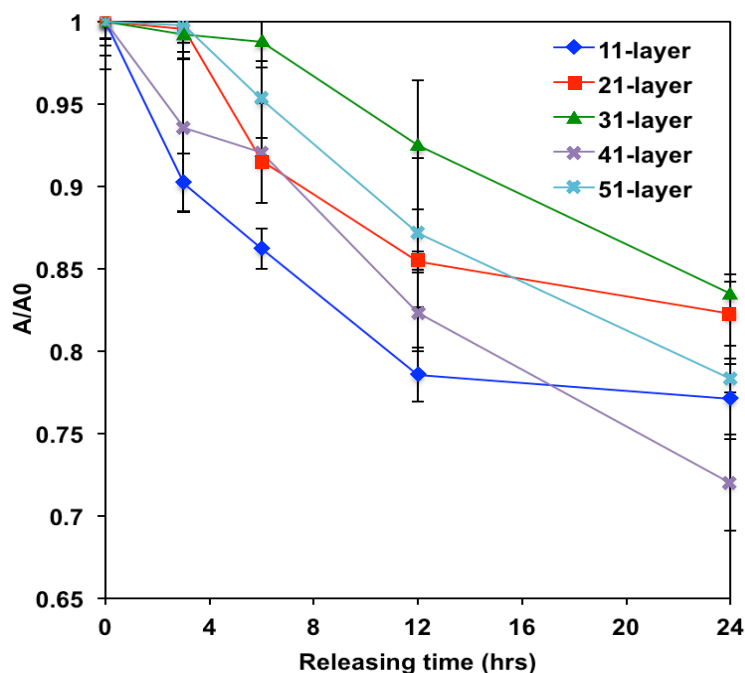


Figure 3.14 The absorbance of Cur loaded PEM when attached on agar as a function of time and a required number of PEM layer.

The films were prepared from 0.1 M PDADMAC and PSS with the different number of layers and then loading with 0.1% w/v Cur in 90:10 water:ethanol at 5°C overnight for accomplishing the maximum amount of Cur loaded into PEM films. The films were attached on agar as the artificial skin to study the releasing of Cur at 37°C and measured the kinetic property of the releasing of Cur by UV-Vis spectroscopy. Figure 3.14 presented that Cur are diffused out from the film to the skin owing to the increasing of releasing time and trend to saturate after 12 h using 11 and 21-layer of PEM while the 31, 41 and 51-layer have still decreased in absorbance indicated that Cur is continuously releasing to 24 h.

Although, the loading of Cur can be enhanced by increase the number of deposited layers, which is infers that Cur diffuses in the bulk of the films depict in increasing of absorbance and the strong yellow color of the films as shown

in Figure 3.15, but the releasing of Cur on agar surface is occur only at the outer layer of PEM film.

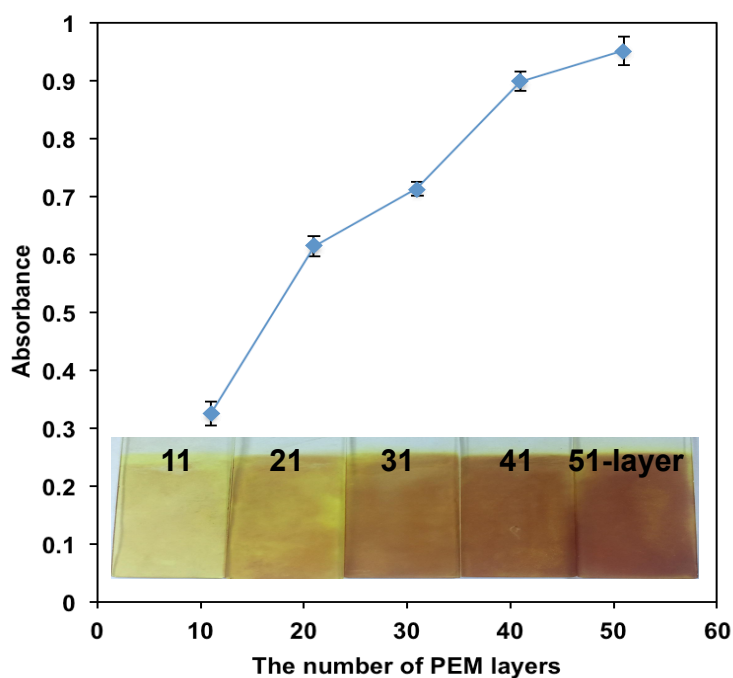


Figure 3.15 The absorbance of Cur loaded PEM when increased the deposition layer of PDADMAC/PSS.

3.3.3 Improved pH Sensing of Cur Loaded PEMs Thin Films

The effect of the top layer electrostatic charge on the Cur sensing properties was investigated. The fabrication of Cur loaded PEM film for pH solution testing shown in Figure 3.16. Preliminary work suggested that the cationic or anionic top layers could affect the pH at which the color change occurs and therefore allow better detection of amine compounds. It was hypothesized that the charge of the top layer PEs, PDADMAC or PSS, would modify the pH response of Cur. These results suggest that the films with PDADMAC on top and loaded with Cur could provide early detection of the decaying seafood and could be of interest in the development of food sensors. PEM thin films were loaded with Cur and tested for their pH sensing properties.

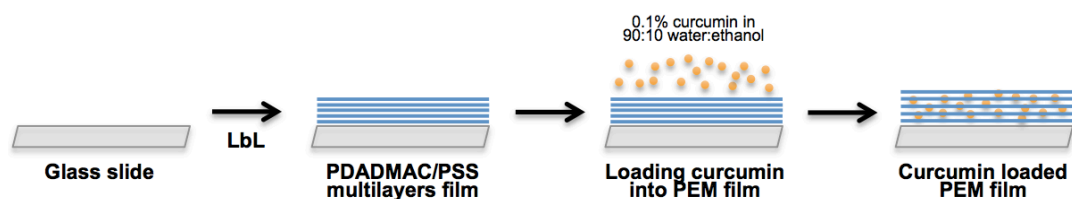


Figure 3.16 Schematic representation of Cur loaded PEM thin film.

The films were fabricated using the LbL deposition of PDADMAC and PSS as shown in Figure 3.17. Cur, a natural essential oil used in food, has the property to change color from yellow (in acid) to orange-red when exposed to pH values above 8. UV-Vis spectroscopy was used to monitor the loading of Cur in the thin films as a function of the number of layers and pH. The effect of the charge of the top layer on the sensing properties was studied and this film could be of interest in the development of food sensors or pH indicator.

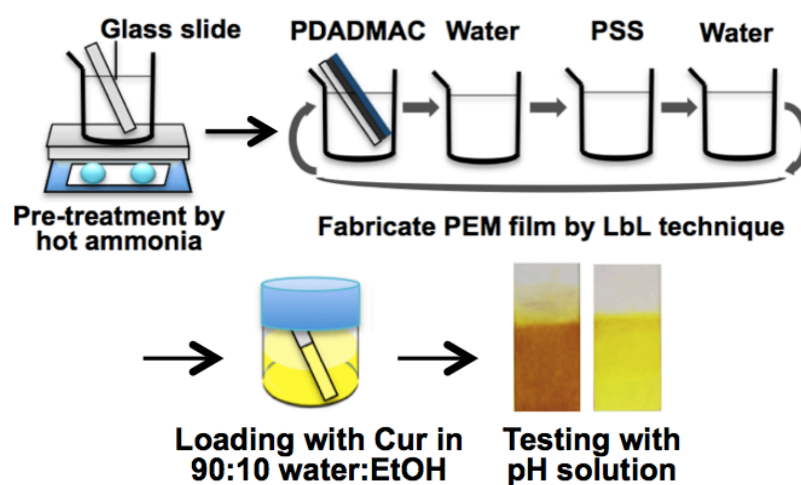


Figure 3.17 Fabrication of Cur loaded PEM thin films for pH solution testing.

Using the LbL technique, nano-thin films can be prepared with tunable bulk and surface properties. This suggests that the physico-chemical, optical and electrical properties of the film can be adjusted both surface and the bulk of film. In previous work, we have described a method to induce the loading of hydrophobic Cur in PEM thin films by tuning the solvent (water:ethanol) composition. It was

demonstrated that the Cur dose loaded in the PEM thin films could be increased with the film thickness suggesting that the drug diffused inside the film (Figure 3.15). The loading time was of about 2 h and the optimum solvent composition was 90:10 %v/v water:ethanol. In the previously published work, only even numbers of layers were used for the film growth (10, 20, 30 and 40 layers) and all the films appeared yellow. In this work odd and even numbers of layers were used and the effect of the top layer electrostatic charge was investigated.

PEM thin films composed of increasing number of layers from 1 to 17 were dipped in 0.1% Cur solution composed of water:ethanol 90:10 %v/v. The loading of Cur as function of the number of layers was studied using UV-VIS spectroscopy. As expected, it can be seen in Figure 3.18(a) that the final absorbance at 440 nm increased with the number of deposited layers due to increased Cur loading with the film. The absorbance at 540 nm plotted in Figure 3.18(b) can be seen to increase for odd layers and decrease for even layers. This rather surprising observation is correlated with the color of the film that appeared either yellow or orange depending on the type of PEs on top of film as seen on the sample picture. When using an even number of layers, which anionic PSS on top, the films appeared yellow while with cationic PDADMAC on top the film appeared orange. The orange and the yellow films have the same peak at 440 nm but in the case of the PDADMAC on top an extra peak at 540 which gives the orange color to the films. The change in color of the Cur films with cationic PDADMAC on top is due to the formation of a complex between cationic PDADMAC and anionic Cur inducing a lowering of the energy gap between the π - π^* transition. This bathochromic (red) shift is observed when Cur is dispersed in more polar solvent or in case of the formation of a metal complex.

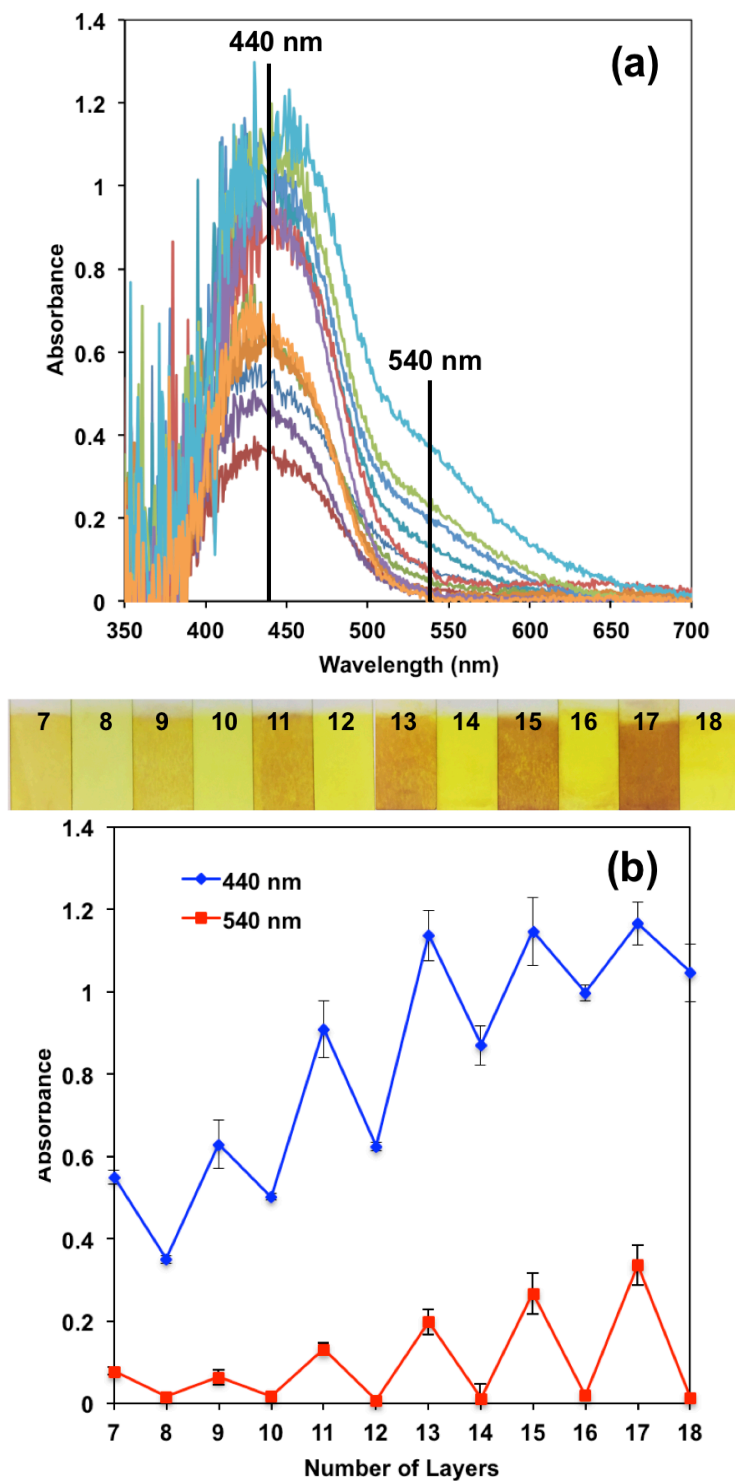


Figure 3.18 (a) UV-Vis spectra and (b) absorbance of Cur loaded in PDADMAC/PSS thin film with different layers.

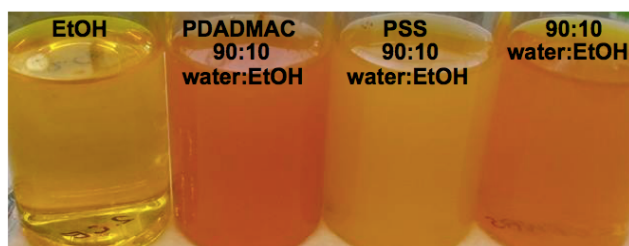


Figure 3.19 Cur (0.1 %w/v) mixed with various solutions.

To confirm that the color of Cur was a result of the interaction with the charge of the cationic PEs, a small amount of Cur was mixed with PDADMAC or PSS solutions in separated beakers. As seen on the Figure 3.19, a turbid orange solution is obtained when Cur is mixed with PDADMAC in contrast with the yellow solution obtained when mixed with PSS. This confirms that PDADMAC interact with Cur through electrostatic interaction and induce the color change of the film.

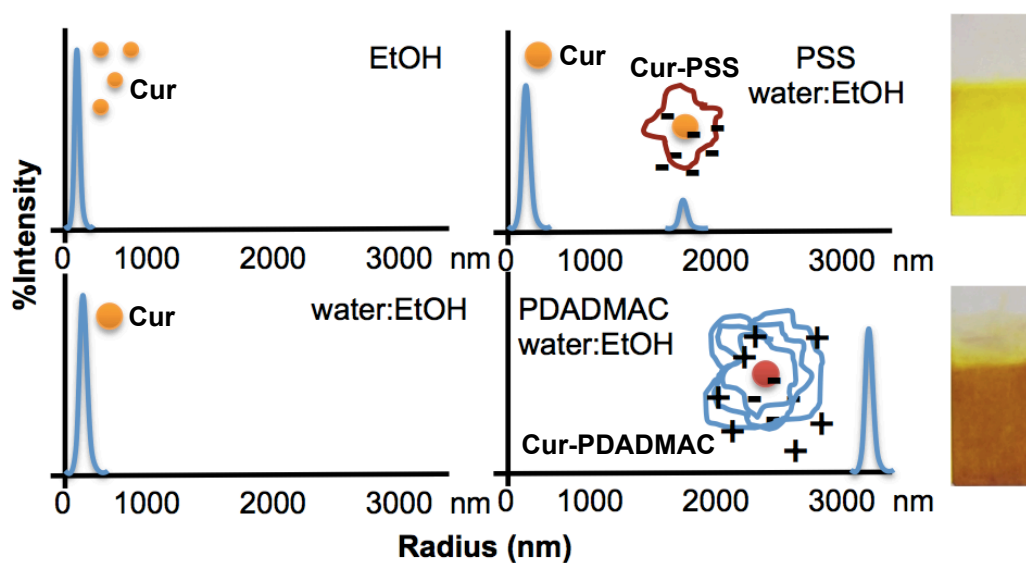
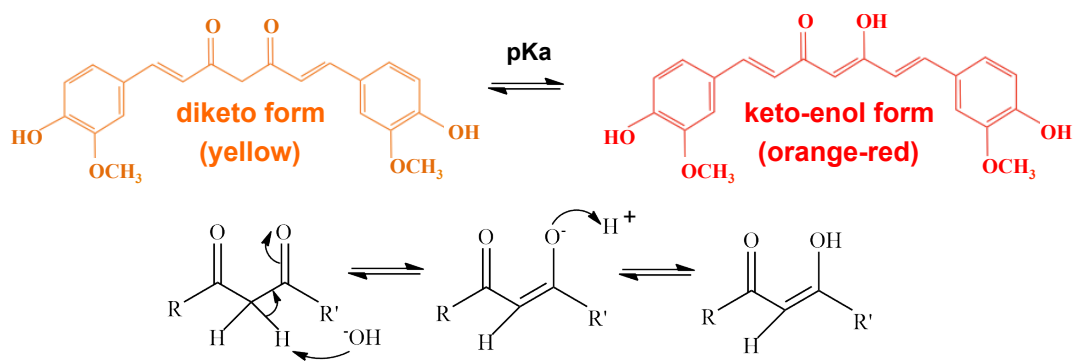


Figure 3.20 Radius of Cur particles in different solution observed by DLS measurement.

Table 3.1 DLS measurement of 1 mg/ml Cur in different solution

Cur in solution	Radius (nm)	% Intensity	% Mass
ethanol	0.701	0.6	99.4
90:10 water:ethanol	166.536	62.3	80.7
PDADMAC in 90:10 water:ethanol	3318.010	85.6	98.6
PSS in 90:10 water:ethanol	165.961	87.0	48.1
	1844.790	13.0	51.9

To study the behavior of Cur in surrounding solvents, dynamic light scattering (DLS) was used to measure the particle size of Cur in different solutions (Figure 3.20 and Table 3.1). Cur powder with the concentration of 0.1 %w/v was dissolved in ethanol, 90:10 water:ethanol, PDADMAC in 90:10 water:ethanol and PSS in 90:10 water:ethanol then sonicated for 30 min before characterized. It can be seen from Figure 3.19 that the solution of Cur in ethanol is clear but in the presence of water (90:10 water:ethanol) solution become turbid because the solubility of Cur was reduced which can confirm by the increase in particle size due to the aggregation of Cur. There was observed the aggregation of Cur in PSS solution due to the possible π - π interactions between the Cur and PSS aromatic structures (Kittitheeranun, 2010). Additionally, the negatively charged Cur was more stabilized by positively charged PDADMAC by electrostatic interaction resulting in the larger particles size.

**Figure 3.21** Keto-enol tautomerization of Cur.

Cur has a characteristic pH dependent spectral absorbance in the visible range and has been used in many applications for its pH sensing of volatile amine compound. As mentioned before, Cur change color from yellow to orange-red above pH 8 as the structure change of diketo to keto – enol form (Figure 3.21). Cur shift toward to diketo form in equilibrium state and when added to an alkaline solution, the shift of a hydrogen atom triggers the Cur change to keto – enol form. Based on our LbL films assembly, two kinds of films can be prepared with either PDADMAC or PSS as a top layer and produce films with different initial color as seen on the picture in Figure 3.22. The work reported hereafter is an investigation of the effect of the top layer on the colorimetric sensing of Cur. It was speculated that since the films had different initial colors, they might also have different response to increasing pH and therefore different sensing properties. More specifically, since the films with PDADMAC on top are already slightly orange, the color change could occur at lower pH and provide better volatile amine detection.

In Figure 3.22(a)-(b) show the UV-Vis spectra of PEM thin films composed of either 11 (PDADMAC on top) or 12 layers (PSS on top) loaded with Cur immersed in different pH. The pH was varied from 6 to 10 to simulate an increase in basicity due to the presence of volatile amine compound in spoiled food. As expected, the films with PDADMAC on top displayed an increase in absorbance at 540 nm, which corresponds to increasing orange color compared to the initial films. On the other hand, the spectra of the films with PSS on top can be seen to remain yellow until pH 9 and slightly orange at pH 10. The sensing properties of the film can be quantified by plotting the changes in absorbance at 540 nm as a function of pH. From the plot in Figure 3.22(c), it can be seen that when PSS is the top layer, this color shift happens for pH values above 9 whereas it starts occurring at pH 7 when PDADMAC is the top layer. The lowering of the apparent pK_a of the Cur is due to the polarization of the carbonyl groups by cationic PDADMAC making the Cur more acidic. This decrease in pK_a of acid groups such as carboxylic or phosphate upon complexation with a cationic species is commonly observed in other systems such as protein or DNA. Upon complexation the weak acids appear more acidic with a lower pK_a (Rmaile, 2002). Due to its lower pK_a , Cur complexed with PDADMAC is an interesting candidate to design optical sensors to be used in food

packaging stickers to evaluate food freshness because the lower pK_a can provide an early detection of the rising concentration in volatile amines.

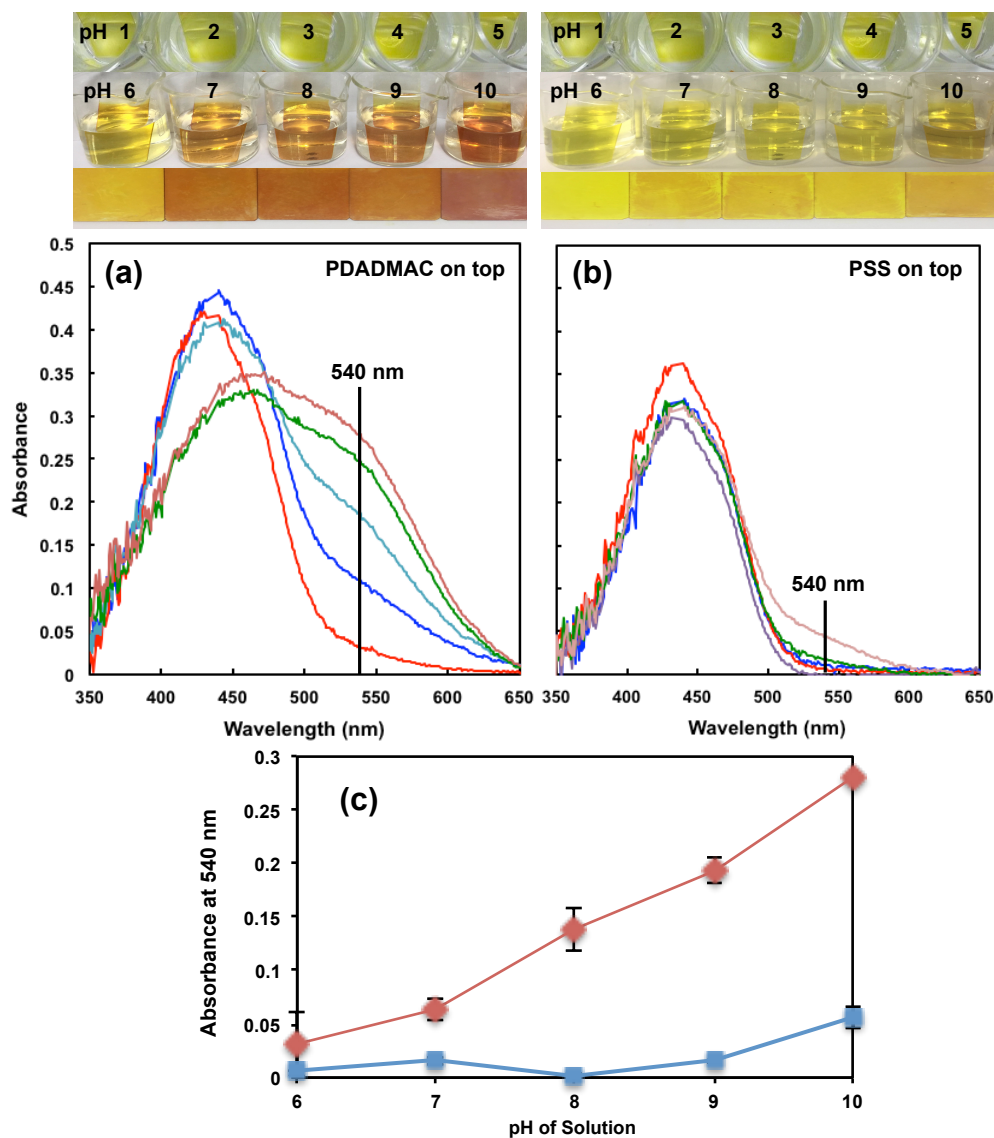


Figure 3.22 The UV spectra of Cur loaded on PEM with PDADMAC on top (a) and PSS on top (a) film dipped at different phosphate buffer pH. The absorbance at 540 nm of Cur loaded PEM film with different polymer on top of layers (c).

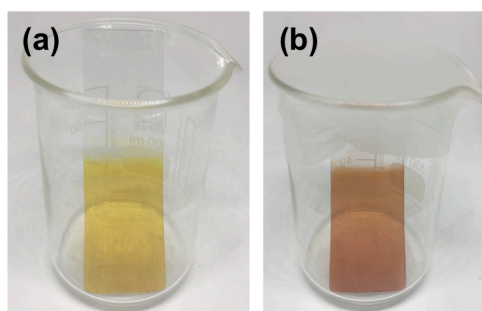


Figure 3.23 Cur loaded 13-layer PEM exposed in air (a) and ammonia vapor (b).

As shown in Figure 3.23, the yellow film of Cur loaded 13-layer PDADMAC/PSS multilayer film appears reddish brown when exposed in strong ammonia vapor and it can be reversible when soaked the film in acid solution. The presence of volatile amine compound releasing from spoiled food is a further interesting study for PEM loaded Cur films as pH detector.

3.4 Conclusion

In the first part, the solvent loading and temperature release of Cur has been investigated. It was demonstrated that the loading of Cur is strongly dependent on the solvent composition and the loading temperature with water:ethanol being a good solvent mixture. It was found that at the lower temperature lead to an increase in the total amount of Cur that could be loaded and in particulate, at 5°C the loading was maximum. Interestingly, the Cur could be released by simply exposing the film to warm water. These results are of interest for the development of temperature triggered drug delivery patch. A second part, PEM thin films with either PDADMAC or PSS as top layers were loaded with Cur to produce films for pH sensors. The sensing properties of the Cur loaded PEM thin films could be tuned due to electrostatic interactions between Cur and cationic PDADMAC. The PDADMAC on top films had a color change occurring at pH 7 but only at pH 9 when PSS was on top. The interactions induce a color change of the film at lower pH, which is critical for the early detection of the volatile amine compound in the spoiled food package.

3.5 Acknowledgements

This work has been financially supported by the Petroleum and Petrochemical College, Grant for International Research Integration: Chula-Research Scholar, Ratchadaphiseksompote Endowment Fund and the Center of Excellence on Petrochemical and Materials Technology, the Integration Project: Innovations for the Improvement of Food Safety and Food Quality for New World Economy, Government Research Budget, Chulalongkorn University, Thailand, Graduate Institute of Science and Technology (TG-55-09-51-034D).

3.6 References

- Anjomshoa, S., Namazian, M., Noorbala, M. R. (2016) The effect of solvent on tautomerism, acidity and radical stability of curcumin and its derivatives based on thermodynamic quantities. *J. Solution Chem.*, 45, 1021–1030.
- Ariga, K., Yamauchi, Y., Rydzek, G., Ji, Q., Yonamine, Y. (2014) K.C.-W. Wu, J.P. Hill, Layer-by-layer nanoarchitectonics: invention, innovation, and evolution. *Chem. Lett.*, 43, 36–68.
- Decher, G., Hong, J. D., Schmitt, J. (1992) Buildup of ultrathin multilayer films by a self-assembly process: III. Consecutively alternating adsorption of anionic and cationic polyelectrolytes on charged surface. *Thin Solid Films*, 210 (211), 831–835.
- Decher, G., Schmitt, J. (1992) Fine-tuning of the film thickness of ultrathin of ultrathin multilayer films composed of consecutively alternating layers of anionic and cationic polyelectrolytes. *Prog. Colloid Polym. Sci.*, 89, 160–164.
- Decher, G. (1997) Fuzzy nanoassemblies: Toward layered polymeric multicomposites. *Science*, 277(5330), 1232-1237.
- Donath, E., Sukhorukov, G. B., Caruso, F., Davis, S. A., Möhwald, H. (1998) Novel hollow polymer shells by colloid-templated assembly of polyelectrolytes. *Angew. Chem. Int. Ed.*, 37 (16) , 2201–2205.

- Dubas, S. T., Schlenoff, J. B. (1999) Factors controlling the growth of polyelectrolyte multilayers. Macromolecules, 32, 8153–8160.
- Dubas, S. T., Schlenoff, J. B. (2001) Swelling and Smoothing of polyelectrolyte multilayers by salt. Langmuir, 17, 7725–7727.
- Gai, M., Frueh, J., Kudryavtseva, V. L., Yashchenok, A. M., Sukhorukov, G. B. (2017) Polylactic acid sealed polyelectrolyte multilayer microchambers for entrapment of salts and small hydrophilic molecules precipitates. Appl. Mater. Interfaces, 9, 16536–16545.
- Gentile, P., Carmagnola, I., Nardo, T., Chiono, V. (2015) Layer-by-layer assembly for biomedical applications in the last decade. Nanotechnology, 26, 422001.
- Goel, A., Kunnumakkara, A. B., Aggarwal, B. B. (2008) Curcumin as “curcumin”: From kitchen to clinic. Biochemical Pharmacology, 75, 787-809.
- Iler, R.K. (1966) Multilayers of colloidal particles. Journal of colloids and interface science, 21, 569-594.
- Jagannathan, R., Abraham, P. M., Poddar, P. (2012) Temperature-dependent spectroscopic evidences of curcumin in aqueous medium: a mechanistic study of its solubility and stability. Phys. Chem., 116, 14533–14540.
- Kittitheeranun, P., Sanchavanakit, N., Sajomsang, W., Dubas, S. T. (2010) Loading of curcumin in polyelectrolyte multilayers. Langmuir, 26(10), 6869-6873.
- Köhler, K., Shchukin, D. G., Möhwald, H., Sukhorukov, G. B. (2005) Thermal behavior of polyelectrolyte multilayer microcapsules. 1. The effect of odd and even layer number. J. Phys. Chem. B, 109, 18250–18259.
- Kong, X., Shi, W., Zhao, J., Wei, M., Duan, X. (2011) Layer-by-layer assembly of electroactive dye/inorganic matrix film and its application as sensor for ascorbic acid. Talanta, 85, 493-498.
- Podsiadlo P., Shim B. S., Kotov N. A. (2009) Polymer/clay and polymer/carbon nanotube hybrid organic-inorganic multilayered composites made by sequential layering of nanometer scale films. Coordination Chemistry Reviews, 253, 2835-2851.
- Priyadarsini, K. I. (2009) Photophysics, photochemistry and photobiology of curcumin: studies from organic solutions, bio-mimetics and living cells. J. Photochem. Photobiol. C, 10, 81–95.

- Richardson, J. J., Cui, J., Björnmalm, M., Braunger, J. A., Ejima, H., Caruso, F. (2016) Innovation in layer-by-layer assembly. Chem. Rev., 116, 14828–14867.
- Rmaile, H. H., Schlenoff, J. B. (2002) "Internal pK(a)'s" in polyelectrolyte multilayers: Coupling protons and salts. Langmuir, 18, 8263-8265.
- Saikaew, R., Bijaisoradat, O., Netcharoensirisuk, P., Dubas, S. T. (2016) Improved pH sensing of curcumin loaded polyelectrolyte multilayers thin films. Sens. Lett., 14 (6), 572–576.
- Tang, Z., Wang, Y., Podsiadlo, P., Kotov, N. A. (2006) Biomedical applications of layer-by-layer assembly: from biomimetics to tissue engineering. Adv. Mater., 18, 3203–3224.
- Wang, L., Wang, X., Xu, M., Chen, D., Sun, J. (2008) Layer-by-layer assembled microgel films with high loading capacity: reversible loading and release of dyes and nanoparticles. Langmuir, 24, 1902–1909.
- Zhang L., Xie A. J., Shen Y. H. (2010) Preparation of TiO₂ films by layer-by-layer assembly and their application in solar cell. Journal of Alloys and Compounds, 505, 579-583.

CHAPTER IV
CURCUMIN BLENDED NONSTOICHIOMETRIC
POLYELECTROLYTE COMPLEX MEMBRANES
FOR THE OPTICAL AMMONIA VAPOR SENSOR

As discussed in Chapter 3, nano-scale polyelectrolyte multilayers (PEMs) thin films loaded with curcumin (Cur) with either poly(diallyldimethylammonium chloride) (PDADMAC) or poly(sodium 4-styrene sulfonate) (PSS) on top provide different color change ability with different pH solution. The concept of an excess PDADMAC or PSS of micro-scale compressed polyelectrolyte complex (PEC) films blended with Cur was studied for the detection of pH solution and ammonia (NH_3) vapor as shown in Figure 4.1.

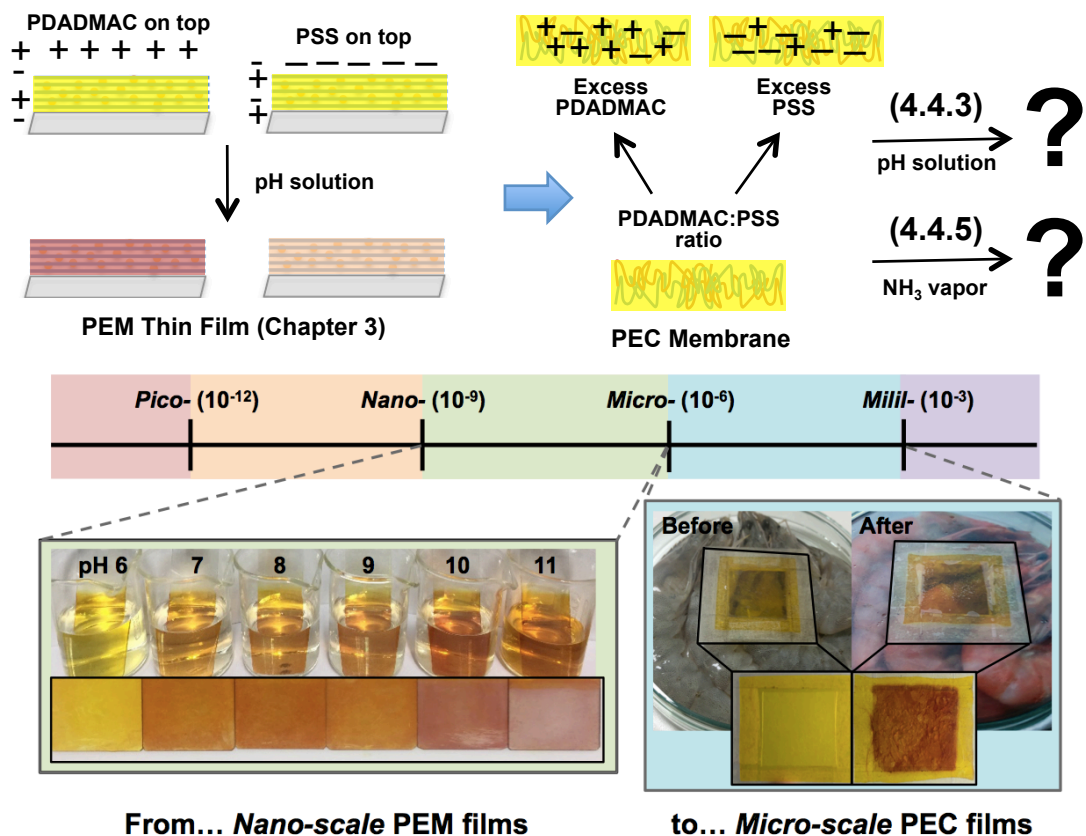


Figure 4.1 The concept of Cur loaded PEM film with different polymer charge on top and Cur blended PEC membrane with various polymer ratio.

4.1 Proposed Research

In previous works we have studied the loading and release of Cur on synthetic polyelectrolyte nano-scale films, which known as PEMs through the layer-by-layer (LbL) self-assembly technique, of cationic PDADMAC and anionic PSS (Kittitheeranun, 2010, Shin, 2014, Saikaew, 2018). It was found that Cur can be loaded into the bulk of film using 90:10% water:ethanol and we hypothesized that the increase in film thickness could be enhanced the sensing properties. Importantly, these PEM films providing an improvement of sensitivity of sensor when PDADMAC on top (Saikaew, 2016) were motivated an idea of preparing nonstoichiometric Cur-polyelectrolyte micro-scale films with excess PDADMAC composition. Although it is known that the response of NH₃ gas detector is sensitive to water vapor content of the environment, this work focused on the NH₃ detection of the different moisture-containing films when exposed to a certain amount of NH₃ vapor under constant RH at ambient temperature. The salt concentration and polymer mixing ratio are the important factors to control the properties of PECs composed of PDADMAC and PSS. The difference in charge density can cause swollen structures (Dautzenberg, 1997, Dautzenberg, 2002). The salt type and content also affect both the degree of hydration and the moisture content of PECs (Schlenoff, 2008). Therefore, the effect of NaCl concentration ([NaCl]) used during complexation-induced the moisture content of compressed stoi- and nonstoichiometric Cur-PEC films on the sensitivity of NH₃ vapor detection was monitored by UV-Vis spectrophotometer. Moreover, the influence of nonstoichiometric PEC with different polycation:polyanion compositions and various salt types on the color change ability was investigated. These Cur-PEC films could be studied for potential used in sensor application and food packaging technology.

4.2 Experimental

4.2.1 Chemicals and Materials

Poly(diallyldimethylammonium chloride) (PDADMAC, medium molecular weight, 20 wt.% in water, typical $M_w = 200,000-350,000$), Poly(sodium 4-

styrene sulfonate) (PSS, typical $M_w = 70,000$), 1,7-bis-(4-hydroxy-3-methoxyphenyl)-1,6-heptadiene-2,5-dione (curcumin, Cur), lithium chloride (LiCl), potassium carbonate (K_2CO_3), sodium chloride (NaCl), potassium chloride (KCl) and calcium chloride ($CaCl_2$) were purchased from Sigma-Aldrich. Potassium acetate (CH_3COOK) and potassium sulfate (K_2SO_4) were obtained from Alfa Aesar. Ethanol was purchased from Labscan asia and ammonia (NH_3) solution (25% for analysis) was from Merck. All solutions were prepared in double distilled (DI) water.

4.2.2 Fabrication of Cur-PEC Membranes

The Cur powder was dissolved in ethanol with a concentration of 0.1% w/v (1000 ppm). The volume of Cur in ethanol dispersed in the final mixture was calculated to 90:10% of water:ethanol (Cur solution). 5 %v/v of Cur solution was then mixed with an aqueous solution of PSS containing NaCl. PECs were prepared by solution mixing of Cur-PSS and 0.1 M PDADMAC solution with stirred for 30 min and adjusted an ionic strength by varying NaCl concentrations ($[NaCl]$). Blob complexes were compacted into dense precipitates by centrifugation at 8,000 rpm for 20 min. Cur-PEC films were fabricated using a Labtech press (model LP200) at 60°C under a pressure of 2,000 psi for 30 min with an aluminum spacer to control the thickness of about 100 μm .

4.2.3 Characterizations of Cur-PEC Membranes

All experiments were performed under room temperature (20°C) with 50% relative humidity (RH) and the results are reports from three independent tests. The NH_3 vapor for the sensing experiments was prepared from the dilution of a 25% NH_3 solution to the 40 ml of final concentrations ranging from 5, 10, 15, 25 to 50 ppm in glass petri dishes (80 ml) and left until NH_3 vapor was equilibrated for 30 min. PDADMAC/PSS films with various $[NaCl]$ during complexation: 0, 0.5, 1 and 1.5 M were cut in a rectangular shape of dimension 1x1 cm and then exposed to NH_3 vapors inside the petri dish containing 40 ml of various NH_3 concentration ($[NH_3]$) solutions. The color change was observed with a UV-Vis spectrophotometer (Red Tide USB650, OceanOptics). The influence of moisture content of PEC films prepared with 1.5 M NaCl was obtained by storing the films in humidity-control chamber (100 ml) containing 20 ml of saturated salt solutions: LiCl, CH_3COOK , K_2CO_3 , NaCl, and K_2SO_4 provide an equilibrium RH of 11, 23, 43, 75 and 97%,

respectively, at 20°C for 7 days before testing (Greenspan, 1977). The saturated salt solutions were used to create a certain RH in an ambient container. After the moisture content of the films was saturated, they were tested for NH₃ vapor sensitivity with a 15 ppm NH₃ solution. The PEC films with different polymer ratio of PDADMAC:PSS containing 1.5 M NaCl stored in 97% RH chamber were studied as stoichiometric (50/50) and nonstoichiometric (67/33 and 33/67 of mol% PDADMAC/PSS) ratio. To determine the moisture content, the dry films of dimension 2x2 cm were dried at 60°C for 48 h and then stored at a certain RH. The moisture content was calculated from their weights of the dried (W_d) and the moistened (W_m) films by this equation:

$$\text{Moisture content (\%)} = \frac{W_m - W_d}{W_d} \times 100 \quad (1)$$

The infrared spectra of stoi- and nonstoichiometric PEC and Cur-PEC films were characterized by Fourier Transform Infrared (FTIR) spectroscopy in Attenuated Total Reflectance (ATR) mode using Thermo Scientific Nicolet iS5 with iD7 detector from 4,000 to 600 cm⁻¹.

4.2.4 Sensing Properties of Cur-PEC film for spoiled shrimp

In order to investigate the potential used of Cur-PEC film for optical sensor application, the nonstoichiometric 2:1 PDADMAC/PSS film, stored in 97% RH chamber for 7 days before testing, was attached inside the petri dish contained 54 g of shrimp (bought from Tesco Lotus) and left at ambient temperature. After 2 days, the color change of film was measured by UV-Vis spectroscopy and the color parameters were observed from portable colorimeter, where L is lightness, a is redness-greenness and b is yellowness-blueness. Furthermore, the effect of salt types during fabrication, KCl, NaCl and CaCl₂ on the sensing ability of these nonstoichiometric Cur-PEC film was studied.

4.3 Results and Discussion

4.3.1 Hydrophilic Dyes Absorption on the Salt-Free Stoi- and Nonstoichiometric PEC Membranes

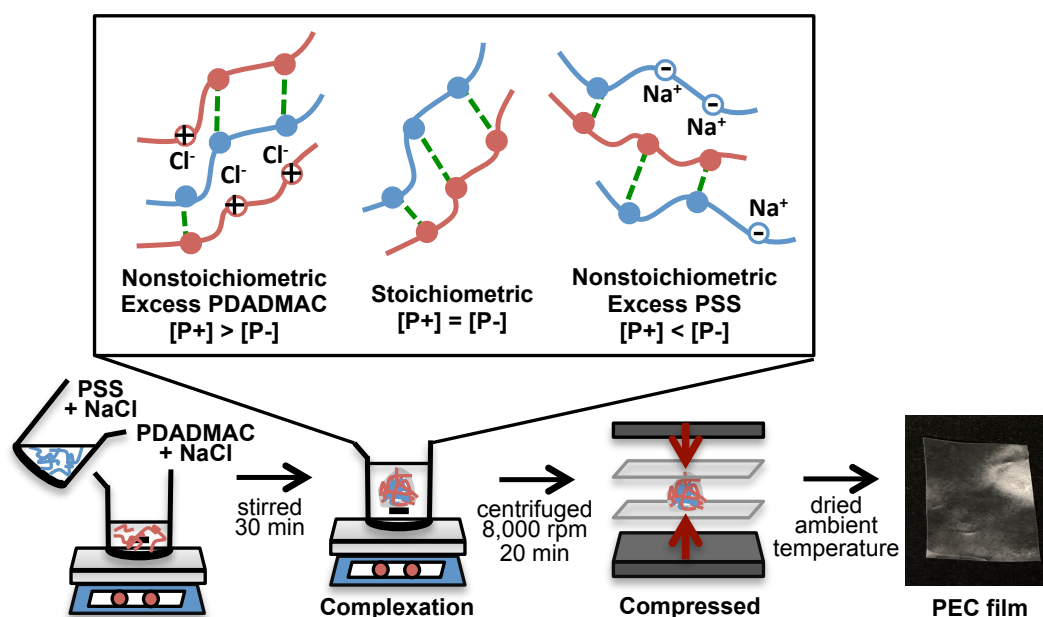


Figure 4.2 The fabrication of compressed stoichiometric and nonstoichiometric PEC membrane of PDADMAC/PSS.

The PEC membranes were fabricated by solution-mixing of aqueous PDADMAC and PSS using 1.5 M NaCl as a plasticizer followed by centrifugation and compression molding into about 100 micron sheets as shown in Figure 4.2. The PECs were prepared using various PDADMAC $[P^+]$:PSS $[P^-]$ molar ratio ranging from [2:1], [1:1] and [1:2] as PEC67/33, PEC50/50 and PEC33/67, respectively, which represent mol% ratio of PDADMAC/PSS.

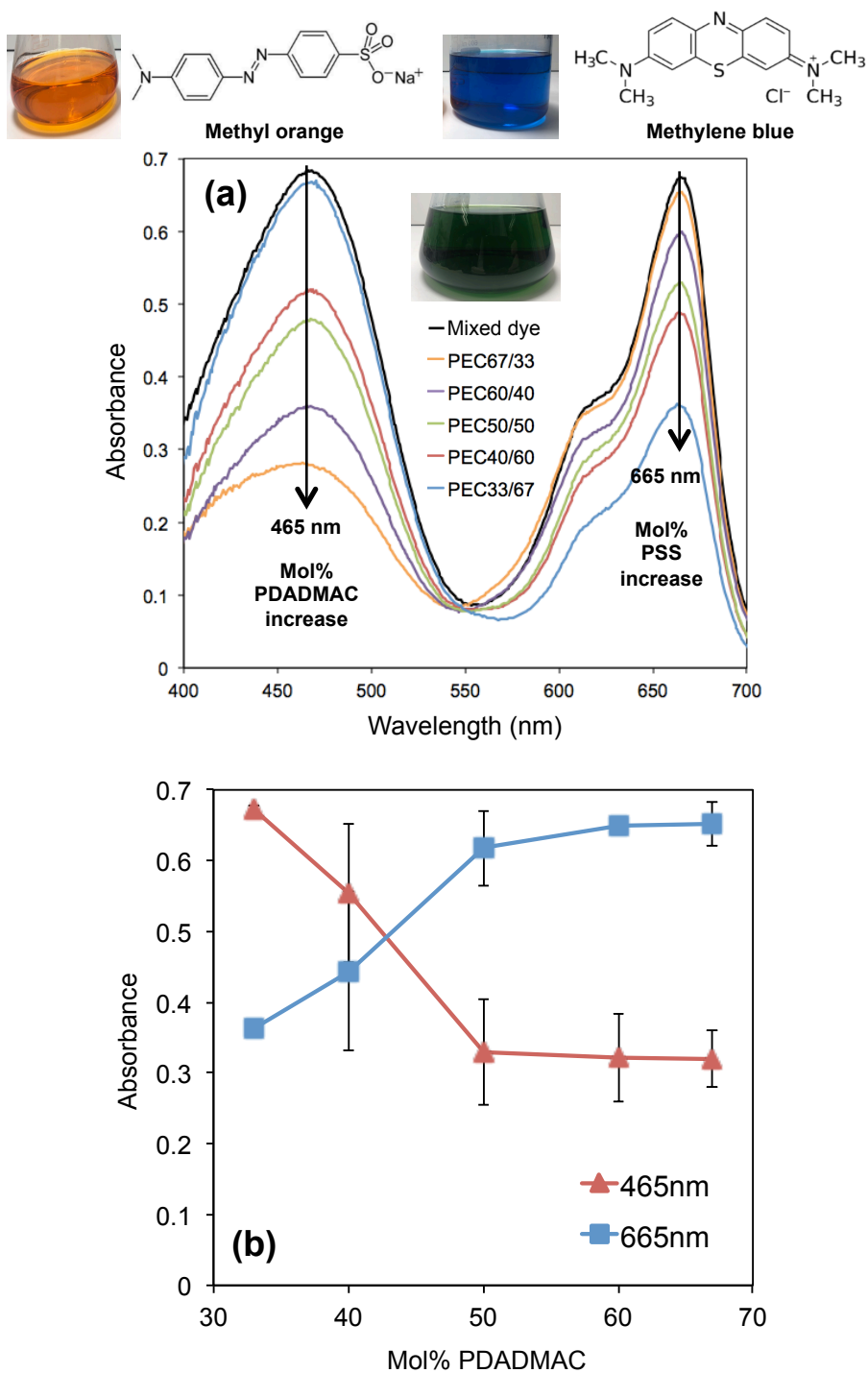


Figure 4.3 UV-Vis spectrum (a) and absorbance (b) of mixed dye solution of MO and MB after dye absorption for 150 min of salt-free PEC(1.5) with various mol% of PDADMAC/PSS.

In order to study the absorption ability of salt-free PEC films, the films with various polymer molar ratio prepared at 1.5 M NaCl were soaked in DI water for 24 h to remove any salt content. The films were cut with the dimension of 20x20 mm and then soaked in mixed dye solution of cationic 3,7-bis(dimethylamino)-phenothiazin-5-ium chloride (methylene blue, MB) and anionic sodium 4-[[4-(dimethylamino)phenyl]diazenyl]benzene-1-sulfonate (methyl orange, MO) dyes. To compare the change in the peak intensity at λ_{max} of both dyes, the concentration of dye was chosen here as 10 and 20 ppm for MB and MO, respectively, to obtain the intensity about 0.7. UV-Vis spectra of dye solutions before testing in Figure 4.3(a) depict two characteristic peaks at 465 and 665 nm, which represent the amount of MO and MB dye, respectively. After dye absorption for 150 min, the intensity peak at 465 nm of anion MO decreases with increasing cation PDADMAC content of the film while the intensity at 665 nm of cation MB drops with increasing anion PSS content (Figure 4.3(b)). It is evident that the film can absorb oppositely charged dye with an excess polymer content in the film.

The kinetic absorption of salt-free PEC films with mixed dye in Figure 4.4 suggest that the fully absorption ability of the films was achieved in both excess PDADMAC and PSS films with oppositely charged dyes within 8 h. This advantage of tuning the excess charge on PDADMAC/PSS films can be used for molecules absorption or removal (Shiratori, 2001). Interestingly, the stoichiometric PEC50/50 seem to displays an excess PDADMAC character that can absorb anionic MO dye with nearly 100% after 8 h and provides homogeneous yellow film (Figure 4.5). It is speculated that PDADMAC prefers to rearrange out to the surface of the film, during the complexation and the rinsing step, because of their hydrophilic nature.

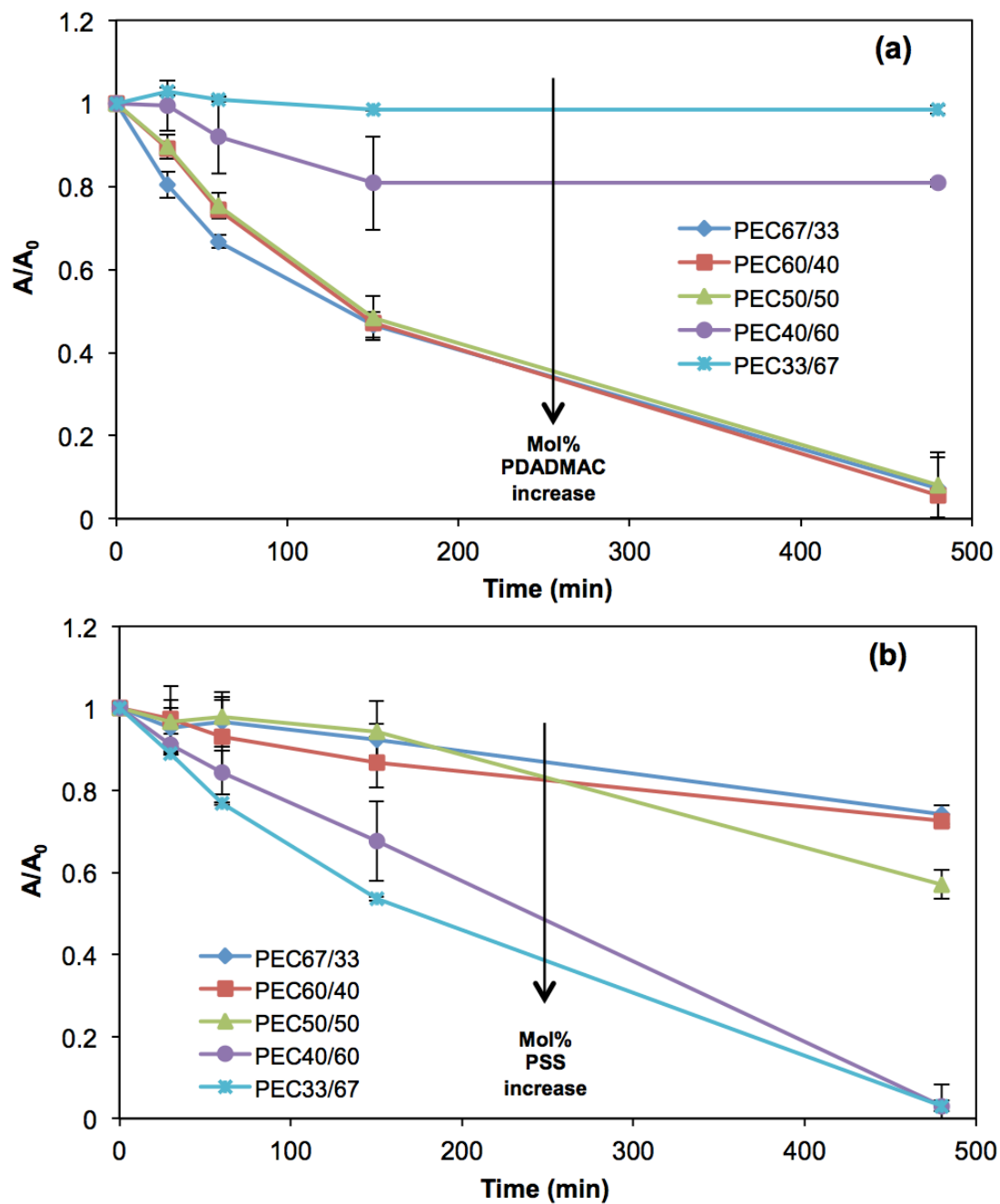


Figure 4.4 Kinetic properties of mixed dye absorption of salt-free PEC film various polymer molar ratio, (a) MO and (b) MB absorption (A is absorbance at 465 and 665 nm, respectively, and A_0 is absorbance of initial mixed dye).

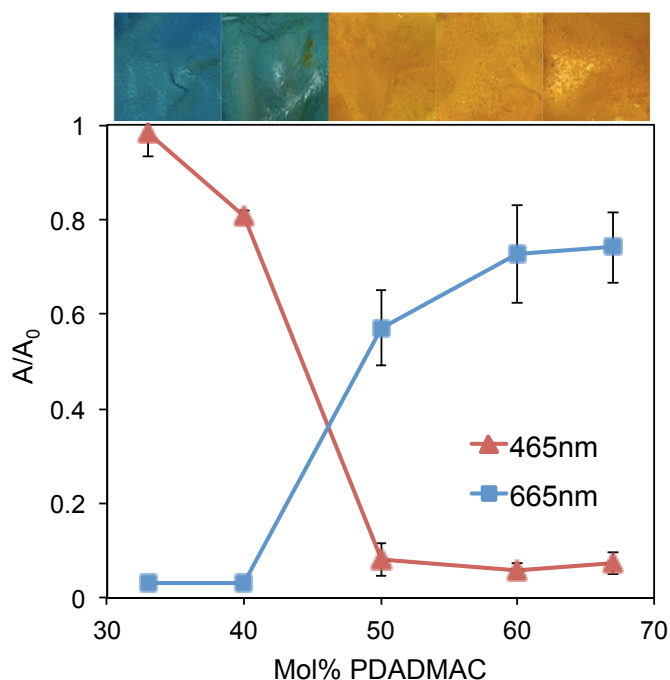


Figure 4.5 Photographic images and dye absorption of salt-free PEC film with various polymer molar ratio after 8 h.

4.3.2 Fabrication of Salt-Free Cur-PEC Films

Unlike thermoplastic polymers, PECs insoluble in water and hardly softened by heat lead to their limitation during processing. It is well known that the plasticizing effect of salt-water is a key for electrolyte complexes fabrication. The Cur-PEC precipitates were prepared under various ionic strength adjusted by NaCl in aqueous PDADMAC and PSS solutions. The fabrication of the Cur-PEC films was shown in Figure 4.6 and described in the Experimental Section. The samples prepared from electrolyte solution containing NaCl “X” M are indicated as PEC(X). After dried under room temperature, the smooth, flexible and transparent yellow Cur-PEC films were performed. The films were all tested for NH₃ vapor sensitivity under ambient condition.

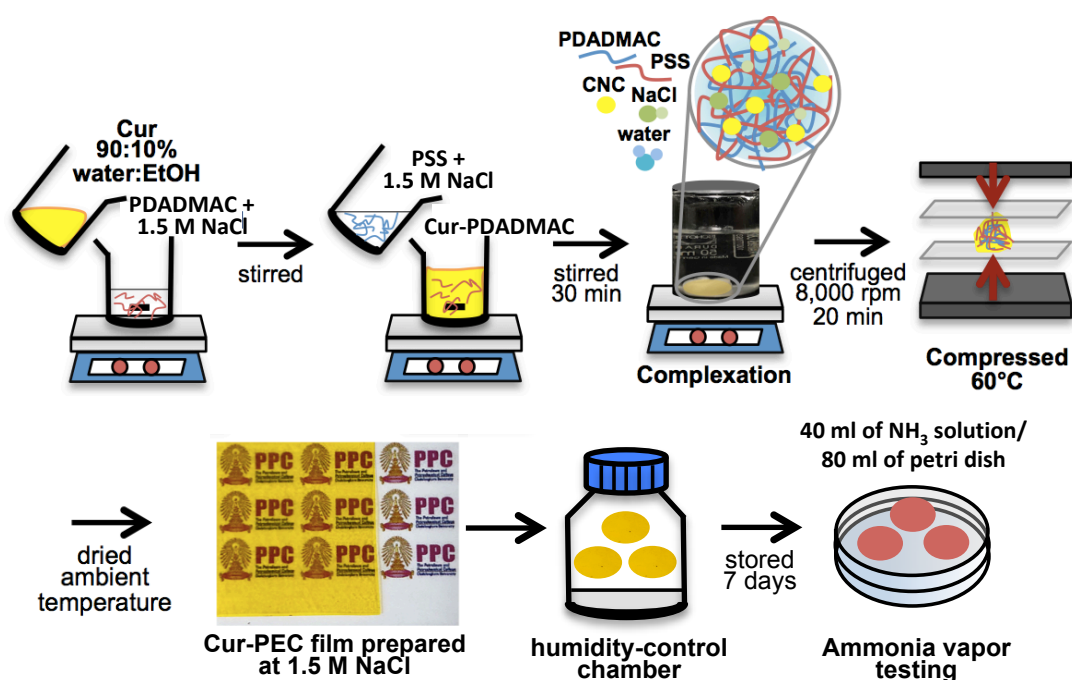


Figure 4.6 Schematic illustrates the fabrication of compressed Cur-PDADMAC/PSS film for NH₃ vapor sensing.

4.3.3 pH Solution Sensing of Salt-Free Cur-PEC Films

Cur-PEC film prepared with stoichiometric 1:1 ratio under 1.5 M NaCl were soaked in DI water overnight to eliminate the effect of salt releasing into solution. The films were immersed in various pH solutions ranging from 6 to 11 and monitored by UV-Vis spectroscopy. It was found from Figure 4.7(a) that the intensity peak at 470 nm, which correspond to the yellow appearance of Cur-PEC film, decrease with immersion time when the film was soaked in high pH solution (pH 11). In the same time, the peak at 535 nm was appeared due to the color change to orange-red. The absorbance at 535 nm of the films immersed in solution pH 6 - 11 was saturated within an hour and the peak intensity increase with increasing pH of solution (Figure 4.7(b)).

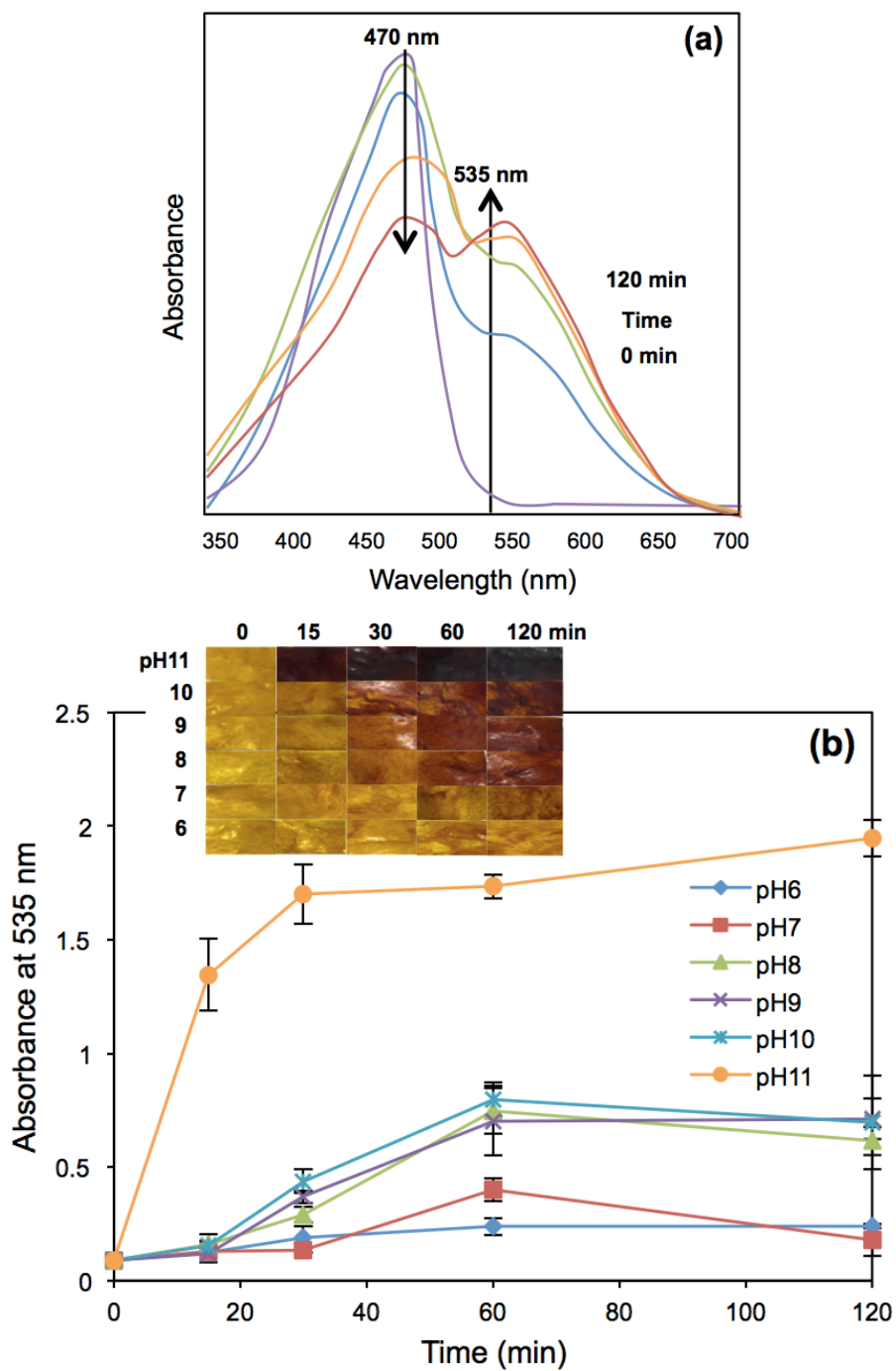


Figure 4.7 (a) UV-Vis spectrum of stoichiometric PDADMAC:PSS of salt-free Cur-PEC(1.5) films immersed to solution pH 11 and (b) absorbance at 535 nm and the color change of the films immersed to various pH solutions as a function of time.

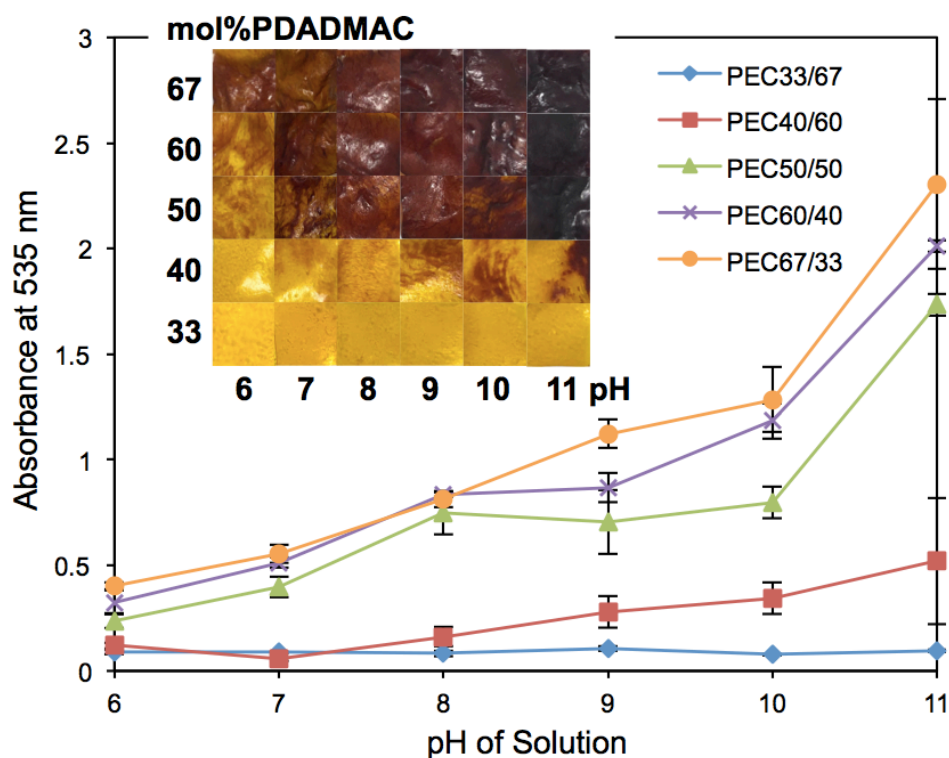


Figure 4.8 Absorbance at 535 nm and the color change of the salt-free stoi- and nonstoichiometric Cur-PEC(1.5) films immersed to various pH solutions after 1 h.

In previous work, PEM films loaded with Cur illustrate pH sensor property by changing from yellow to reddish brown when exposed to different pH solutions. The charged of electrolytes plays an important role to control the pH sensing properties. As expected from Figure 4.8, the stoichiometric (1:1) and nonstoichiometric (2:1, 1.5:1, 1:1.5 and 1:2) PDADMAC:PSS films depict different color change ability from yellow to orange-red when soaking in different pH of phosphate buffer solutions. PDADMAC-rich films depict the highest pH sensing character while excess PSS (PEC33/67) films do not show the color change property.

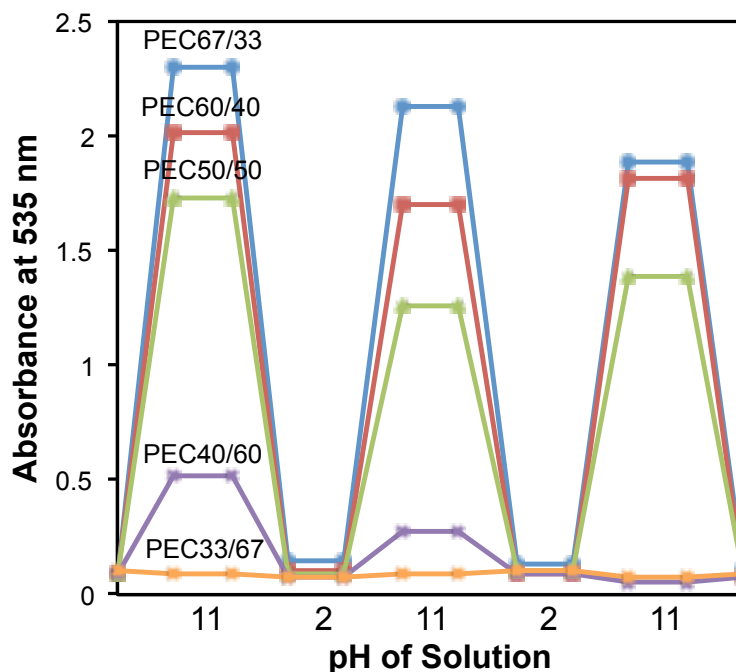


Figure 4.9 The reversible color change of the salt-free stoichiometric and nonstoichiometric Cur-PEC(1.5) films immersed to pH 11 and pH 2.34 solutions.

Moreover, these films can maintain their yellow or red color under ambient temperature and the red film can turn back to yellow again by soaking in an acidic solution. The second and third cycles of the reversible color change of Cur-PEC film in Figure 4.9 reveal that these films can be reused many times as they provide the ability to monitor pH change of solution.

To confirm that Cur can react with PDADMAC lead to the strong color change ability, Cur solution was mixed with PDADMAC or PSS in 90:10 %water:EtOH at different pH. We observed from Figure 4.10 that yellow solution of Cur turn to orange-red at pH 11 in both PDADMAC and PSS solutions but the intensity at 535 nm of Cur in PDADMAC is higher than in PSS solution, which is due to the electrostatic interaction of the carbonyl groups of Cur with cationic PDADMAC and then the pK_a of Cur was decreased. Moreover, it can be seen that Cur mixed with PSS in all range of pH show strongly yellow, which confirmed by the fading of the intensity of peak at 535 nm, owing to the π - π interactions between the Cur and PSS aromatic structures (Kittitheeranun, 2010).

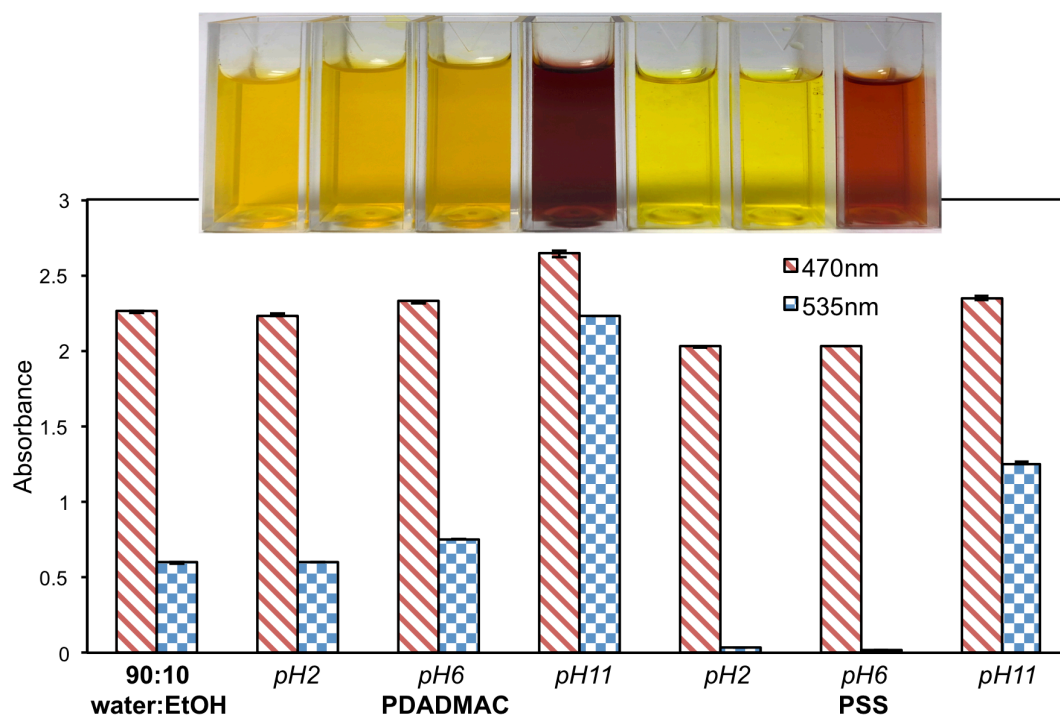


Figure 4.10 Absorbance at 470 and 535 nm represent the yellow and orange-red color of Cur solution dissolved in different polymer and pH solution.

4.3.4 The Effect of [NaCl] used during Complexation on the Moisture Content and the NH₃ Vapor Sensing of Cur-PEC Films

The change in color of Cur-PEC films from yellow to orange-red after exposed to NH₃ vapor was observed by UV-Vis spectroscopy at the maximum absorbance wavelength (λ_{\max}) of about 535 - 540 nm, which corresponds to the orange-red appearance. Figure 4.11 is plotted the UV-Vis absorbance at λ_{\max} of stoichiometric 50/50 mol% of PDADMAC/PSS films prepared at different [NaCl] during processing: 0, 0.5, 1 and 1.5 M. After exposed the films to NH₃ vapor releasing from various concentration of NH₃ solution ([NH₃]): 0, 5, 10, 15, 25 and 50 ppm for an hour, the high salt film depicts high color change. It could be hypothesized that Cur-PEC film with high salt content will absorb more water in the atmosphere, so, the moisture content of the film was tested at different RHs.

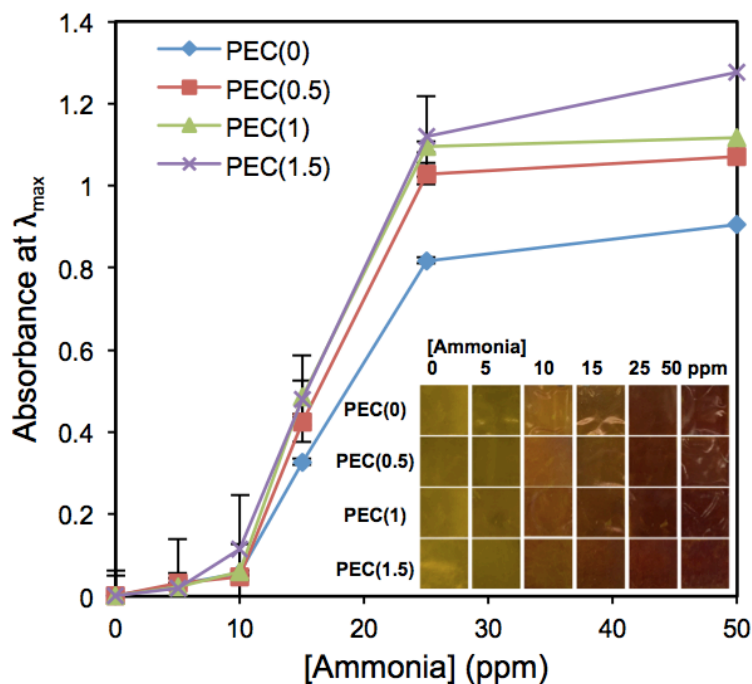


Figure 4.11 Absorbance at λ_{\max} of Cur-PEC films exposed to vapor of various $[\text{NH}_3]$ as a function of $[\text{NaCl}]$ during processing.

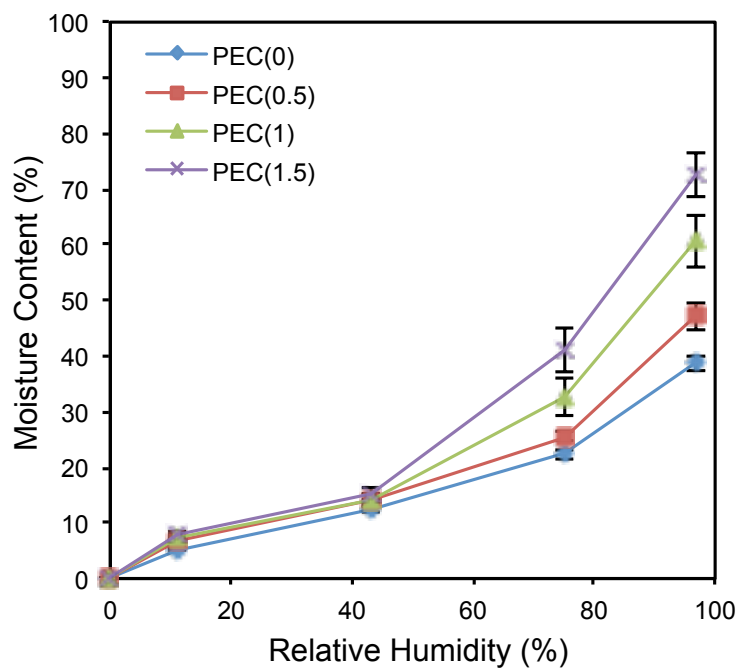


Figure 4.12 The moisture content of PEC films as a function of % RH at various $[\text{NaCl}]$ during processing.

The relation between moisture content and RH is shown in Figure 4.12. The weight increase with respect to the dry state, which shows in %moisture content, describes the sorption isotherm or water activity of films. The water adsorption of PEC films is increasing with both humidity and [NaCl] increase. High [NaCl] used during mixing causes the increase in salt-trapped inside the films, which shows more hydrophilicity lead to more moisture absorption. The highest difference in moisture uptake was observed from PEC(1.5) of 0 - 70% with the range of 0 - 97% RH and the saturated adsorption was obtained after 7 days, so, 1.5 M NaCl was used to fabricate the Cur-PEC films in all afterward experiments.

To cross-check for the moisture content of PEC films could be affected the NH₃ sensitivity, the Cur-PEC(1.5) films were stored in various RHs: 0, 23, 75 and 97 % for 7 days and then exposed to the vapor of NH₃ solution with a concentration of 15 ppm. As can be seen in Figure 4.13(a), the bathochromic red shift was observed when the films adsorb more NH₃ vapor due to their complexation.

The high moisture content provides high NH₃ gas dissolve in the water phase of the films as an equation: $\text{H}_2\text{O} + \text{NH}_{3(\text{g})} \rightarrow \text{NH}_4^+ + \text{OH}^-$ as a result of the moisture content of film increases with % RH of storage chamber (Figure 4.13(b)). The result facilitates the alkaline (basic) environment govern the phenolic structure of Cur from diketo (yellow) to keto-enol (red) form, which is an obvious color change from yellow to red as illustrated by Figure 4.14. In the same time, the high moisture content in the film under high RH generated more $\text{NH}_4^+ + \text{OH}^-$ result in the RH accelerated the color change (Ma *et al.*, 2017). It also appeared that even 0% RH film (dried at 60°C for 48 h) displays the visible color change, which indicated that these films could be utilized in a wide range of RH (0 – 97%) under ambient temperature with as many as 2.5-times in difference.

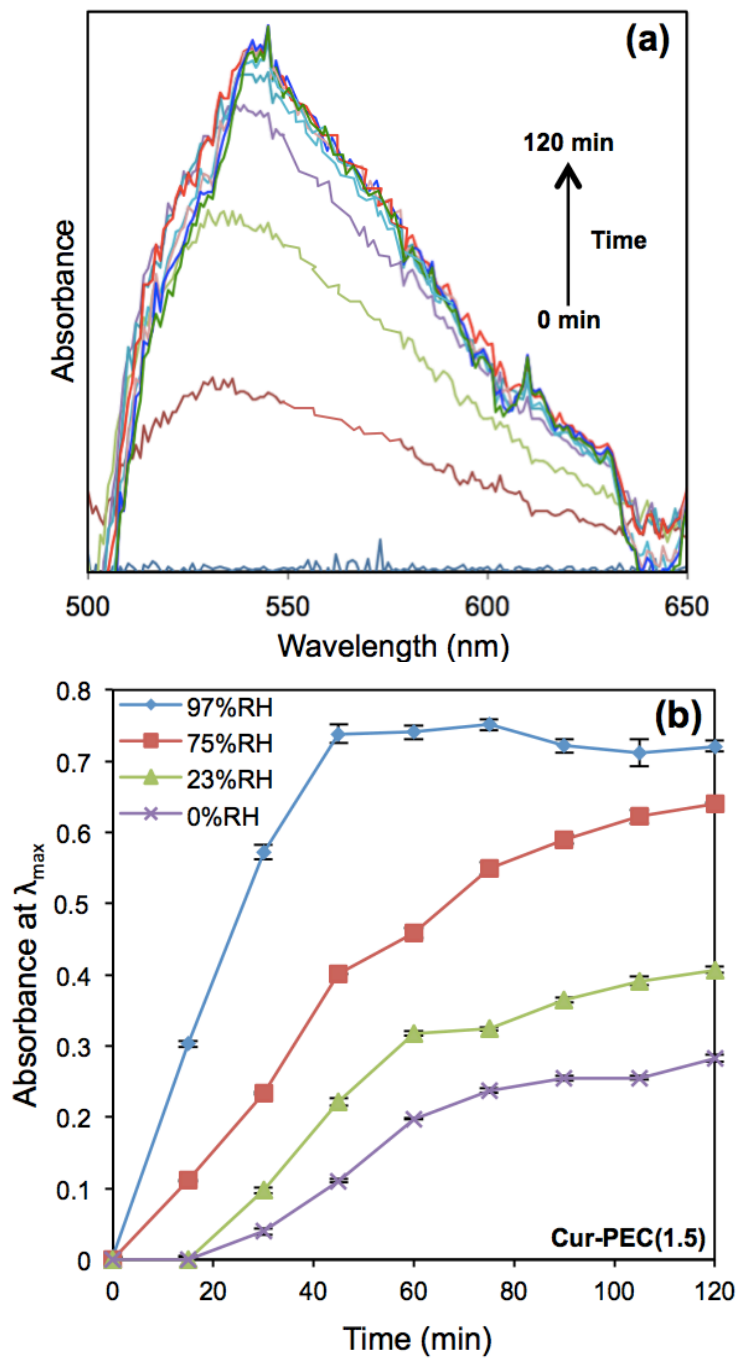


Figure 4.13 (a) UV-Vis spectrum of moisted Cur-PEC(1.5) film and (b) kinetic properties the films stored in various % RHs exposed to vapor of 15 ppm $[\text{NH}_3]$.

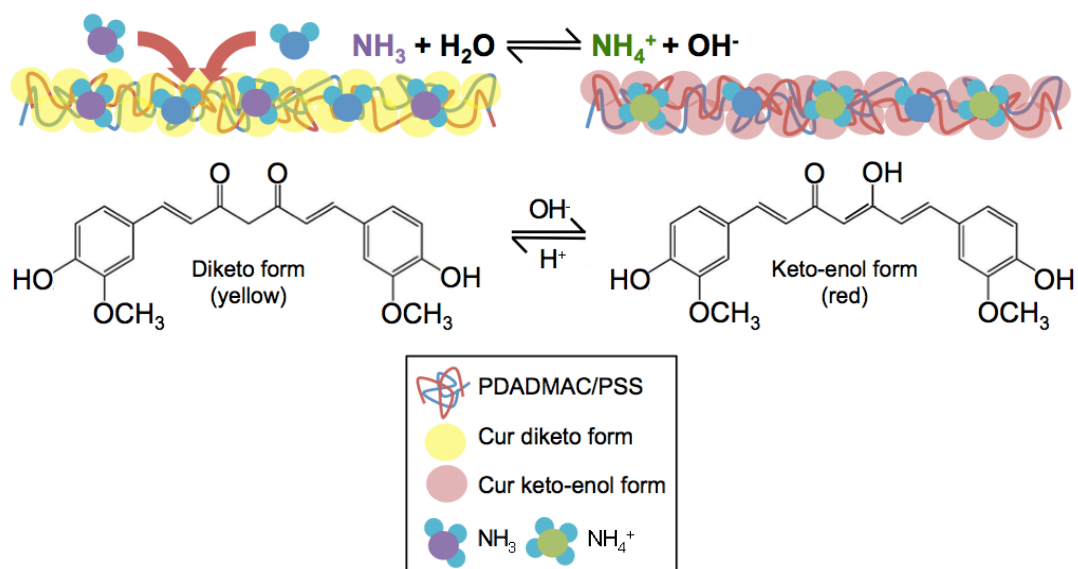


Figure 4.14 Schematic representation of the color change of moistened Cur-PEC films when exposed to NH_3 vapor.

4.3.5 Enhanced the NH_3 Vapor Sensing of Cur-PEC Films Based on Nonstoichiometric Ratio

Previous investigation on Cur loaded with either PDADMAC or PSS on top of PEM nano-scale films provide different inspection when immersed in various pH aqueous phases (Saikaew, 2016). It was assumed that nonstoichiometric PEC with PDADMAC- or PSS-rich embedded Cur may establish the different color change behavior. The PEC films were defined as $\text{PEC}_X/(100 - X)$, where X is mol% fraction of PDADMAC and $(100 - X)$ is mol% fraction of PSS in the initial complex. It can be seen from Figure 4.15 that the absorbance at λ_{max} was saturated after an hour and the nonstoichiometric PEC with PDADMAC-rich (PEC67/33) provides the highest color change in NH_3 vapor sensing according to PEM loaded Cur films with PDADMAC used on top, which provides better pH aqueous sensitivity.

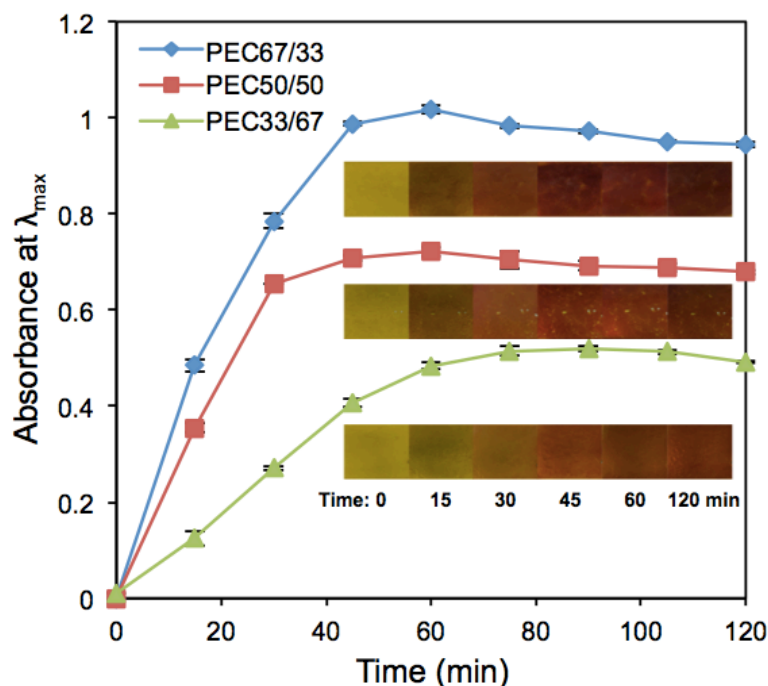


Figure 4.15 Response time of moisted Cur-PEC(1.5) films fabricated from stoi- and nonstoichiometric PDADMAC/PSS exposed to vapor of 15 ppm $[\text{NH}_3]$.

The moisture content of Cur-PEC films at 97% RH in Figure 4.16 indicates the highest moisture uptake of PEC67/33 film, which is consistent with the strongest color change with NH_3 vapor. The moisture significantly increases with the amount of PDADMAC composition because of their hydrophilic nature. This behavior may be described as in the nonstoichiometric film the NaCl counterions are required to balance the excess polyelectrolytes, resulting in salt doping, as ion-compensated extrinsic sites, in PEC structure (Fu, 2017) and leads to an increase in NaCl content of the films. The unexpected results were observed when the moisture content values of PEC50/50 and PEC33/67 films are quite similar, whereas an excess PSS film depicts significant low NH_3 sensing compared to stoichiometric film. It can be stated that not only the moisture content of the film controlling the NH_3 sensitivity but also the electrostatic interaction between anionic Cur and cationic PDADMAC lead to the lowering of the pK_a of Cur and the enhancing of the sensing ability.

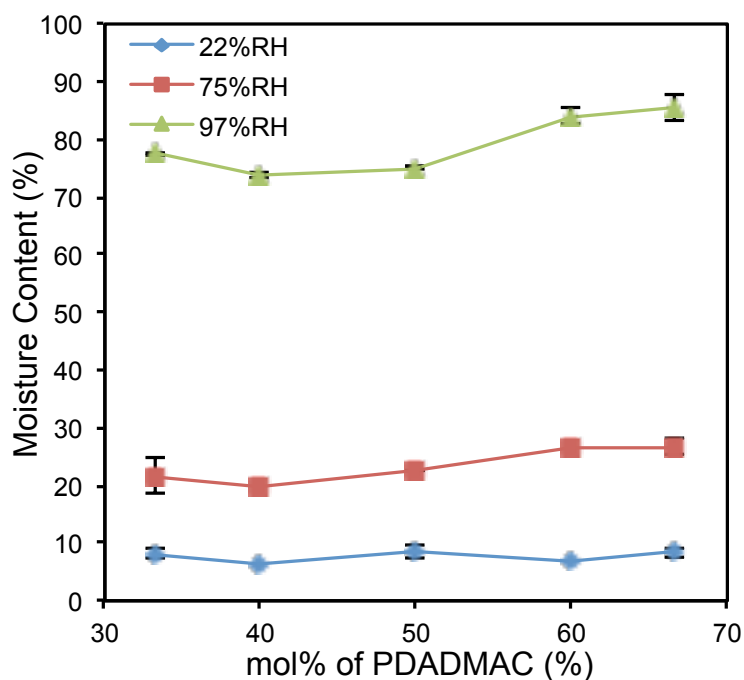


Figure 4.16 The moisture content of the Cur-PEC films as a function of RHs.

The changes in the intensity of characteristic peaks were observed from ATR-FTIR and labeled to the compositions of the film (Figure 4.17). The peaks at 1005 and 1033 are attributed to the S=O symmetric stretching vibration of the sulfonate (SO_3^-) group and the peak at 1170 cm^{-1} is designated to the SO_3^- asymmetric stretching while the peak at 1120 cm^{-1} is aromatic C-H in-plane bending, which confirms the increasing of PSS of excess PEC film. The Cur-PEC films provide the low intensity of characteristic peaks of PSS, which can attribute to the π - π interaction between the Cur and PSS aromatic structures. In the same way, the peak at 1466 and 1630 cm^{-1} derived from the amine (NH_4^+) group and N-H asymmetric deformation of PDADMAC, respectively (Bragaru, 2013) were found to decrease with the presence of Cur in the film because of the electrostatic force between PDADMAC and Cur. Since the amount of Cur content is very low compared to PDADMAC/PSS matrix, the characteristic peaks of C=C and C=O vibration at 1626 and 2928 cm^{-1} assigned to the presence of Cur (Ma, 2017) were not observed. A broad peak at 3390 – 3410 cm^{-1} , corresponding to the O-H stretching vibration of water, decrease as a result of the increasing hydrophobic Cur molecules.

Additionally, it was found that the O-H vibration peak shifted to 3392, 3396 and 3397 cm^{-1} denoting a hydrogen bonding interaction between Cur with increasing the amount of PDADMAC content in the films (Liu, 2016).

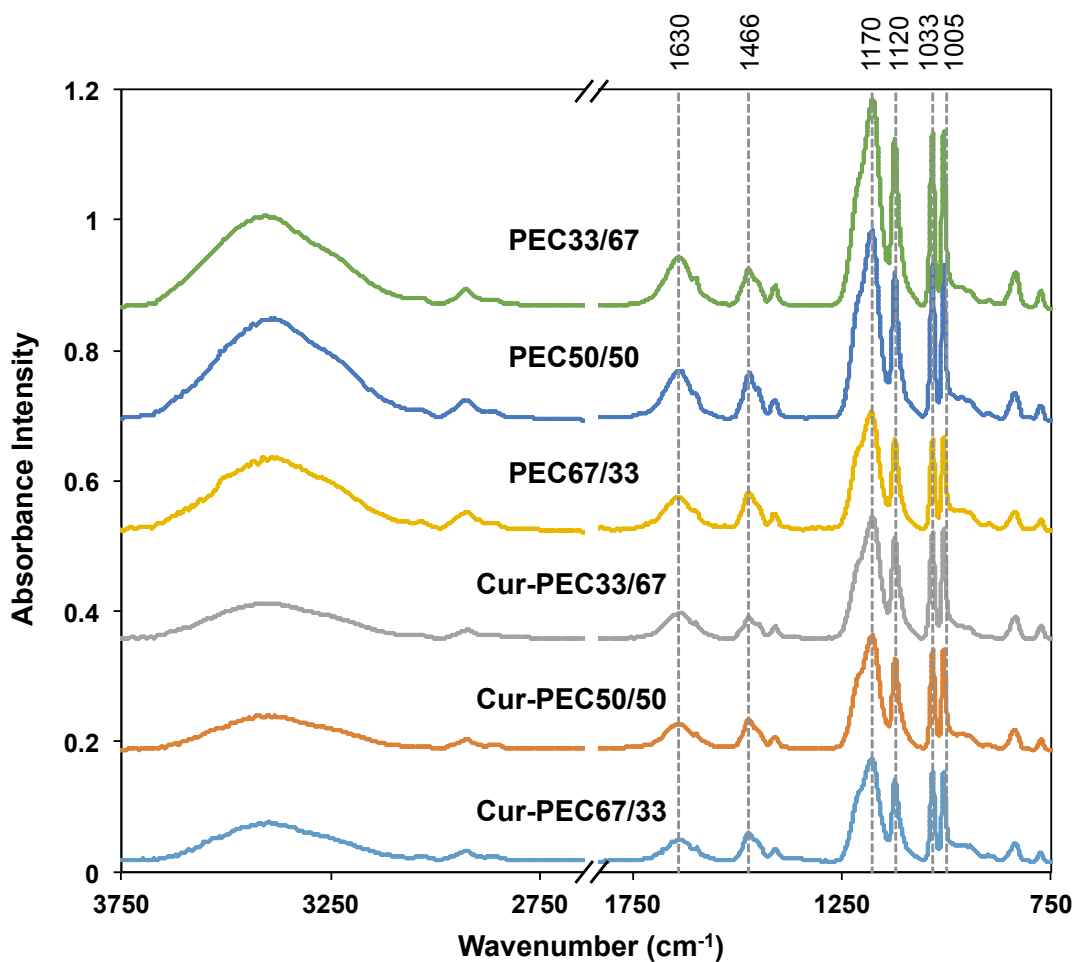


Figure 4.17 The ATR-FTIR spectra of PEC and Cur-PEC films with different polymer ratio.

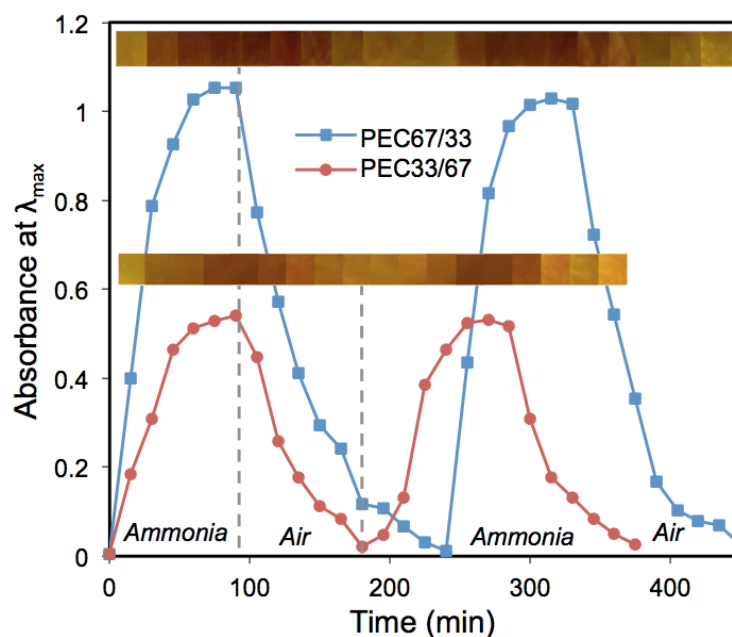


Figure 4.18 The reversible color change cycling of nonstoichiometric PEC films when exposed to NH_3 vapor and air condition.

In order to investigate that whether the color change of Cur-PEC film was reversible, the nonstoichiometric PEC67/33 and PEC33/67 films were stored in 97% RH chamber and then exposed to NH_3 vapor (15 ppm of NH_3 solution). As seen in Figure 4.18, the absorbance at λ_{max} was saturated within an hour after exposed to NH_3 vapor and then the red color return back to yellow again after left under ambient condition within 100 – 120 min. This indicates that the sensing ability of Cur-PEC films was reversible. Although the PSS-rich film depicts faster reversible change than PDADMAC-rich film, the lower amount of NH_3 vapor dissolved in the water phase of the PSS matrix leads to the lower sensitivity. Moreover, the color change of Cur-PEC films when exposed to NH_3 vapor is faster than the reversible change due to the evaporation of NH_3 . This behavior of these Cur-films could broaden their potential uses, especially in sensing applications.

4.3.6 Cur-PEC Film for Optical Detection of the Spoiled Shrimp

The spoilage of fresh food products is related to microorganisms. The microorganisms degradation mainly generate total volatile basic nitrogen (TVBN) including volatile amines, dimethylammonium, trimethylamine, etc, which may

increase the pH value of the media environment. From this viewpoint, the sensing property for the spoilage of seafood products was investigated to verify that these Cur-PEC films could be used to detect NH_3 vapor created from the spoiled shrimp (Figure 4.19(a)). The color of the moistened film was changed from yellow to orange-red after stored for 2 days. As seen in Figure 4.19(b)-(c), the color difference observed from UV-Vis spectroscopy at λ_{max} was found to increase in the film after testing as well as the a value of the color parameters from colorimeter, which represents the reddish of film, was increased. The enhanced of NH_3 vapor detection ability on asymmetric excess PDADMAC composition of Cur-PEC films can be used for optical sensing application to estimate the spoilage of food with convenient way under ambient conditions.

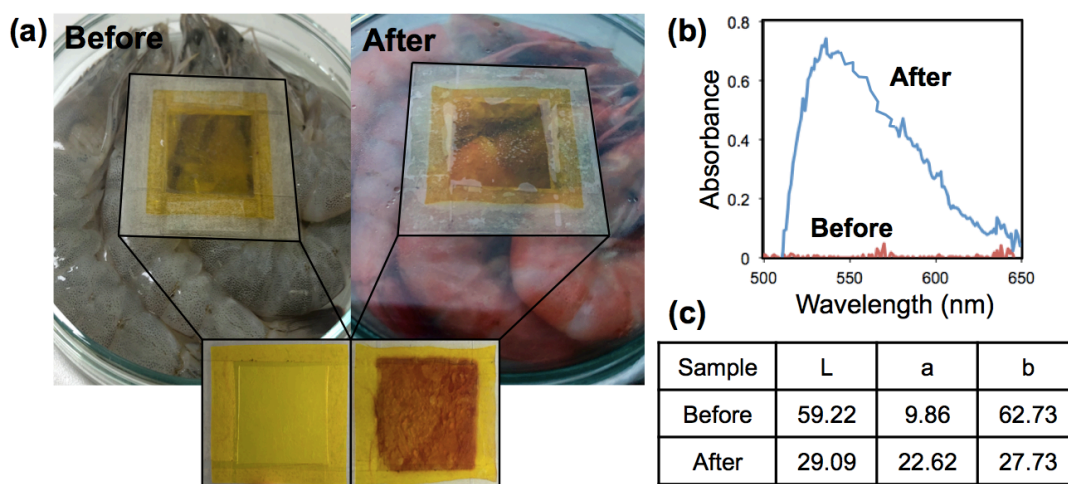


Figure 4.19 Sensing properties for the spoiled shrimp of Cur-PEC film with excess PDADMAC composition. The visible color change of film (a) was observed from (b) UV-Vis spectroscopy and (c) colorimeter (the table shows the color parameters of film).

4.3.7 Cur-PEC Film Prepared with Different Types of Salt

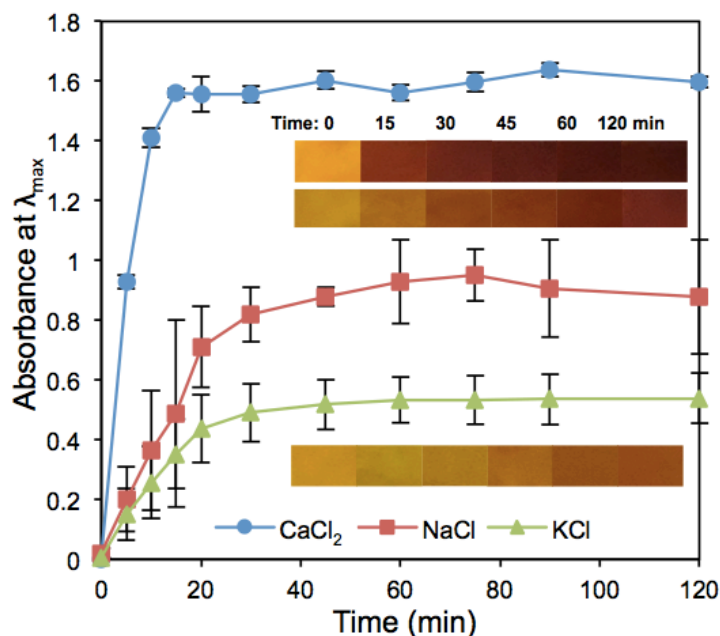


Figure 4.20 Response time of moisted Cur-PEC(1.5) films of PEC67/33 at different types of salt used during fabrication exposed to vapor of 15 ppm [NH₃].

In accordance with previous findings, PEC films of PDADMAC and PSS can be fabricated in the presence of different types of salt during mixing and may affect the color change ability of the Cur-PEC film. The yellow Cur-PEC films prepared under KCl, NaCl and CaCl₂ with the concentration of 1.5 M were stored in 97% RH chamber and then exposed to NH₃ vapor (15 ppm of NH₃ solution). These films depict different color change ability as seen in as shown in Figure 4.20. The moisted Cur-PEC film with CaCl₂ displays not only the highest intensity of absorbance at λ_{\max} , which correspond to the highest moisture uptake of the film after stored at 97% RH for a week (Figure 4.21), but also the fastest visible color change to orange-red within 30 min. This evidence is due to the hygroscopicity of salts contained in the film. Comparison between the RH provided from these salts, KCl, NaCl and CaCl₂ are about 85, 75 and 9% RH (Greenspan, 1977), respectively, meaning that CaCl₂ acts as desiccant salt and can absorb more moisture from the surrounding environment (Kallenberger, 2018). Future work should therefore include

the study of Cur-PEC film prepared with CaCl_2 for detection of lower NH_3 vapor concentration released from the spoilage of food and the scale-up of film fabrication for revealing the gas leak from the automotive and industrial factory.

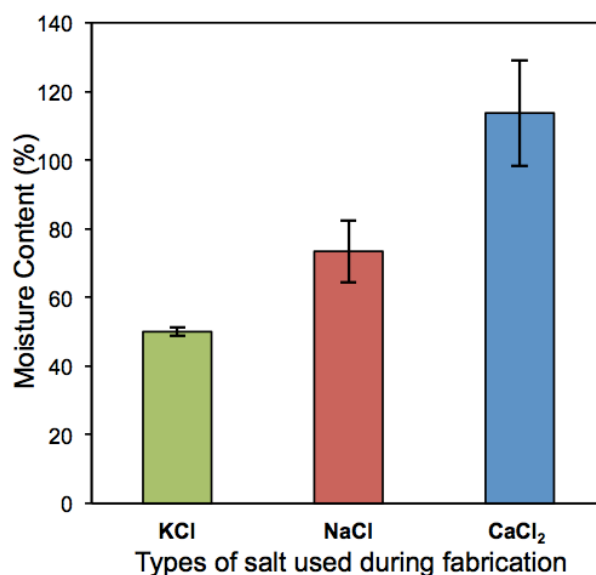


Figure 4.21 The moisture content of Cur-PEC(1.5) films of PEC67/33 with different types of salt at 97% RH.

4.4 Conclusion

The influence of moisture content and polymer ratio on the NH_3 vapor sensitivity based on Cur-PEC films with various PDADMAC:PSS composition was studied. A visual color change of the films from yellow to reddish-orange can be obtained under low concentration of NH_3 vapor at sufficient moisture content and can be accelerated the color change ability by increasing the moisture content in the films. The type of salt contained in the final films provide different color change ability due to the moisture content also. A potential used for these Cur-PEC could be motivating for the development of sensor applications and food packaging industries. Furthermore, the tuning of the positive or negative ratio of PEC-based materials is an interesting strategy for further study towards other specific applications that the requirement of charge possibly was concerned.

4.5 Acknowledgements

This work has been financially supported by the Petroleum and Petrochemical College, Grant for International Research Integration: Chula-Research Scholar, Ratchadaphiseksompot Endowment Fund and the Center of Excellence on Petrochemical and Materials Technology, Chulalongkorn University and the Development and Promotion of Science and Technology Talents (DPST) Project jointly administered by the Ministry of Science and Technology, the Ministry of Education.

4.6 References

- Bragaru, A., Kusko, M., Radoi, A., Danila, M., Simion, M., Craciunoiu, F., Rascu, R., Mihalache, I., Ignat, T. (2013) Microstructures and growth characteristics of polyelectrolytes on silicon using layer-by-layer assembly. Cent. Eur. J. Chem., 11(2), 205-214.
- Dautzenberg, H. (1997) Polyelectrolyte complex formation in highly aggregating systems. 1. Effect of salt: Polyelectrolyte complex formation in the presence of NaCl. Macromolecules, 30, 7810-7815.
- Dautzenberg, H., Jaeger, W. (2002) Effect of charge density on the formation and salt stability of polyelectrolyte complexes. Macromol. Chem. Phys., 203, 2095-2102.
- De, S., Cramer, C., Schönhoff, M. (2011) Humidity dependence of the ionic conductivity of polyelectrolyte complexes. Macromolecules, 44, 8936-8943.
- Fu, J., Abbett, R. L., Fares, H. M., Schlenoff, J. B. (2017) Water and the glass transition temperature in a polyelectrolyte complex. ACS Macro Lett., 6, 1114-1118.
- Gai, M., Frueh, J., Kudryavtseva, V. L., Mao, R., Kiryukhin, M. V., Sukhorukov, G. B. (2016) Patterned microstructure fabrication: Polyelectrolyte complexes vs polyelectrolyte multilayers. Sci. Rep., 6, 37000.

- Gorga, R. E., Cohen, R. E. (2004) Toughness enhancements in poly(methyl methacrylate) by addition of oriented multiwall carbon nanotubes. J. Polym. Sci. Part B: Polym. Phys., 42(14), 2690.
- Greenspan, L. (1977) Humidity fixed points of binary saturated aqueous solutions. J. Res. Nat. Bur. Stand. Sect. A. Phys. Chem., 81A(1), 89-96.
- Imre, Á. W., Schönhoff, M., Cramer, C. (2008) A conductivity study and calorimetric analysis of dried poly(sodium 4-styrene sulfonate)/poly(diallyldimethylammonium chloride) polyelectrolyte complexes. J. Chem. Phys., 128, 134905.
- Kallenberger, P. A., Fröba, M. (2018) Water harvesting from air with a hygroscopic salt in a hydrogel-derived matrix. Commun. Chem., 1:28.
- Kittitheeranun, P., Sanchavanakit, N., Sajomsang, W., Dubas, S.T. (2010) Loading of curcumin in polyelectrolyte multilayers. Langmuir, 26(10), 6869-6873.
- Liu, Y., Cai, Y., Jiang, X., Wu, J., Le, X. (2016) Molecular interactions, characterization and antimicrobial activity of curcumin-chitosan blend films. Food Hydrocoll., 52, 564-572.
- Ma, Q., Du, L., Wang, L. (2017) Tara gum/polyvinyl alcohol-based colorimetric NH₃ indicator films incorporating curcumin for intelligent packaging. Sens. Actuator B-Chem., 244, 759-766.
- Michaels, A. S. (1965) Polyelectrolyte complexes. Ind. Eng. Chem., 57, 32.
- Saikaew, R., Bijaisoradat, O., Netcharoensirisuk, P., Dubas, S.T. (2016) Improved pH sensing of curcumin loaded polyelectrolyte multilayers thin films. Sensor Letters, 14(6), 572-576.
- Saikaew, R., Marsal, P., Grenier, B., Dubas, S.T. (2018) Temperature controlled loading and release of curcumin in polyelectrolyte multilayer thin films. Materials Letters, 215, 38-41.
- Schlenoff, J. B., Rmaile, A. H., Bucur, C. B. (2008) Hydration contributions to association in polyelectrolyte multilayers and complexes: Visualizing hydrophobicity. J. Am. Chem. Soc., 130, 13589-13597.

- Shin, Y., Cheung, W. H., Ho, T. T. M., Bremmell, K. E., Beattle, D. A. (2014) Insights into hydrophobic molecule release from polyelectrolyte multilayer films using in situ and ex situ techniques. Phys. Chem. Chem. Phys., 16, 22409.
- Shiratori, S., Inami, Y., Kikuchi, M. (2001) Removal of toxic gas by hybrid chemical filter fabricated by the sequential adsorption of polymers. Thin Solid Films, 393, 243–248.

CHAPTER V
INFLUENCE OF THE SALT CONCENTRATION
DURING PROCESSING ON THE PROPERTIES OF
SALT-FREE POLYELECTROLYTE COMPLEX MEMBRANES

It was illustrated in the previous chapter that charged electrolytes can be used as a nanostructured coating, polyelectrolyte multilayers (PEMs), loaded with biomolecules to use be as a sensor or in the medical field. Although, the PEMs produces very thin, smooth and homogenous coating films their limitation is they are so thin and can not be held, so, they can only be used as coating. To accelerate the assembly of electrolyte films into thicker films, polyelectrolyte complexes (PECs) have become interesting materials. The same electrolytes can be mixed together under optimized condition by tuning the ionic strength to form PECs. They can be fabricated in a variety of shapes and also loaded with additive fillers. As mention in Chapter 4 stoi- and nonstoichiometric PEC films with different polymer [P⁺]:[P⁻] ratio provided different properties that required for many specific applications, this work focusses on the other parameters controlling the properties of PEC films. The thermomechanical properties and characteristics of PECs made from poly(diallyldimethylammonium chloride) (PDADMAC) and poly(sodium 4-styrene sulfonate) (PSS) as a function of NaCl concentration ([NaCl]) during processing are investigated.

5.1 Proposed Research

While several studies have investigated the influence of salt annealing *after* PEC formation (Fu, 2017), the study presented here was focused on examining the effect of salt addition *as a processing aid during* mixing and formation of the polymer complex. Smooth and transparent PEC films can be produced by mixing aqueous NaCl-containing solutions of cationic PDADMAC and anionic PSS, shaping the materials formed via compression molding into thin films, and extracting the NaCl by a rinse step. Varying the [NaCl] during processing and hydrating the materials after salt extraction, it was shown that the T_g of the hydrated salt-free PEC

films increases with the [NaCl] used during the mixing step. This trend appears to reflect improved mixing during the polymer complex formation and an increased entanglement density in the final materials. Processing the PEC films in the presence of salt also had an interesting effect on their shape memory characteristics. PEC films prepared under high-salt conditions were shown to maintain a programmed temporary shape better than materials prepared with low salt concentration, while recovery was possible within a short period of time when then immersed in hot water.

5.2 Experimental

5.2.1 Chemicals and Materials

Poly(diallyldimethylammonium chloride) (PDADMAC, medium molecular weight, 20 wt.% in water, weight-average molecular weight, M_w , = 200,000-350,000 g/mol), poly(sodium 4-styrene sulfonate) (PSS, M_w = 70,000 g/mol), and sodium chloride (NaCl) were purchased from Sigma-Aldrich. Double distilled (DI) water was used throughout.

5.2.2 Fabrication of Polyelectrolyte Complex (PEC) Films

PEC films were prepared as follows. PDADMAC and PSS were individually dissolved in water at a concentration of 0.1 M (16.12 g/L for PDADMAC and 20.62 g/L for PSS) by stirring with a magnetic stir bar and adding NaCl to the solutions after the polymers were completely dissolved. The NaCl concentration in the two solutions ([NaCl]) was adjusted in a range of 0 – 1.5 M. Aliquots of the solutions (30 mL of each solution) were combined, stirred for 30 min, and the solid complexes that had formed were compacted into dense precipitates by centrifugation at 8,000 rpm for 20 min. The solids were separated from the supernatant solution and, without further drying, compressed in a Carver press at 40°C under a pressure of 2,000 psi for 30 min using spacers to control the thickness to 100 μ m. The samples were dried at ambient temperature overnight. To prepare the salt-free films, the films were immersed in 100 mL of water for 24 h and the water was changed every 8 h.

5.2.3 Characterization of PEC Films

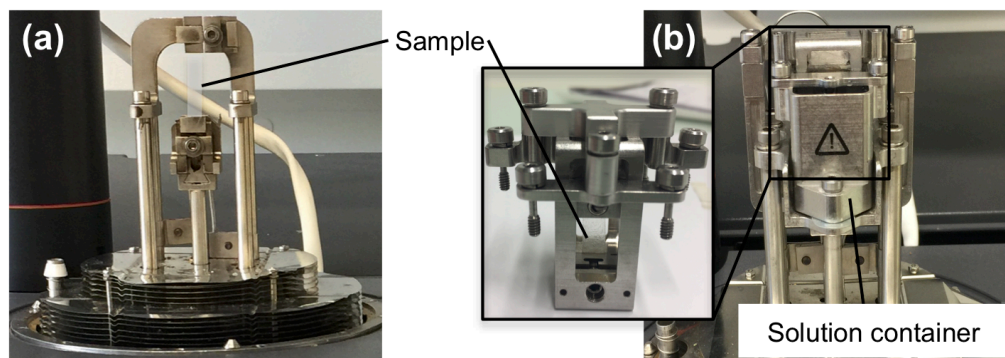


Figure 5.1 Photographic images of tension (a) and submersion (b) clamps for dynamic mechanical analysis (DMA).

All the results quoted are averages of three independent experiments. The thermal stability and salt content of the PEC films were measured by thermogravimetric analysis (TGA) on ca. 3 mg of dry salt-containing as well as salt-free samples with a Mettler-Toledo STAR^e system under inert N₂ atmosphere in the temperature range of 25 to 600°C and applying a heating rate of 10°C/min. Differential scanning calorimetry (DSC) measurements with heating and cooling cycles from 0 to 250°C were performed using a heating/cooling rate of 10°C/min. The mechanical behavior of the PEC films was characterized by dynamic mechanical analysis (DMA) using a TA Instruments Model Q800. A tension clamp and a heating rate of 5°C/min were employed for measurements of dry, salt-containing films. A submersion clamp and a heating rate of 0.5°C/min with samples immersed in water were used for measurements of hydrated, salt-free films (Figure 5.1) and in this case, the temperature range was limited to 5 – 55°C. The DMA tests were conducted in multi-frequency strain mode using a temperature ramp, a frequency of 1 Hz, and a strain amplitude of 15 μ m. The experiments were conducted with PDADMAC/PSS film samples of dimension 6x15 mm and samples were studied as a function of [NaCl] during mixing: 0, 0.5, 1 and 1.5 M. Stress-strain measurements were conducted on the hydrated, salt-free films on the same instrument at room temperature with a strain rate of 20%/min. The tensile moduli were calculated from

the initial slopes of the linear regions, i.e., in the strain range of 0 – 5%. To measure the water uptake, the dry salt-free films with dimension of 20 x 20 mm (dried for 48 h at 60°C) were soaked in water for 24 h, and the water uptake was calculated from the weights of the dry (W_d) and the hydrated (W_h) samples by:

$$\text{Degree of swelling (\%)} = \frac{W_h - W_d}{W_d} \times 100 \quad (5.1)$$

5.2.4 Shape Memory Behavior of PEC films

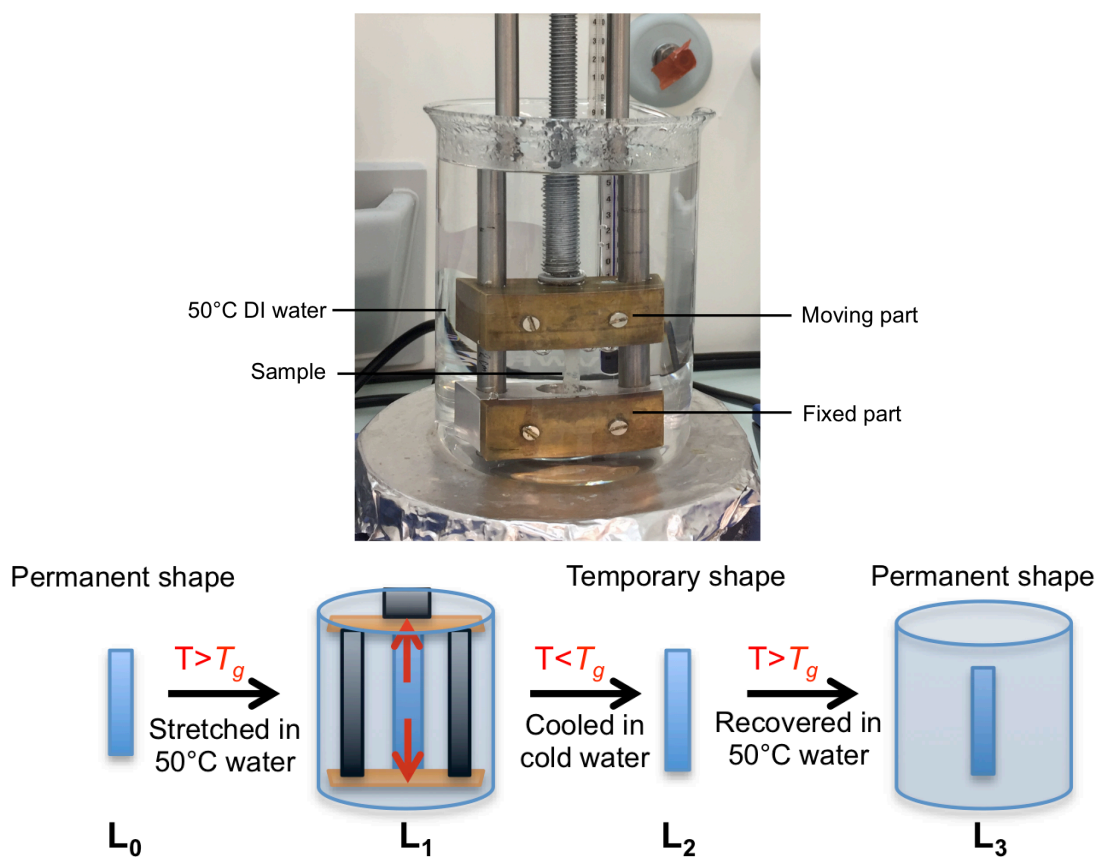


Figure 5.2 Photographic image of the manual stretching device (model) and schematic procedure for shape memory experiment.

In order to monitor the water-induced shape memory effect (SME) of the PEC films, 6 mm wide strips of an initial length of 2 cm (L_0) were immersed in water maintained at 50°C, stretched to a length of $L_1 = 4$ cm (i.e. to a strain $S = (L_1 - L_0)/L_0 = 100\%$) in a manual stretching device (model) as shown in Figure 5.2. With

the strain applied, the samples were placed in cold water and held at this stage for 5 min, before they were allowed to dry under ambient conditions. After removing the force, the temporary shape (L_2) was determined. Finally, the shape recovery was triggered by placing the samples into water heated at 50°C and the recovered length L_3 was measured. The shape fixity (R_f) and shape recovery (R_r) were calculated using eqs. 5.2 and 5.3:

$$\% \text{ Shape fixity } (R_f) = \frac{L_2 - L_0}{L_1 - L_0} \times 100 \quad (5.2)$$

$$\% \text{ Shape recovery } (R_r) = \frac{L_2 - L_3}{L_1 - L_0} \times 100 \quad (5.3)$$

5.3 Results and Discussion

5.3.1 Fabrication of Salt-Free PEC Films

A variety of salts, including NaCl, have been used to screen electrostatic interactions between cationic and anionic polymers and soften PECs, thereby making them processable by extrusion or compression molding. Unlike several previous studies, in which the influence of salt water on the thermal transition (T_g) of the PEC was investigated, the materials reported here did not contain any salt during testing, but NaCl was merely used during processing and subsequently removed. This approach was explored based on the hypothesis that it would (i) allow adequate processing, (ii) support the formation of chains entanglements, and (iii) possibly allow tailoring of the thermomechanical properties of the salt-free PEC films.

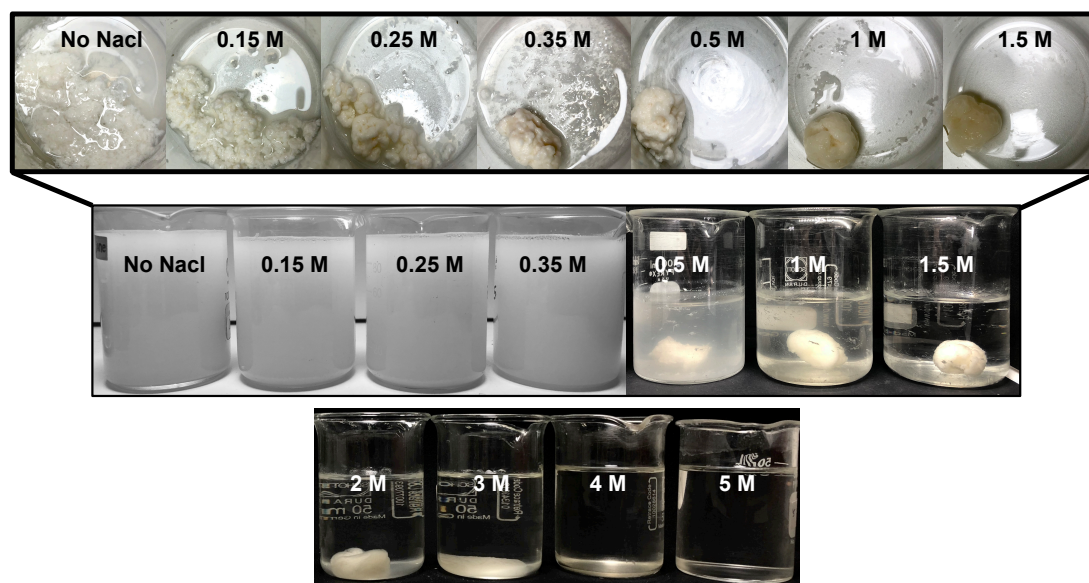


Figure 5.3 PECs formation of PDADMAC and PSS prepared at various $[\text{NaCl}]$.

The influence of salt on the PEC formations is displayed in Figure 5.3. The stoichiometric 1:1 ratio of PDADMAC and PSS with a concentration of 0.1 M prepared at no salt condition produces white colloidal particles. At low ionic strength, PECs spontaneously aggregate to form solid-like morphologies due to macroscopic flocculation (Dautzenberg, 1997). When the $[\text{NaCl}]$ increase to 2 - 3 M, PECs dissociate to an elastic liquid, namely coacervate, which are liquid-like, mobile, and reversible structure (Biesheuvel, 2004). Eventually when $[\text{NaCl}]$ above 4 M, the PECs dissolve in salt water and both PDADMAC and PSS exist as free polyelectrolytes in solution. The NaCl during complexation dominates the conformation of complex driven by salt screening effect, induces the aggregation of complex and creates repulsion force between the electrolyte pair follow by breaking the chain interaction. As mentioned in the introduction, PECs are brittle and infusible when dry therefore the fabrication of complex at adequate NaCl is the important key for the processing step.

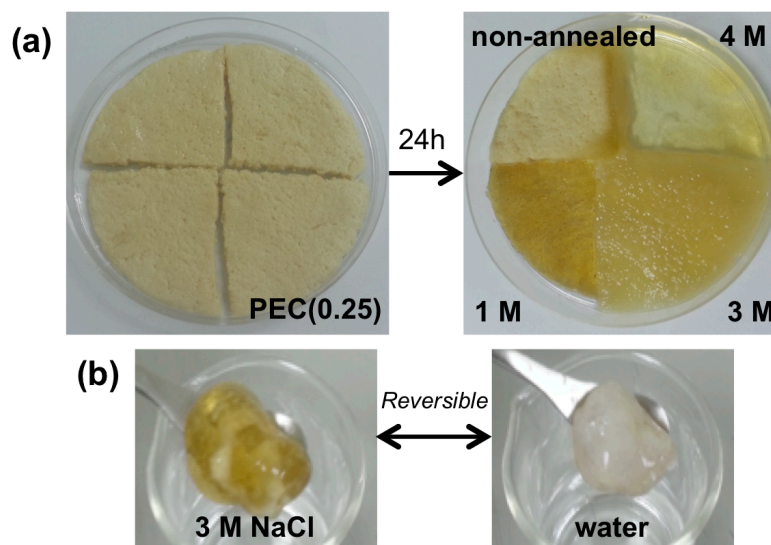


Figure 5.4 (a) PEC(0.25) after annealing for 24 h in different [NaCl] solutions for 24 h and (b) PEC coacervate soaked in 3 M NaCl and became solid in water.

The complexes of PDADMAC/PSS prepared under 0.25 M NaCl were packed into petri dish as a compact solid and then cut into 4 pieces. After annealing each PEC in different [NaCl] solutions for 24 h (Figure 5.4(a)), non-annealing PEC maintains a rubber property, which is tough and hard to deform the shape. When [NaCl] increases, PECs become softer and start to swell. Finally, the PEC dissolved in a high concentration of annealing salt and reform to a gel governed by the salt screening effect, which breaks the electrostatic crosslink between PE ion pairs. As illustrated by Figure 5.4(b) the PEC soaked in 3 M NaCl, a yellow and transparent gel, can change to the turbid white complex after soaking in DI water for a min and this behavior could be reversible. Likewise, extended the immersion time to 1 h, the PEC became a rubber material because NaCl was got out from the complex lead to increases the interaction force between two opposite charge polymers. It can be concluded that salt plays a role in screening charge and reduces the viscosity of complex.

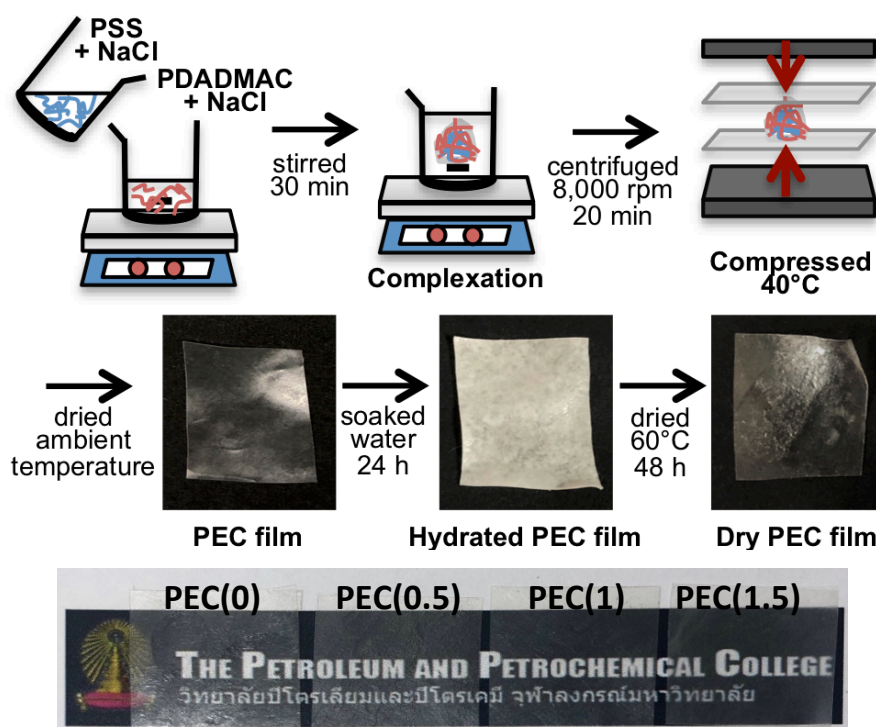


Figure 5.5 Schematic representation of the fabrication process used to create PDADMAC/PSS based PEC films and PEC films with different [NaCl] during complexation.

The PEC films were prepared as schematically shown in Figure 5.5 and detailed in the Experimental Section. PDADMAC and PSS were individually dissolved in water containing NaCl in a concentration of 0 – 1.5 M. The solutions were combined and stirred, and the solid complexes that had formed were compacted into dense precipitates by centrifugation. In preliminary work, the complexes were compressed at high temperature (80 - 100°C) and obtained the films trapping bubble inside as seen in Figure 5.6. It is due to the temperature accelerates the evaporation of water inside the materials and the lack of relaxation time for chain rearrangement. Then, the materials were compressed at 40°C into films of a thickness of 100 μm and dried under ambient conditions. At this point, the NaCl used during mixing of the PEs was still trapped in the film, which were transparent, smooth, and of homogeneous appearance. The NaCl was subsequently removed by soaking the PEC films in deionized (DI) water. After thorough drying, smooth salt-free PEC films

were obtained, which are referred to as PEC(X), where “X” denotes the [NaCl] in the original solution from which the material was processed.

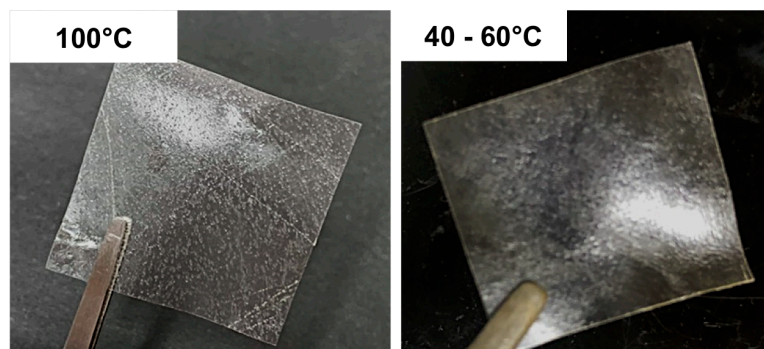


Figure 5.6 The PEC films when compression molding at different temperature.

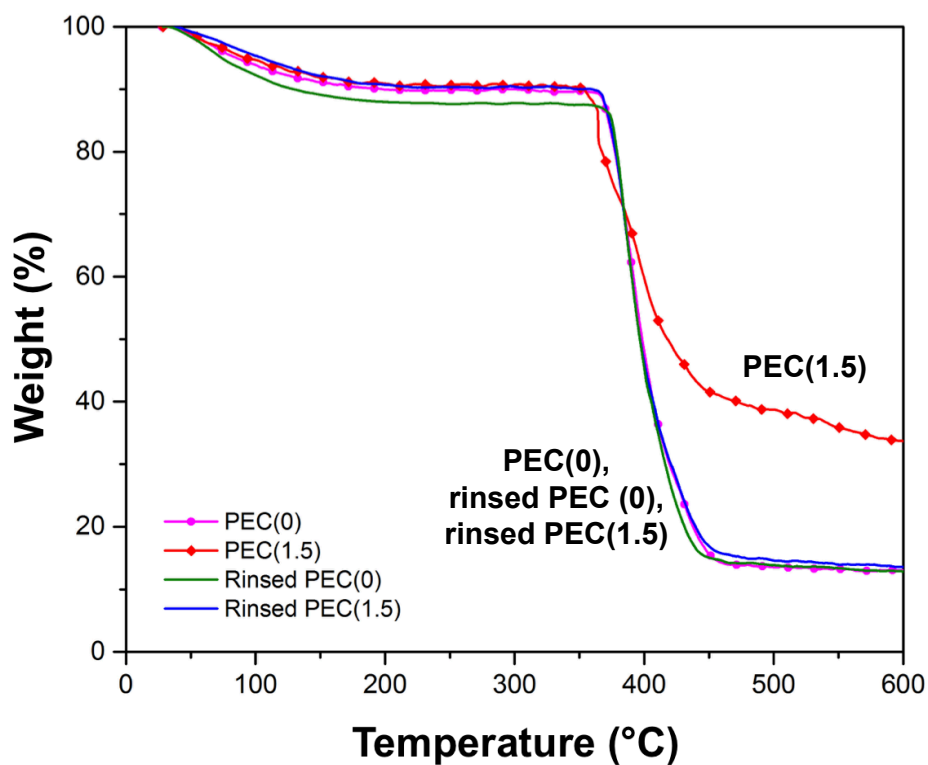


Figure 5.7 TGA thermogram of dry, PEC(0) and PEC(1.5) films before and after rinsed with water for 24 h and then dried at 60°C for 48 h (heating rate 10°C/min).

The removal of NaCl was confirmed by TGA of the PEC film prepared with 1.5 M NaCl, PEC(1.5), before and after the salt extraction. It can be seen from the thermograms (Figure 5.7) that the remaining weight of the sample without rinse is 30%, while the water-soaked film degrades without leaving any residue, confirming the complete removal of NaCl upon extraction with DI water.

5.3.2 Effect of [NaCl] during Processing on the T_g of Hydrated PEC Films

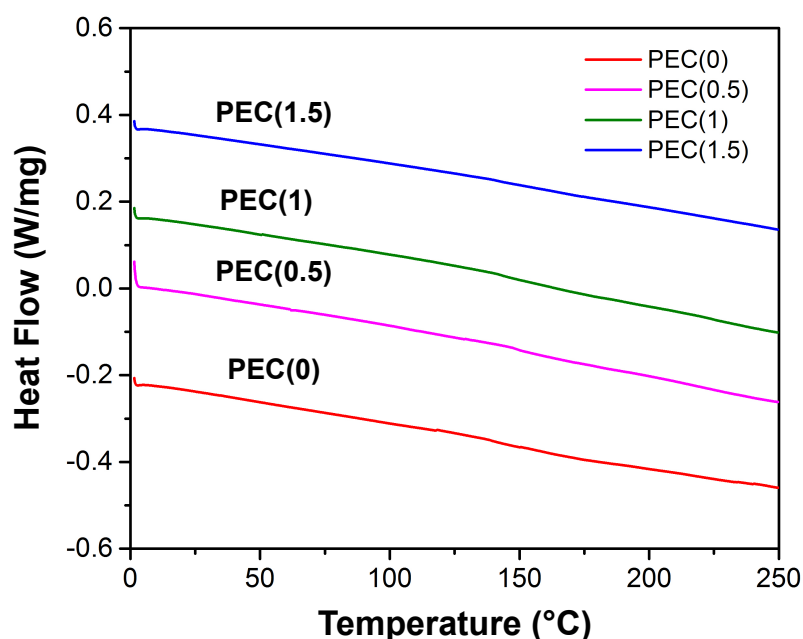


Figure 5.8 DSC thermogram (second heating scan with rate 10°C/min, exotherm up) of dry, salt-containing PDADMAC/PSS films.

In an initial step, the thermal and mechanical properties of the dry PEC films were investigated using differential scanning calorimetry (DSC) and dynamic mechanical analysis (DMA). As reported by other groups, no glass transition could be observed in either the DSC scans (Figure 5.8) or the DMA measurements (Figure 5.9), due to the lack of chain mobility of the dry PECs prepared from all salt conditions. Because the T_g transition of PECs is largely thermal-independence, it is difficult to observe by calorimetry (Shamoun, 2012). The DMA measurements were particularly difficult to perform, as the dry PEC films were very brittle and could hardly be held in position with the clamp. It is in fact

somewhat expected that the dehydrated PECs would become very rigid and brittle, which makes them impractical for high temperature applications.

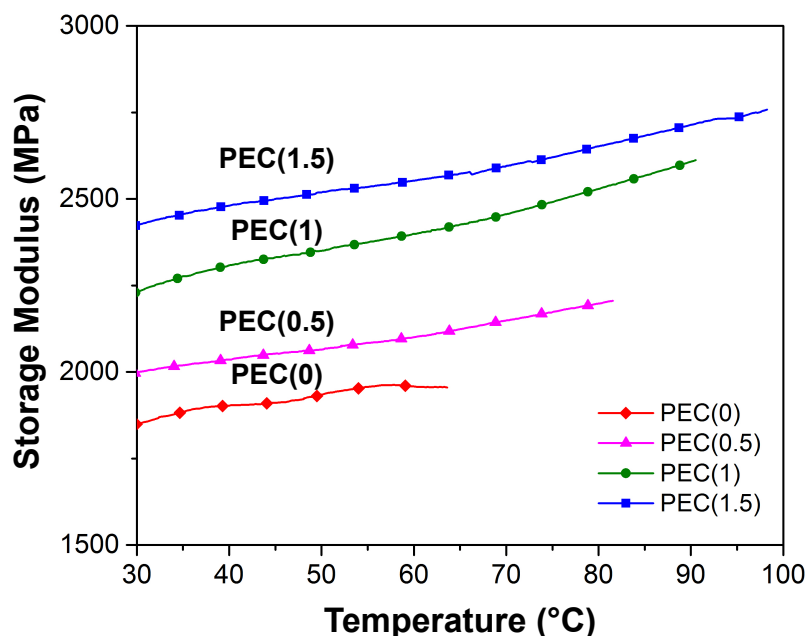


Figure 5.9 Storage modulus at room temperature with heating rate 5°C/min using tension clamp of dry, salt-containing PDADMAC/PSS films.

The thermomechanical behavior of fully hydrated PDADMAC/PSS films, which had been equilibrated by immersion in DI water, was studied using DMA of samples submersed in water. Figure 5.10 show the shear storage modulus E' and $\tan(\delta)$ as a function of temperature and the [NaCl] used during processing. The traces are characteristic of glassy polymers with a glass transition (as established by the maximum of the $\tan(\delta)$ curves) of around 25 – 40°C, a glassy regime with an E' of a few hundred MPa at lower temperature, and a rubbery regime characterized by an E' of around 1 MPa above T_g (Table 5.1). It is interesting to note that both, the T_g and also E' in the glassy state, increase seemingly linearly with the [NaCl] used during processing (Figure 5.11). Since all samples were salt-free during the testing, the shift in T_g cannot be attributed to the persence of NaCl (and related plasticizing effects). Thus, the data suggest that the polymer complex is characterized by either a more tightly bound network or a higher degree of chain entanglements. Indeed, at

low $[\text{NaCl}]$, the PEC is expected to rapidly form and stabilize by the formation of ion pairs without the possibility of much chain motion and therefore few entanglements (Jaber, 2006). On the other hand, at high $[\text{NaCl}]$ the electrostatic charge screening imparted by the salt addition reduces the ionic interaction strength, enables more extensive chain movements, and leads to an intricate mixing of the polymer chain and an inducement of the PEC aggregation (Zhang, 2015), which tend to increase the modulus and T_g of the polymer complex.

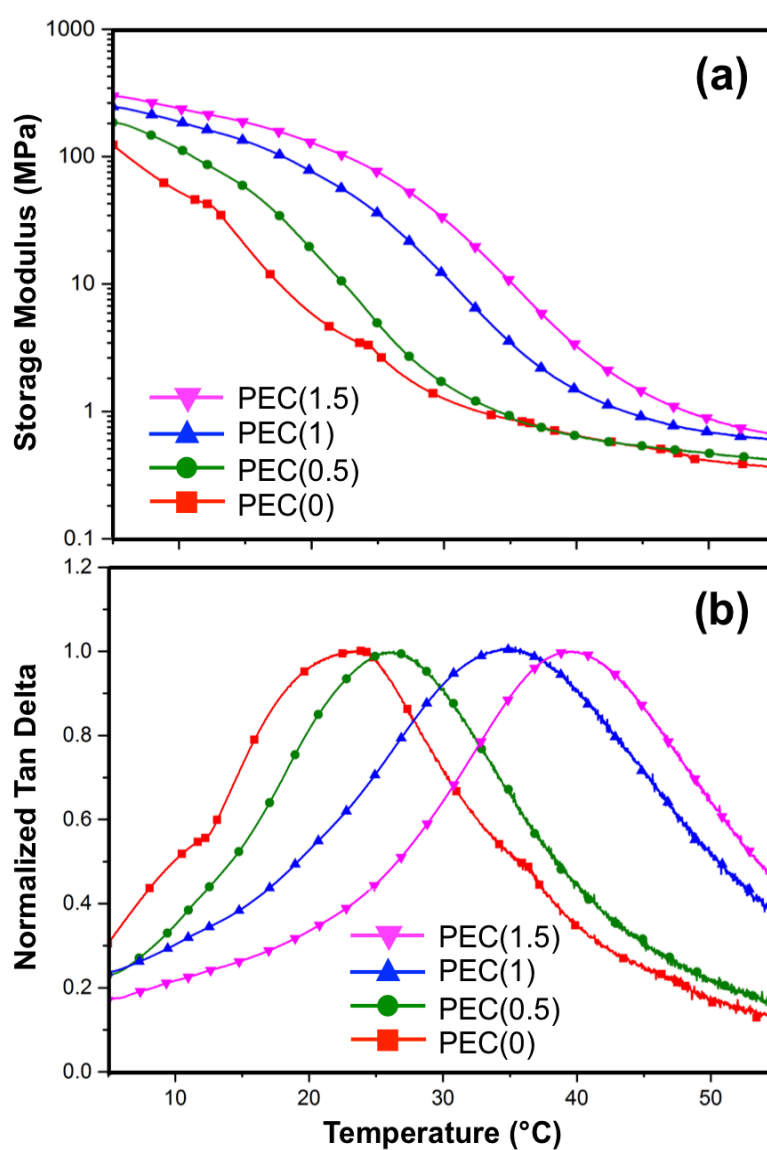


Figure 5.10 DMA traces of hydrated PDADMAC/PSS PEC films measured in water. (a) Storage modulus E' and (b) normalized $\tan(\delta)$.

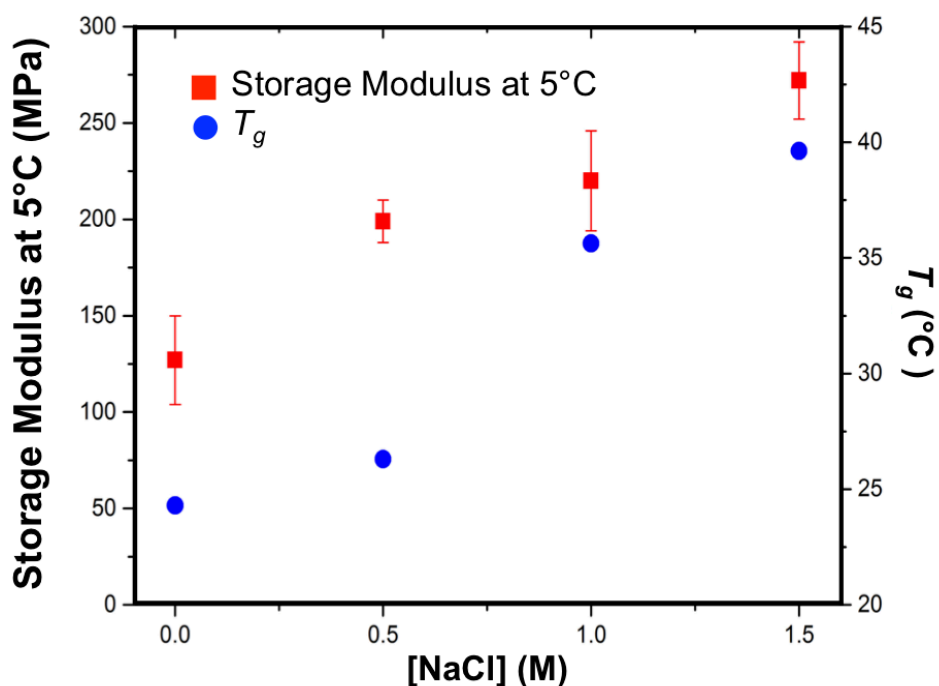


Figure 5.11 E' at 5°C extracted from the graphs shown in (a) and glass transition temperature (T_g) established from the maxima of the $\tan(\delta)$ peaks shown in (b) as a function of [NaCl] used during processing.

Table 5.1 The storage modulus of PEC films in the dry, salt-containing (rate 5°C/min, tension clamp) and hydrated, salt-free (rate 0.5°C/min, submersion clamp) state

[NaCl] (M)	Storage Modulus (MPa)					T_g (°C) (hydrated)
	Dry, salt-containing films		Hydrated, salt-free films			
	At 25°C	At 37°C	At 5°C	At 25°C	At 37°C	
0	1823 ± 118	1912 ± 36	127 ± 23	2.9 ± 1	0.8 ± 0	24.3
0.5	1842 ± 133	2002 ± 76	199 ± 11	6.6 ± 1	0.9 ± 0	26.3
1	2034 ± 60	2226 ± 32	220 ± 26	35 ± 5	2.0 ± 1	35.6
1.5	2384 ± 73	2541 ± 111	272 ± 20	63 ± 9	4.2 ± 2	39.6

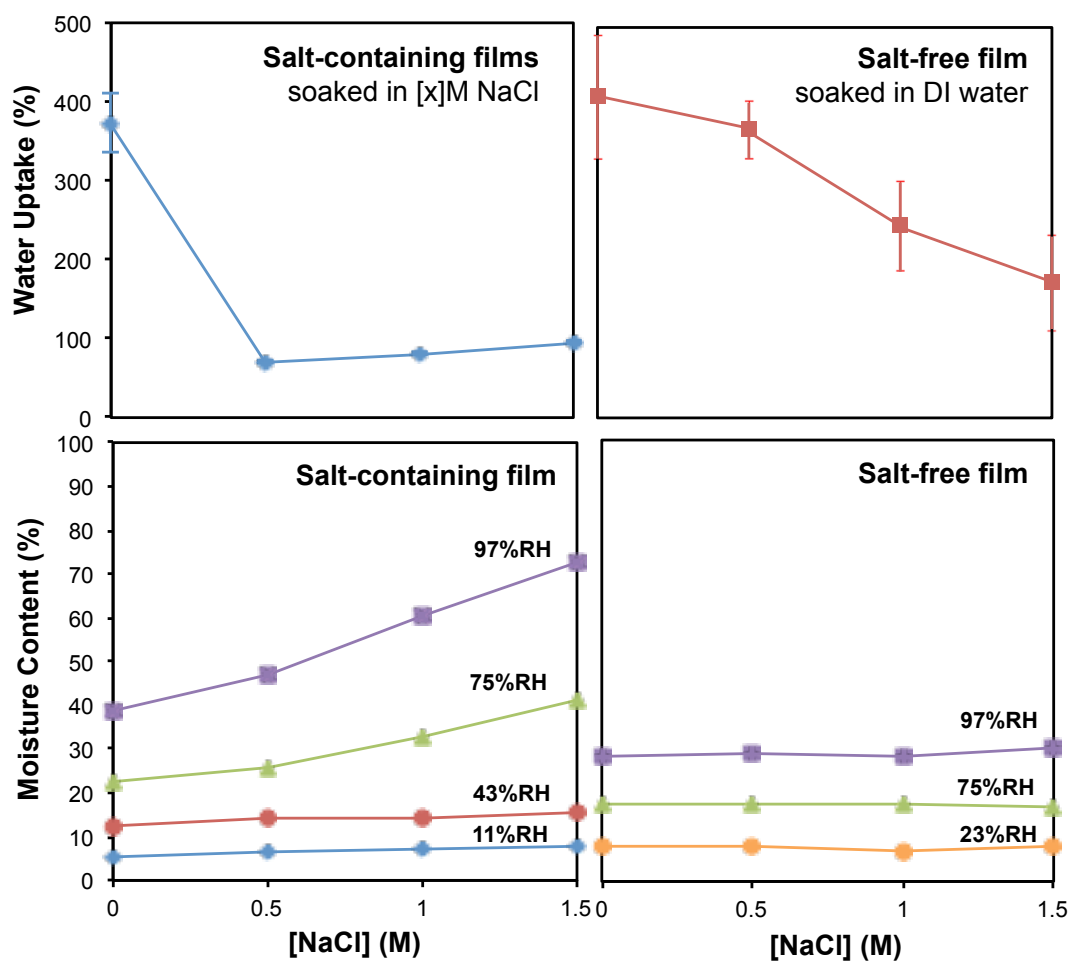


Figure 5.12 Equilibrium water uptake and moisture content of salt containing and salt-free PDADMAC/PSS films at 25°C as a function of [NaCl] used during processing.

It has been reported in a number of papers that water hydrating the polyionic structure in PECs can act as a plasticizer and that, consequently, the T_g usually decreases as the degree of hydration increases (Hariri, 2012, Sadman, 2017). Therefore the water uptake of the salt-free films prepared here was measured in order to elucidate to what extent the [NaCl] used during processing influences the water content of the samples and how it latter impacts the T_g . The PEC films were thus immersed for 24 h in water, in order to achieve equilibrium swelling. As seen in Figure 5.12, the water uptake of salt-free film soaked in DI water decreases from ca. 400 to 150% as [NaCl] used during processing is increased. This result is a

somewhat unexpected, since the films are salt-free, and as they have the same composition, one might think that the water uptake should be nearly constant. However the fact that T_g (Figure 5.11) increases with decreasing water content, and therefore decreasing extent of plasticization (Figure 5.12) is consistent, and suggests that the water uptake is not only governed by the mere chemical composition of the PECs, but also conformation changes that occur during mixing the components under different salt concentrations. With salt containing films soaking in the same [NaCl] solution that used to fabricate the films, the uptake of PEC(0.5) – PEC(1.5) is less than 100% due to the equilibrium concentration of [NaCl] inside and outside the films. To measure the moisture content of salt containing and salt-free films, the films were stored in a humidity-control chamber (100 ml) at 20°C for 21 days before testing. These chamber contain 20 ml of saturated salt solutions: LiCl, CH₃COOK, K₂CO₃, NaCl, and K₂SO₄ to provide an equilibrium relative humidity (RH) of 11, 23, 43, 75 and 97%, respectively, It was found that the moisture uptake of salt containing film increase with both increasing [NaCl] during mixing and %RH, which is consistent to the hygroscopic salt absorb water from the surrounding atmosphere. The salt-free film also shows the increasing in moisture uptake with increasing %RH but the influence of [NaCl] during complexation do not dominate. This might be due to the less changed in moisture content that cannot detect with gravimetric analysis.

The mechanical behavior of hydrated salt-free PEC films was further investigated by way of tensile testing at room temperature. The stress-strain curves shown in Figure 5.13(a) show strikingly that the mechanical properties are significantly impacted by the processing conditions. In accordance with the DMA data, the Young's modulus increased considerably with the [NaCl] employed during processing from 3.0 ± 0.4 MPa for the salt-free solutions to 40 ± 3 MPa for samples processed with [NaCl] = 1.5 M. At the same time, the maximum stress rose from 3.0 ± 1.0 MPa to 10 ± 0.9 MPa, while the elongation at break was reduced from 138 ± 13 to $65 \pm 15\%$. Despite the significant reduction of the strain at break, the films maintained a considerable toughness from 1.3 ± 0.03 to 3.9 ± 0.6 MJ/m³ (Figure 5.13(b)).

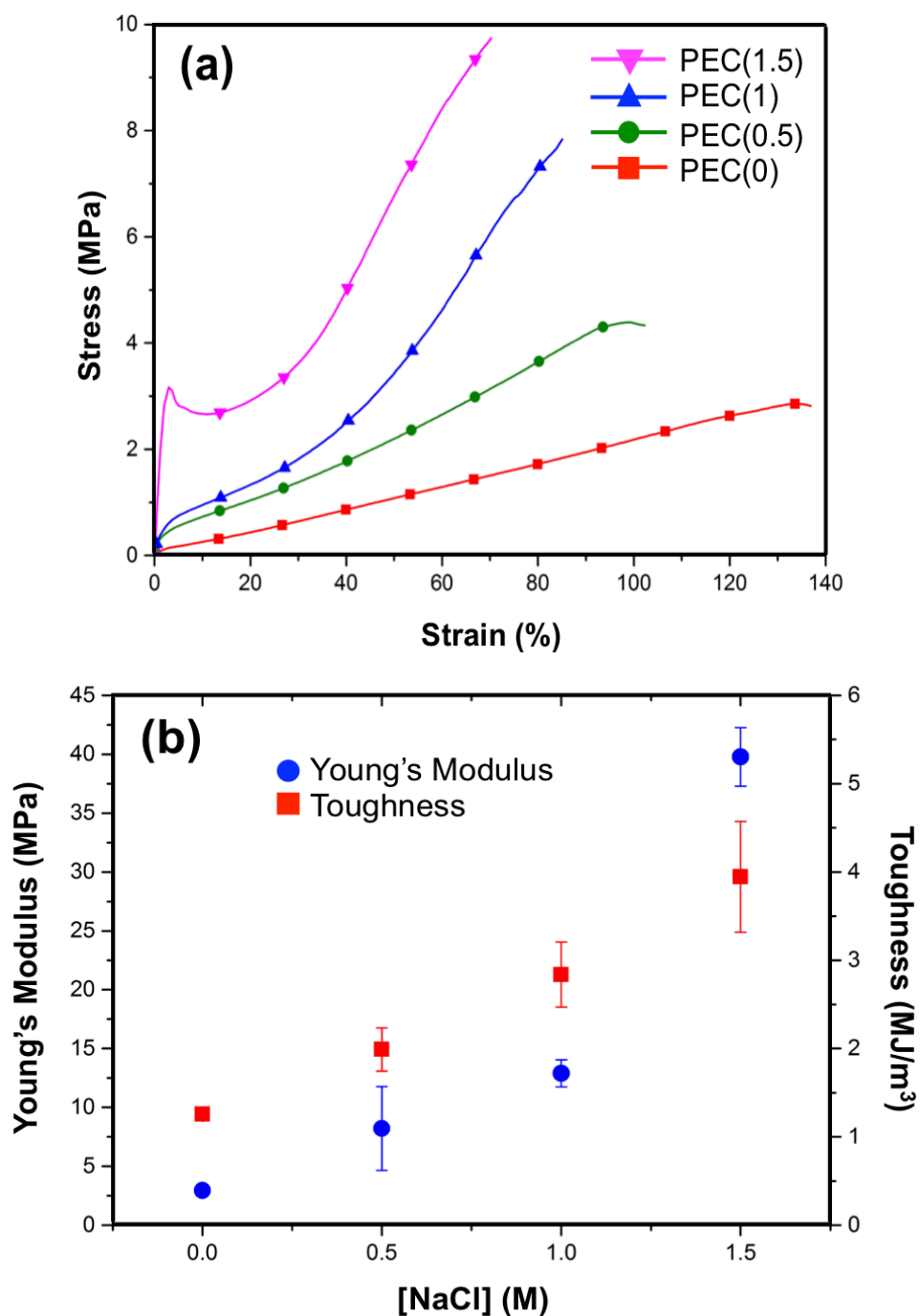


Figure 5.13 (a) Stress-strain curves (strain rate of 20%/min) and (b) Young's modulus and toughness of hydrated PDADMAC/PSS films as a function of [NaCl] used during processing.

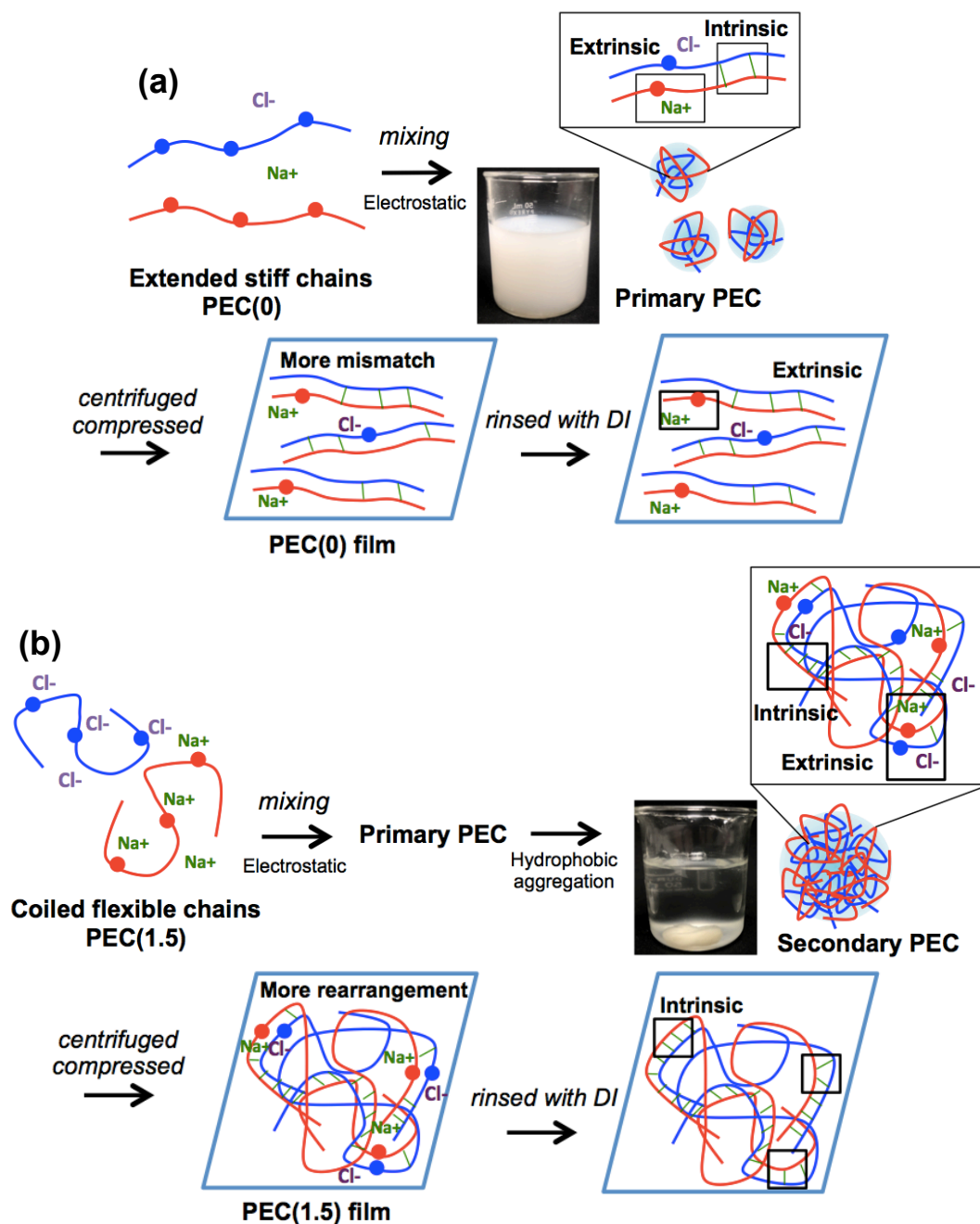


Figure 5.14 Schematic representation of salt influence PE chain conformation with (a) no add salt and (b) 1.5 M NaCl during complexation.

Results discussed here and in previous publication (Jaber, 2006) suggest that there is a strong interplay between the $[NaCl]$ used during the complexation and temperature. These two parameters having a strong effect on the

T_g and mechanical properties of the PEC. The complexes compose of “extrinsic” pairs of Na^+/Cl^- counterions-polymer and “intrinsic” sites of polyanion-polycation. Without salt, (Figure 5.14(a)), polymer chains behave as stiffly extended chains and create primary PEC during mixing. In compression step, these polymer pairs are rapidly packed without chain motion and then more “mismatch” extrinsic pairs were trapped in the polymer network after rinsing. In the latter case in Figure 5.14(b), the electrolyte chains prepared under 1.5 M NaCl exhibit as a flexible coiled structure. The primary PEC becomes more complicated structure, as secondary complex, govern by hydrophobic aggregation. At high salt concentration, the extrinsic compensation from added NaCl is the key to lowering the friction and the activation energy barrier lead to simplify the chain rearrangement and promote entanglement points (Liu *et al.*, 2017). After compression and rinsing step, these extrinsic sites convert to intrinsic polyanion-polycation pairs due to more chain rearrangement from salt softening effect (Shamoun, 2012). These phenomena provide free volume in an ionic network by electrostatic charge screening, enhance chain mobility, modify chain interaction and improve mixing during complexation. Both films provide different T_g because of the amount of intrinsic and extrinsic charge compensation coexist in the PEC (Das, 2017, Markarian, 2012), so, it can be stated that the mechanical properties of PEC films can be enhanced by preparing at high salt content due to the reduction of the ratio between extrinsic/intrinsic sites and the entanglement between polymer chains.

5.3.3 Effect of Polymer Molar Ratio on the Thermomechanical Properties of Salt-Free PEC Films

To investigate that the nonstoichiometric excess PDADMAC or PSS composition may affect the thermomechanical behavior of the PEC films, the E' of hydrated salt-free films were measured by DMA with submersion clamp. As seen in Figure 5.15, a glassy plateau with some hundred MPa of E' at low temperature suddenly drops to a few MPa of the rubbery regime when crossing a glass transition temperature (T_g) around room temperature (25 – 40°C). Interestingly, the shear E' as a function of temperature (Table 5.2) were found to increase with decreasing mol% of PDADMAC and the modulus of excess PSS film (PEC 33/67) remain nearly

hundred MPa while the E' of excess PDADMAC film (PEC67/33) decrease to only 6.2 ± 1.5 MPa at room temperature.

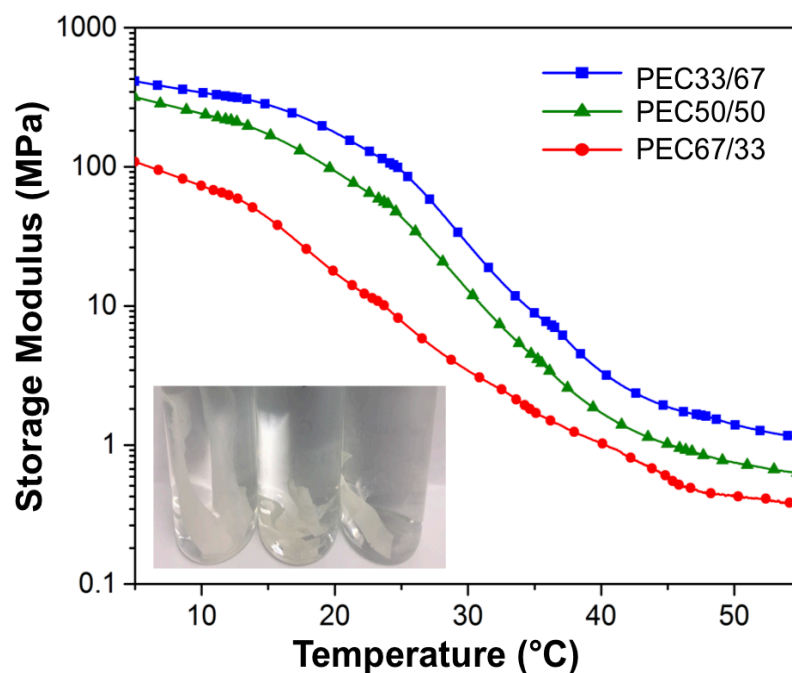


Figure 5.15 Storage modulus E' (rate $0.5^{\circ}\text{C}/\text{min}$, submersion clamp) with photographic images of PEC(1.5) films with different molar ratio after soaked in DI water overnight.

Table 5.2 The storage modulus of hydrated salt-free PEC at different molar ratio

Mol% fraction PDADMAC/PSS	Storage Modulus (MPa)		
	At 5°C	At 25°C	At 37°C
67/33	110.8 ± 17.2	6.2 ± 1.5	1.0 ± 0.4
50/50	314.2 ± 15.8	57.4 ± 14.1	3.6 ± 0.9
33/67	439.1 ± 40.7	94.3 ± 19.3	6.0 ± 0.4

The excess PDADMAC films reveal lower E' values due to the higher extrinsic charge compensation from counterion-balance and their hydrophilic nature, which confirm by the greater swelling behavior of PEC films with higher mol%

fraction of PDADMAC after soaking in water overnight (Figure 5.16). There are parameters controlling the E' of PEC films including the water absorption, films swelling caused by the breaking of ion pair cross-links and also extrinsic charged sites, which create the osmotic pressure within nonstoichiometric complexes leading to the swelling (Hariri, 2012).

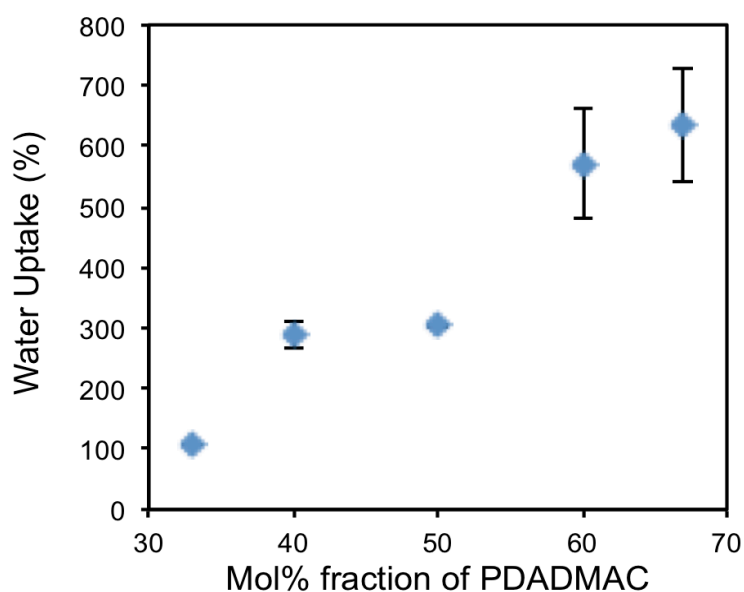


Figure 5.16 Water uptake at room temperature of PDADMAC/PSS films with various molar ratio of polymer.

It is evident that the DMA results obtained here are in good agreement with the stress-strain curve of hydrated PEC films from tensile testing at room temperature as in Figure 5.17(a). The decreasing of PDADMAC content significantly increases the maximum stress from 0.5 ± 0.4 MPa to 8.8 ± 1.1 MPa while the elongation at break decrease from 226.3 ± 43.6 % to 93.8 ± 6.7 %. Figure 5.17(b) illustrates Young's modulus (the initial slope of stress/strain) and toughness (area under the stress-strain curve) of hydrate PEC films. It was found that the modulus decrease with increasing PDADMAC fraction consistent with the reduction of crosslink density (Shamoun, 2012). However, the maximum toughness was observed with stoichiometric 1:1 film of about 5.5 MJ/m^3 , which depicts good mechanical

properties higher than poly(methylmethacrylate) used for tendons replacement of about 2 MJ/m^3 (Gorga, 2004). This is probably due to the higher “matching” polyanion-polycation pairs compare to “mismatch” species within nonstoichiometric PECs (Gai, 2016).

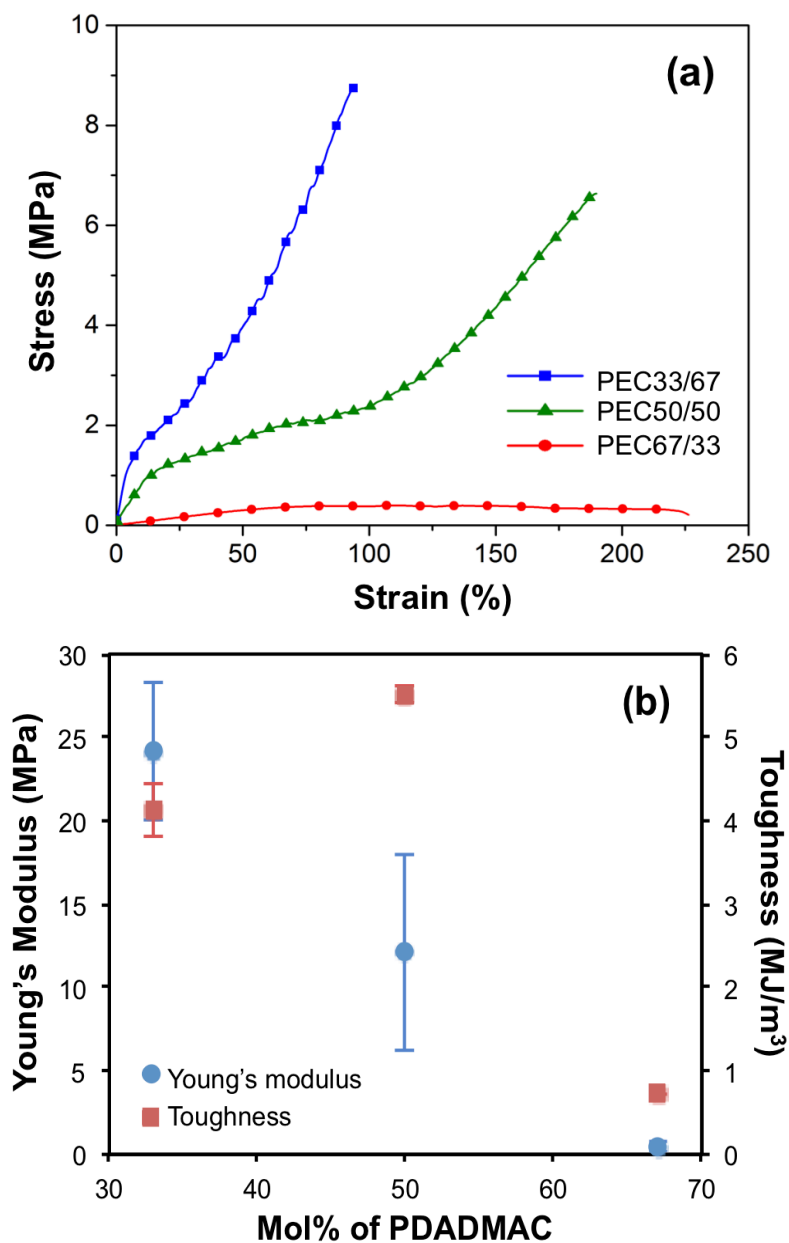


Figure 5.17 (a) Stress-strain curves (strain rate of 20%/min) and (b) Young's modulus and toughness of hydrated PEC(1.5) films with various the molar ratio of PDADMAC/PSS.

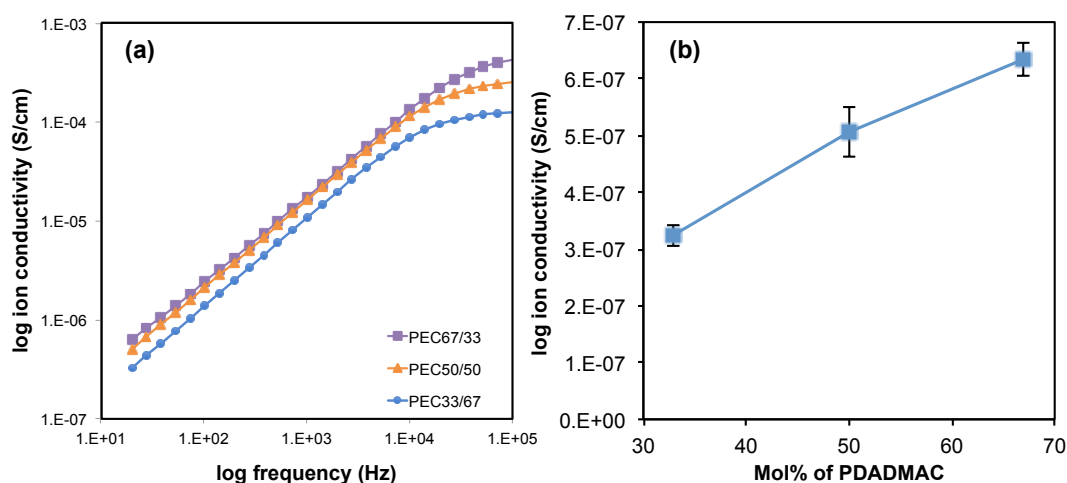


Figure 5.18 Ionic conductivities of hydrated PEC films prepared at different molar ratio of polymer after soaked in DI water.

The frequency dependent properties of hydrated salt-free PEC film (dimension of 1.7x1.7 cm) were studied by impedance spectroscopy. The ion conductivity (σ) was calculated according to eq. (5.4):

$$\text{The ion conductivity } (\sigma) \text{ (S/cm)} = \frac{L}{R \times A} \quad (5.4)$$

where L is the thickness of the film in cm, R is the resistance measured from the impedance spectroscopy using LCR meter (Agilent E4980A) with 1mV and A is a cross-sectional area between electrodes and membrane (2.89 cm²). Surprisingly, it can be observed from Figure 5.18 that at a given frequency the σ values of the film increase with increasing the amount of PDADMAC in the film, which is in contrast to the results from previous studies that the PSS-rich complexes provided high conductivity because the mobility of the positively charged Na⁺ counterions in excess PSS is higher than Cl⁻ ions in excess PDADMAC complexes (Imre, 2008, De, 2011). This might be speculated that the increase of the σ in PDADMAC-rich sample due to the lowering of crosslink density gain from temporary water screening Coulombic interaction between polycation - polyanion pair, which could accelerate the ion mobility. As known that the conductivity of PEC film increase with relative humidity (Michaels, 1965), this increasing σ of PDADMAC-rich film is consistent

with water uptake result obtained in Figure 5.16 that the PDADMAC-rich film had higher water content.

5.3.4 Shape Memory Effect of PEC Membranes

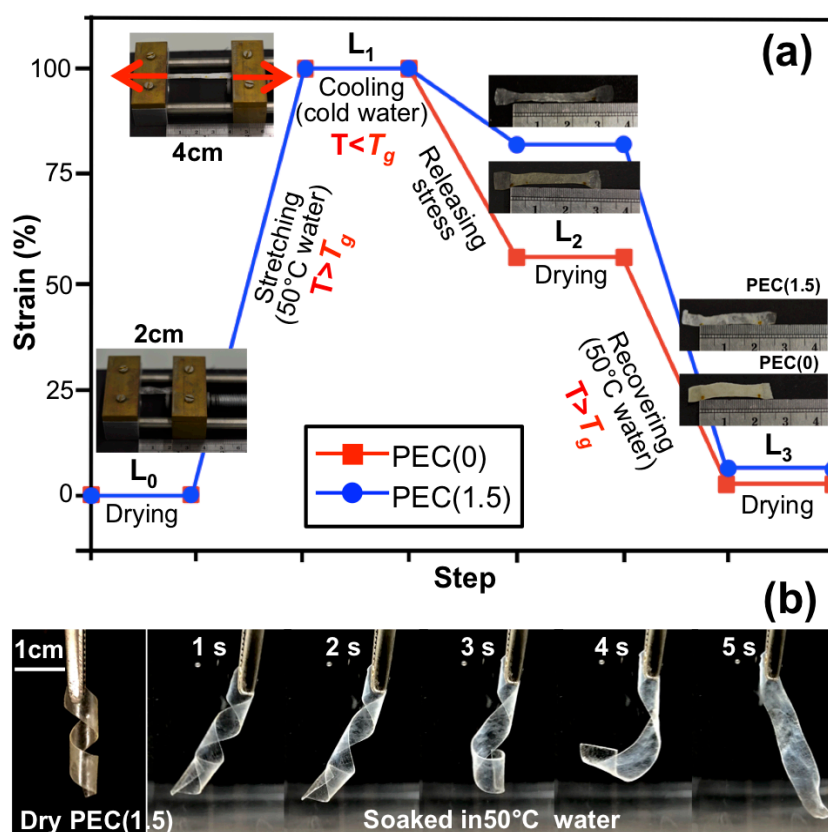


Figure 5.19 (a) Strain as a function of step during shape memory programming and release of compressed PDADMAC/PSS films and (b) a series of photographs illustrating the shape recovery of twisted PEC(1.5) film in 50°C water.

The use of PECs as water-activated shape memory materials has been proposed and demonstrated by Schlenoff *et al.* who programmed and released a temporary shape in extruded PDADMAC/PSS fibers by placing them in hot water (Wang, 2014). Figures 5.10 - 5.11 show that the materials studied here display the features necessary for shape memory, i.e., elastic behavior above T_g , which is necessary to recover the original (permanent) shape (Wang, 2016, Ledlein, 2002, Erkeçoğlu, 2016), and a glass transition around a convenient temperature that can

serve to fix a temporary shape. The shape memory behavior of films made from PEC(1.5) and PEC(0) is illustrated in Figure 5.19(a). Films having an original shape that was characterized by an original length $L_0 = 2$ cm were placed in 50°C water, and thus heated to a temperature $T > T_g$. The heated hydrated samples were stretched to a length $L_1 = 4$ cm and cooled while the strain $S = (L_1 - L_0)/L_0$ remained fixed at 100% by placing them in cold water, i.e., at $T < T_g$. When the stress was subsequently removed and the films were allowed to dry under ambient conditions, samples contracted slightly to the temporary shape (L_2). It was found that the PEC(1.5) film had an appreciable shape retention of $R_f = 80\%$ while PEC(0) had an $R_f =$ of 58%. One can speculate that this difference is mainly related to the different T_g s of the PECs and the fact that fixing was done at ambient temperature, where PEC(1.5) is already glassy, whereas PEC(0) still displays a significant chain mobility. When re-immersed in 50°C water ($T > T_g$), both films contracted within 5 s. In both cases, the recovered length (L_3) was slightly longer than the original length, with PEC(1.5) showing a higher recovery rate ($R_r = 72 \pm 6\%$) than PEC(0) ($52 \pm 2\%$). We speculate that the incomplete recovery is due to some reorganization of the ionic cross-links during deformation. The data acquired in the 1st heating, 1st cooling, and 2nd heating cycle of a submersion DMA experiment (Figure 5.20) can be nicely correlated to the shape memory behavior of the PEC films. When heating through T_g at about 30 – 40°C, the PEC(1.5) film can be stretched, as the film softens at this temperature. Upon cooling, the sample passes the glass transition at the same temperature, which leads to fixing by hardening of the film. The 2nd heating cycle confirms the ability to recover when E' is again decreased as the sample passes through T_g .

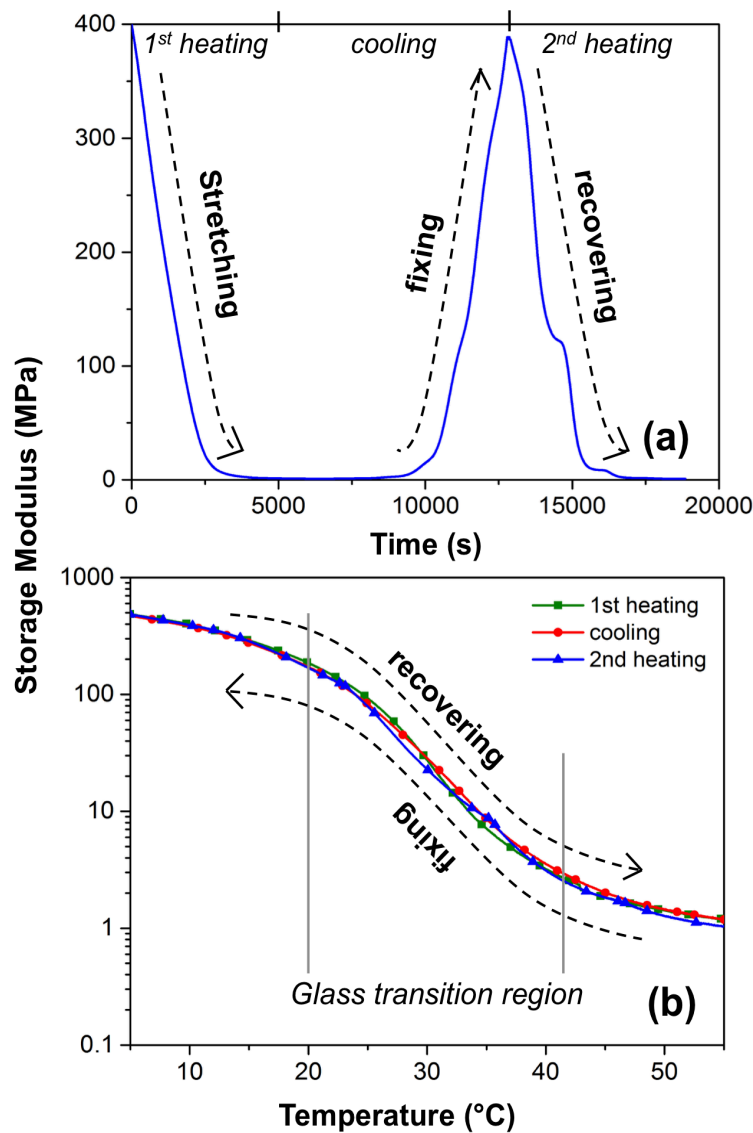


Figure 5.20 Storage modulus of PEC(1.5) film soaked in water measured during three cycles in which the temperature was increase to 55°C, decreased to 5°C, and increased again to 55°C (heating rate 0.5°C/min) as a function of time (a) and temperature (b).

In Figure 5.19(b), the deformation of a PEC(1.5) film into a spiral shape is shown as another example of the shape memory potential of the PEC membranes. After stretching in hot water, the film was rolled around a metal rod and dried at ambient to program a temporary spiral shape. This film returns autonomously to its original shape when immersed in 50°C water within 5 s and

displays a 10-times faster recovery speed than when hydrated at room temperature (within a minute). In the first case (recovery in 50°C water) the dry PEC film is rapidly heated above T_g of the water-swelled material (and the effect is largely diffusion limited), while in the latter case (recovery in room temperature water) the recovery occurs at a temperature where even after water take-up the glass transition has not fully been passed. The PEC films studied here are most useful when fully hydrated and the improved mechanical properties and higher cross-link density should render them useful for potential applications in medical devices where shape recovery is triggered by external humidity or body fluids (Lange, 2004), electrical devices such as flexible electrodes used in contact with aqueous electrolyte solutions, and also separating membranes for wastewater treatment.

5.4 Conclusion

The effect of added salt during the complex formation of PECs has been studied. The T_g of hydrated PEC was observed near room temperature and found to shift towards higher temperature when the [NaCl] during the mixing step was increased. At the same time, the materials became stronger and stiffer, while the elongation at break was reduced. Taken together, the data suggest that the polymer complex has either a more tightly bound network or a higher degree of chain entanglements. This is consistent with the expectation that at low [NaCl], the PEC is expected to rapidly form and stabilize by the formation of ion pairs without the possibility of much chain motion and therefore few entanglements. On the other hand at high [NaCl], the electrostatic charge screening imparted by the salt addition reduces the ionic interaction strength, enables extensive chain movements, and leads to an intricate mixing of the polymer chain and faster PEC aggregation. The PEC films also display interesting shape memory behavior, which certainly need to be further explored although a main limitation is the fact that the PEC needs to be in a moist environment. Further work with composite PEC could be interesting to further extend the T_g range as well as the shape memory behavior.

5.5 Acknowledgements

This work has been financially supported by the Petroleum and Petrochemical College, Grant for International Research Integration: Chula-Research Scholar, Ratchadaphiseksompot Endowment Fund and the Center of Excellence on Petrochemical and Materials Technology, Chulalongkorn University and the Development and Promotion of Science and Technology Talents (DPST) Project. The authors also acknowledge funding from the Adolphe Merkle Foundation, the Swiss National Science Foundation (Ambizione Grant no. PZ00P2_167900 to J.Z.) and the Swiss Confederation (doctoral scholarship to W.M.).

5.6 References

- Das, B. P., Tsianou, M. (2017) From polyelectrolyte complexes to polyelectrolyte multilayers: Electrostatic assembly, nanostructure, dynamics, and functional properties. *Advances in Colloid and Interface Science*, 244, 71-89.
- De, S., Cramer, C., Schönhoff, M. (2011) Humidity dependence of the ionic conductivity of polyelectrolyte complexes. *Macromolecules*, 44, 8936-8943.
- Erkeçoğlu, S., Sezer, A.D., Bucak, S. (2016) Smart delivery systems with shape memory and self-folding polymers. *InTechOpen*, DOI: 10.5772/62199.
- Fu, J., Abbett, R. L., Fares, H. M., Schlenoff, J. B. (2017) Water and the glass transition temperature in polyelectrolyte complex. *ACS Macro Lett.*, 6, 1114-1118.
- Hariri, H. H., Lehaf, A. M., Schlenoff, J. B. (2012) Mechanical properties of osmotically stressed polyelectrolyte complexes and multilayers: Water as a plasticizer. *Macromolecules*, 45, 9364-9372.
- Imre, Á. W., Schönhoff, M., Cramer, C. (2008) A conductivity study and calorimetric analysis of dried poly(sodium 4-styrene sulfonate)/poly(diallyldimethylammonium chloride) polyelectrolyte complexes. *J. Chem. Phys.*, 128, 134905.
- Jaber, J. A., Schlenoff, J. B. (2006) Mechanical properties of reversibly cross-linked ultrathin polyelectrolyte complexes. *J. Am. Chem. Soc.*, 128, 2940-2947.

- Lange, R., Tirrel, D. A. (2004) Designing materials for biology and medicine. Nature, 428, 487-492.
- Ledlein, A., Kelch, S. (2002) Shape-memory polymers. Angew. Chem. Int. Ed., 41, 2034-2057.
- Liu, Y., Momani, B., Winter, H. H., Perry, S. L. (2017) Rheological characterization of liquid-to-solid transitions in bulk polyelectrolyte complexes. Soft Matter, 13, 7443.
- Markarian, M. Z., Hariri, H. H., Reisch, A., Urban, V. S., Schlenoff, J.B. (2012) A Small-angle neutron scattering study of the equilibrium conformation of polyelectrolytes in stoichiometric saloplastic polyelectrolyte complexes. Macromolecules, 45, 1016-1024.
- Sadman, K., Wang, Q., Chen, Y., Keshavarz, B., Jiang, Z., Shull, K. R. (2017) Influence of hydrophobicity on polyelectrolyte complexation. Macromolecules, 50, 9417-9426.
- Wang, Q., Schlenoff, J. B. (2014) Tough strained fibers of polyelectrolyte complex: pretensioned polymers. RSC Adv., 4, 46675.
- Wang, W., Liu, Y., Leng, J. (2016) Recent developments in shape memory polymer nanocomposites: acuation methods and mechanisms. Coord. Chem. Rev., 320-321, 38-52.
- Zhang, Y., Yildirim, E., Antila, H. S., Valenzuela, L. D., Sammakorpi, M., Lutkenhaus, J. L. (2015) The influence of ionic strength and mixing ratio on the colloidal stability of PDAC/PSS polyelectrolyte complexes. Soft Matter, 11, 7392.

CHAPTER VI
IMPROVING THE MECHANICAL PROPERTIES OF
COMPOSITE POLYELECTROLYTE MULTILAYER THIN FILMS
AND COMPLEX MEMBRANES BY REINFORCEMENT WITH
CELLULOSE NANOCRYTALS

The possible utilization of polyelectrolyte systems both polyelectrolyte multilayers (PEMs) and polyelectrolyte complex (PEC) films was investigated toward the fabrication of composite films. As already discussed in previous chapters, these films were fabricated at nearly room temperature that suitable for preserving the activity of additive molecules. These hydrophilic and hydrophobic compounds can be loaded into PEMs or blended with PECs both during the fabrication and after the films were formed. However, to improve the mechanical properties of these polyelectrolyte membranes for specific purposes, such as drug delivery applications, bio or chemical sensors, fuel cell membrane or electrode for energy storage devices, need to be investigated. Numbers of polymer are commonly used as composite to improve their mechanical properties. In this chapter cellulose nanocrystals (CNCs) were deposited into layer-by-layer (LbL) PEM thin films or used as fillers in PEC membranes.

6.1 Proposed Research

As previous results, the hydrated PEC films prepared at high salt display not only stronger but also less swelling compared to these films fabricated at low salt concentration. Although these PEC films can be used in a wide range of pH and temperature, the hydrated films are swelled in hot water, which could limit the utilization of the films. Solving this weakness is an important objective and this study here aims to enhance their mechanical properties by reinforcement with cotton CNCs. The CNCs were synthesized from sulfuric acid hydrolysis of filter papers, which provides sulfate ester groups on the surface of cellulose nanoparticles. CNCs decompose below the melting transition of many polymers that make them not suitable for direct melt blending with polymer matrixes but our systems are

performed at room temperature, fabrication of PDADMAC/PSS films by solution mixing method and compression molding at 40°C (Figure 6.1(a)), can prevent the degradation of CNCs during the processing step.

The reinforced PEC membrane contributes to the study of improving the mechanical properties of free-standing based on PEM films using LbL deposition of cationic PDADMAC and anionic CNC. Before the multilayer film was fabricated on a sacrificial layer, which is later dissolved to release the multilayer film from the substrate making it free-standing. In this work, cellulose acetate (CA) was chosen as the sacrificial layer. CA is non-soluble in water but bears a negative-charge when immersed in neutral water because of the partial hydrolysis of the ester group (Ogawa *et al.*, 2007) and then PDADMAC/PSS primer layer was deposited on CA followed by PDADMAC/CNC layers as seen in Figure 6.1(b).

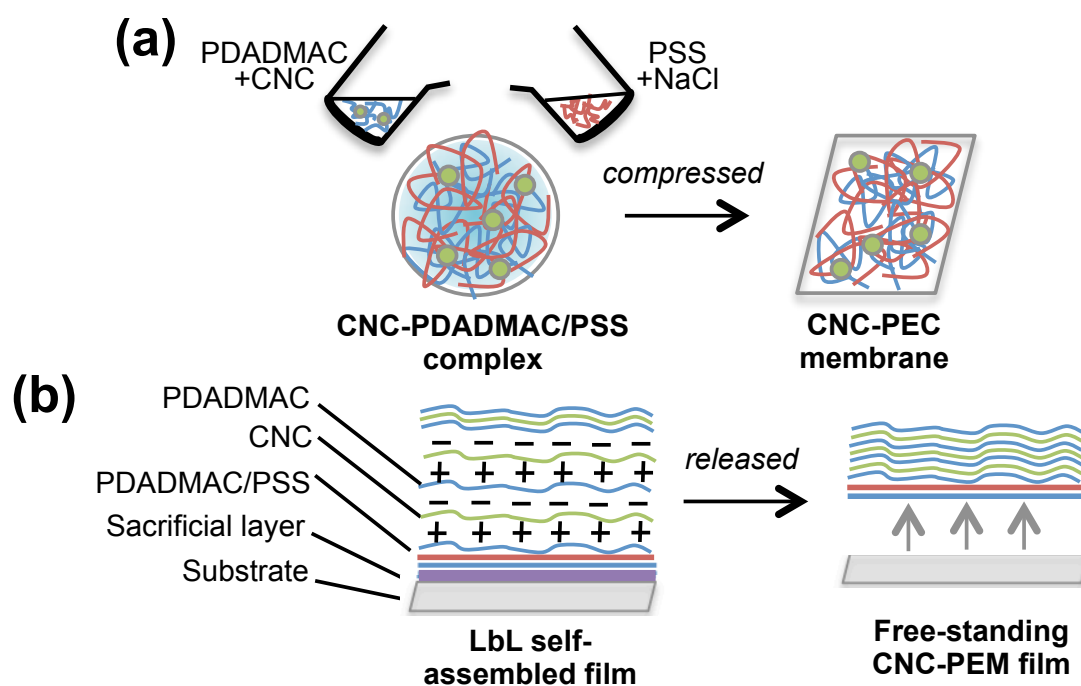


Figure 6.1 Schematic representation of CNC reinforced (a) PEC membrane and (b) free-standing PEM thin film.

6.2 Experimental

6.2.1 Chemicals and Materials

Poly(diallyldimethylammonium chloride) (PDADMAC, medium molecular weight, 20 wt.% in water, $M_w = 200,000-350,000$), Poly(sodium 4-styrene sulfonate) (PSS, $M_w = 70,000$), cellulose acetate (CA), sodium chloride (NaCl), and sulfuric acid were purchased from Sigma-Aldrich. Double distilled (DI) water was used for the aqueous phase.

6.2.2 Synthesis of Cotton CNCs

CNCs were isolated from Whatman No.1 filter paper by sulfuric acid hydrolysis. The 5.2 g of filter paper was cut and soaked in 250 ml DI water overnight. Then, vigorously blended with a kitchen blender to obtain pulp-like slurry and transferred to a beaker which cooled in an ice bath. The 140 ml of sulfuric acid was slowly dropped into the reaction that was kept below 30°C. After that the beaker was placed in 50°C oil bath and stirred for 3.5 h. The slightly yellow mixture was cooled in an ice bath to room temperature. Then the CNCs were separated from the liquid by centrifugation at 3500 rpm for 20 min and washed with DI water. This procedure was repeated until the supernatant was colorless and neutral. The CNC dispersion was dialyzed against DI water for 7 days, to remove any remaining salts, and the water being changed every day. The dispersion was frozen in liquid nitrogen and left it in the freezer at -20°C overnight. Finally, the CNC were lyophilized in a VirTis BenchTop 2K XL lyophilizer with a condenser temperature of -78°C for 3 days. The dry CNCs as white fluffy powder are achieved.

6.2.3 Improving the Mechanical Properties of PEC Membranes by Reinforcement with CNCs

6.2.3.1 *Fabrication of CNC-PEC Films by Compression Molding*

CNC-PEC were prepared by solution mixing of equimolar PDADMAC and PSS with a concentration of 0.1 M by stirring for 30 min and adjusted an ionic strength with vary NaCl concentration ($[NaCl]$). The 10 mg/ml of CNC was sonicated with DI water in a Badelin Sonorex Technik RL 70 UH ultrasound bath for 2 h at room temperature before adding to electrolyte solution. Blob complexes were compacted into dense precipitates by centrifugation at 8,000

rpm for 20 min and then compressed into a film by a Carver® press at 40°C under pressure of 2000 psi for 30 min using spacers to control the thickness of 100 μm .

6.2.3.2 Characterizations of the CNC-PEC Films

To eliminate NaCl effect, the PEC and CNC-PEC films were immersed in water for 2 days before the measurements. Mechanical behaviors of films were characterized by dynamic mechanical analysis (DMA) using a TA Instruments Model Q800 with submersion (rate 0.5°C/min) clamp at varied temperatures over the range 5 - 55°C. CNC-PEC films were investigated in term of preparation methods and CNC content: 5, 7.5, 10, 15 and 20 %w/w. Samples were cut in rectangular shapes of dimension 6 mm x 15 mm. The measurements were showed in multi-frequency strain mode using a temperature ramp, frequency sweep of 1 Hz, and a strain amplitude of 15 μm . The glass transition temperature (T_g) was determined at the glass-rubber transition, from the midpoint of the specific heat increment. While the thermal stability of films were characterized by thermogravimetric analysis (TGA). The temperature regime of 25 to 600°C with a heating rate of 10°C/min was used to analyze the dry samples. To determine the water uptake, the films were dried and soaked in water for 24 h, their dried and hydrated weights were calculated for %water uptake by:

$$\text{Water uptake (\%)} = \frac{W_h - W_d}{W_d} \times 100 \quad (1)$$

6.2.4 Improving the Mechanical Properties of Free-Standing PEM Thin Films by Reinforcement with CNCs

6.2.4.1 Preparation of Free-standing CNC-PEM Films

The PDADMAC and PSS solutions were prepared at a concentration of 10 mM with DI water, adjusted an ionic strength by 1 M NaCl. The 7%w/v CA was dissolved in acetone to fabricate a sacrificial layer. Glass slides cut to a size of 1.9 x 2.5 cm, were pre-treated with fresh piranha solution (3:1 v/v of 70% H_2SO_4 and 30% H_2O_2) for 1 hr and then rinsing with DI water. CA solution was dropped onto the pre-treated glass slides and then the substrated was rotated at 3000 rpm for 30 s. the CA-coated glass slide was immersed in PDADMAC solution for 30 mins and then fabricated the multilayer film by a LbL diped-coating with alternative polyelectrolyte solutions of PDADMAC and PSS with deposition time 1 min. Then

the film was rinsed with DI water for 1 min before immersing the film into the next solution and drying in air. For CNC-PEM films, the CA-treated glass slide was coated with a primer 5-layer PDADMAC/PSS. Then replaced the PSS solution with 10% CNC dissolved in DI water and used LbL to deposit the PDADMAC/CNC film. When the desired number of layers was achieved, the sacrificial layer was dissolved in acetone. The PEM slowly released from the edges of the glass slide withing a few minutes of immersion in acetone.

6.2.4.2 Characterization of the Freestanding CNC-PEM Films

The films with the desired number of PEM layers and CA-coated on glass slide were characterized by infrared spectroscopy (IR) in Attenuated Total Reflectancy (ATR) mode (Digilab FTS 7000). The thickness of the PEM films on pre-treated silicon wafer were measured by null-ellipsometer in polarizer-compensator-sample-analyzer mode (Multiskop, Optrel Berlin). The surface morphology of the free-standing films on mica substrate were observed by Atomic Force Microscopy (AFM) in Tapping mode (Park Systems).

6.3 Results and Discussion

6.3.1 Improving the Mechanical Properties of Composite PEC Membranes by Reinforcement with CNCs

6.3.1.1 *Fabrication of Salt-Free CNC-PEC Films*

The mechanical properties of PEC films, which were prepared by solution mixing of cationic PDADMAC and anionic PSS followed by centrifugation and compression of dense precipitates, can be enhanced by adding NaCl during processing. Although, these transparent and flexible films could be used in contact with aqueous solutions at a wide range of operating conditions, the hydrated films swelled in hot water, which could limit the usage of the films. To improve their mechanical properties, PEC films were reinforced with cotton CNCs. The fabrication of salt-free CNC-PEC membrane illustrates in Figure 6.2 and described in the Experimental Section. The order of mixing of CNCs in different electrolyte solutions and the amount of CNC content were studied in term of E' modulus and T_g transition

temperature. The slightly opaque and flexible membranes with a thickness in micron size were obtained after compression molding.

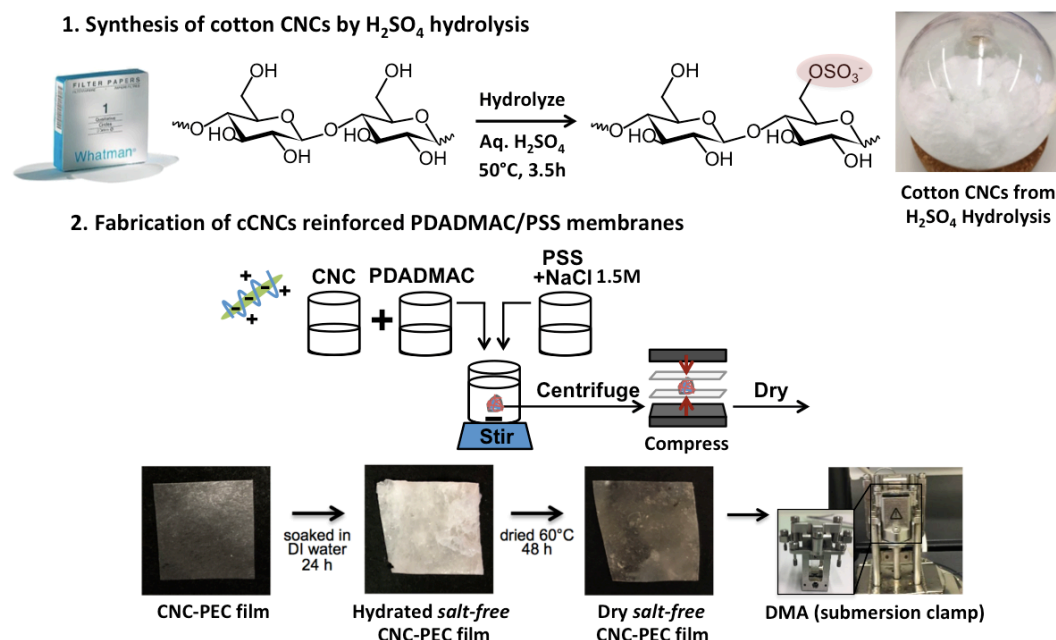


Figure 6.2 The fabrication of CNC-PDADMAC/PSS films prepared using a compression molding.

6.3.1.2 Effect of the Order of Mixing on the Storage Modulus of hydrated CNC-PEC Films

In this case, it cannot observe the T_g for dry CNC-PEC films from DMA because the films crack upon heating. So, the E' was measured with hydrated instead of dry films. The films were soaked in water overnight, in order to eliminate the effect of salt trapped inside the films, before characterization by DMA with submersion clamp. An important factor dominated the properties of films is the order of mixing and the presence of NaCl in solution as in Figure 6.3 and Table 6.1. The 10% CNC was stabilized by PDADMAC or PSS solution and then mixed with another oppositely charged electrolyte. The highest E' value was obtained from anionic CNC stabilized with cationic PDADMAC first and then mixed with PSS. In contrast, CNCs first mixed with the same charged PSS provides low E' value due to the competition between CNCs and PSS to form a complex with PDADMAC.

Additionally, the excess CNCs and free chain PSS trapped inside the polymer matrix allow to release out upon heating (Hariri, 2010), leads to increase osmotic pressure according to the Van't Hoff equation so that film swelling occurs (Köhler, 2005). Low E' value was observed when mixed CNCs with electrolyte solution containing NaCl because electrostatic repulsion between each particle was reduced by salt screening effect, which lead to the aggregation of CNCs (Qi, 2015). Using this method to prepare CNC-PEC complex by stabilized CNC with PDADMAC and then mixed with PSS containing 1.5 M NaCl (noted that overall final concentration of NaCl during complexation is 0.75M), the reinforcement of PEC film by CNC would be feasible.

Table 6.1 The storage modulus of CNC-PEC films at different the order of mixing

	PDADMAC Solution	PSS Solution	Storage Modulus (MPa)		
			At 5°C	At 25°C	At 37°C
A	CNC	-	313.8 ± 11.0	45.6 ± 10.1	8.0 ± 0.9
B	CNC	NaCl	479.0 ± 7.6	135.8 ± 2.9	18.7 ± 1.9
C	CNC+NaCl	NaCl	306.2 ± 7.9	24.8 ± 1.2	4.2 ± 0.8
D	NaCl	CNC	226.6 ± 12.2	17.4 ± 1.4	4.1 ± 0.0
E	NaCl	CNC+NaCl	152.9 ± 9.5	13.8 ± 2.2	4.1 ± 0.3

*when CNC = 10%CNC and NaCl = 1.5 M NaCl in each solution

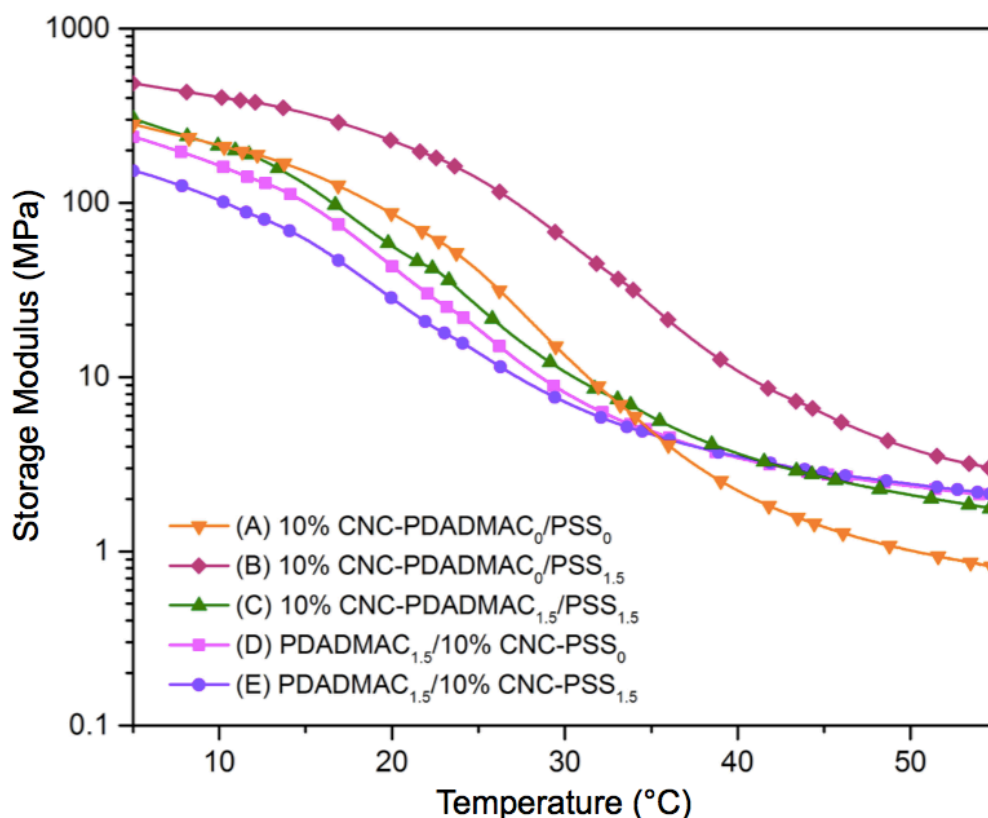


Figure 6.3 E' of hydrated PDADMAC/PSS films reinforced with 10% CNC at different conditions and the order of mixing (Rate $0.5^{\circ}\text{C}/\text{min}$), (A) CNC-PDADMAC mixed with PSS, (B) CNC-PDADMAC mixed with PSS-NaCl, (C) CNC-PDADMAC-NaCl mixed with PSS-NaCl, (D) PDADMAC-NaCl mixed with CNC-PSS, and (E) PDADMAC-NaCl mixed with CNC-PSS-NaCl ([NaCl] in each solution is 1.5 M).

6.3.1.3 Effect of the CNC Content on the Mechanical Properties of Hydrated PEC Films

The CNC contents also affect the mechanical properties of hydrated PDADMAC/PSS films as seen in Figure 6.4 and Table 6.2 that T_g occurs at 23.78 , 29.11 , 29.73 , 40.53 , 38.2 and 37.57°C for the films with 0, 5, 7.5, 10, 15 and 20% CNC, respectively. A significant shift of T_g to a higher temperature when adding CNCs may be understood to the result from the interaction of CNC fillers with PEC matrix. There are adequate of hydrogen atoms of CNCs that create the three-

dimensional hydrogen bonding with PDADMAC/PSS matrix and the strong network reinforcement was produced (Zhu, 2012). Increasing the CNC content up to 10%, the completely physical crosslink was created passing through a percolation point, which illustrates by the constant in T_g value at about 40°C. At this optimum point, the decrease in polymer chains mobility causes a slower rearrangement as a result of E' value at high temperature is higher than that of neat PEC film without CNCs (Köhler, 2005). After that the slight decrease in modulus and T_g were observed due to the aggregation of CNC and air-filled gaps at high reinforcement level (Hubbe, 2017) (Figure 6.5).

Table 6.2 The storage modulus of CNC-PEC films at different CNC content

%CNC	Storage Modulus (MPa)			T_g (°C)
	At 5°C	At 25°C	At 37°C	
0	230 ± 1	4.0 ± 0	1.1 ± 0	23.6
5	216 ± 15	20 ± 3	3.2 ± 1	29.1
7.5	232 ± 29	28 ± 7	3.8 ± 1	29.7
10	460 ± 25	126 ± 17	16 ± 2	40.5
15	429 ± 71	98 ± 36	14 ± 5	38.2
20	420 ± 47	114 ± 14	19 ± 2	37.6

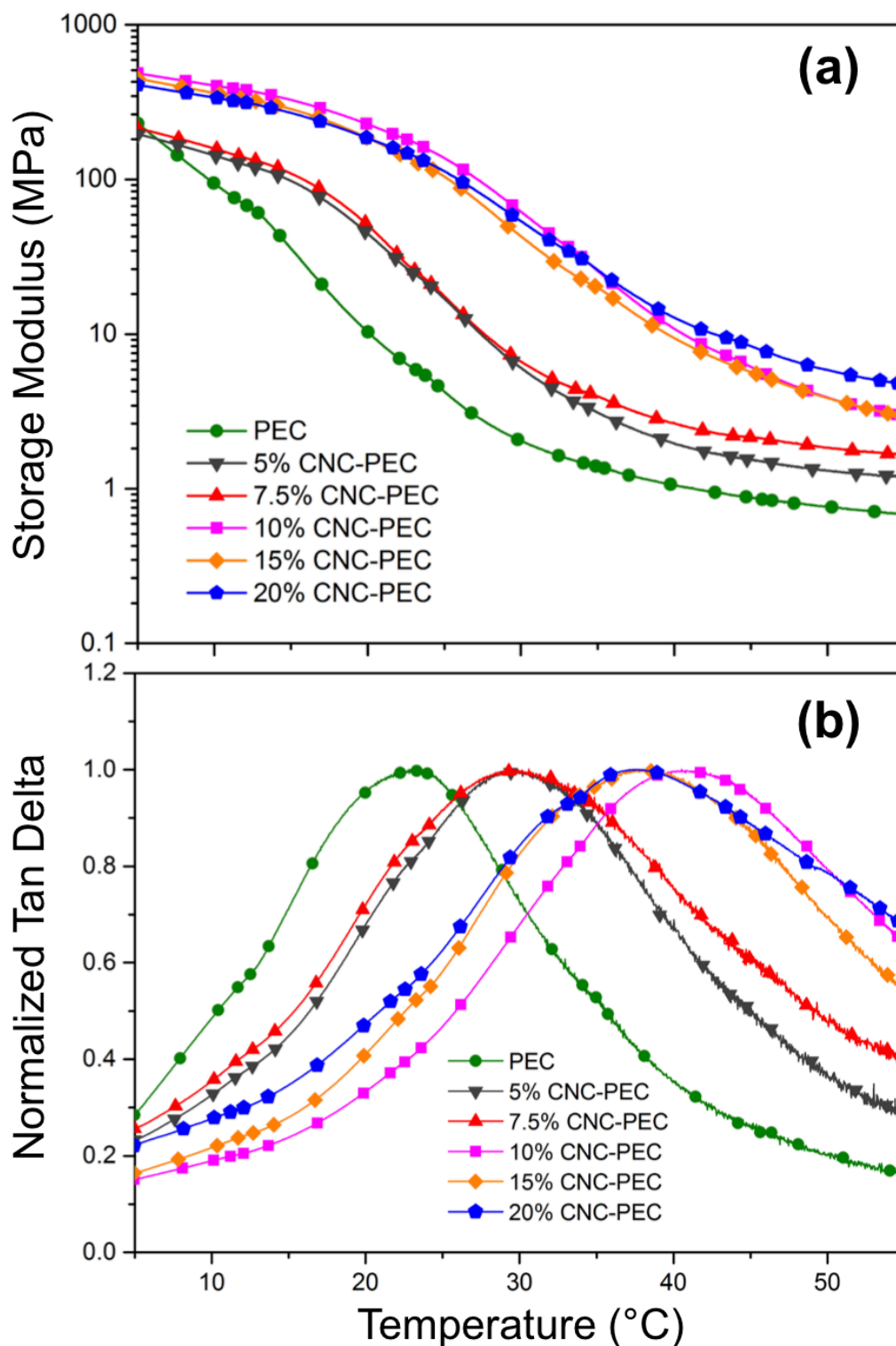


Figure 6.4 DMA measurement of hydrated PDADMAC/PSS films reinforced with different CNCs content. (a) Storage modulus E' and (b) normalized $\tan(\delta)$ (rate $0.5^\circ\text{C}/\text{min}$).

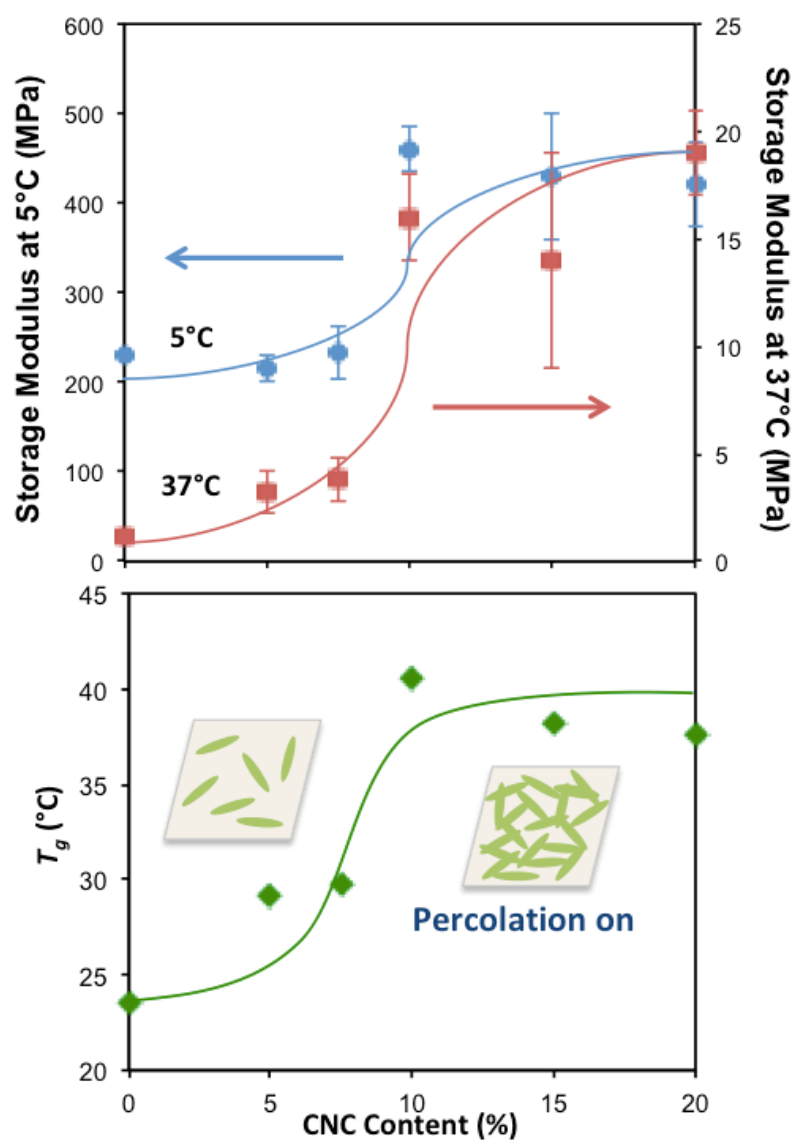


Figure 6.5 E' at 5°C from the graphs shown in Figure 6.4(a) and T_g extracted from the maxima of the $\tan(\delta)$ peaks shown in Figure 6.4(b) for the hydrated PDADMAC/PSS films as a function of CNCs content.

As seen in Figure 6.6, the water uptake of the film starts to decrease when adding CNC from 406 ± 12 % of pure PEC to 350 ± 39 % of 5%CNC-PEC and suddenly drop to 228 ± 38 % when passing through the percolation point at 10%CNC. The water content continuously decreases to 141 ± 19 % when the amount of CNC is 20 %. This evidence confirmed that the hydrophobic

CNC could be reinforced into PDADMAC/PSS matrix, which prevents both water adsorption and swelling effect lead to the increase in T_g values.

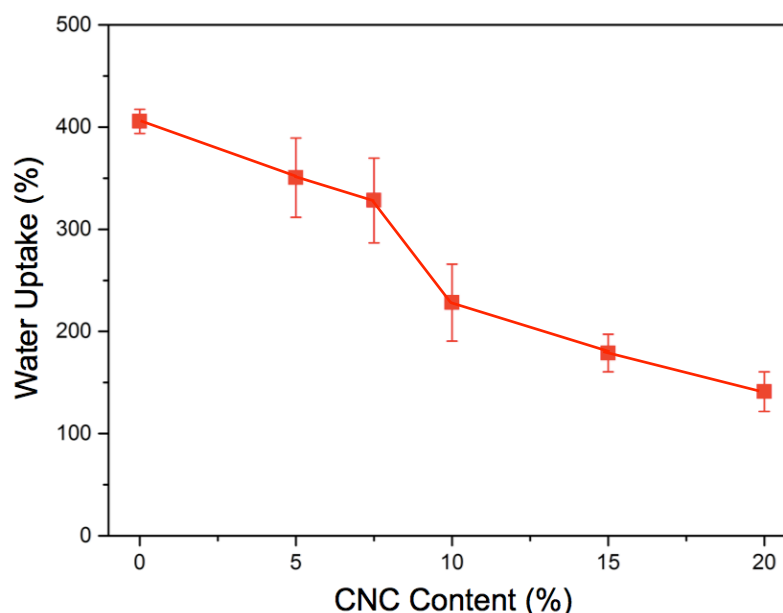


Figure 6.6 Water uptake for the hydrated PDADMAC/PSS films reinforcing with different CNCs content.

For practical use of CNC-PEC films, the thermal stability of the films was investigated. The films were dried in an oven at 60°C for 2 days before analysis with TGA. Thermogram in Figure 6.7 shows the significant weight loss occurred above 350°C for PEC films and decrease to 300°C when the CNC content increase to 20% due to the lower degradation temperature of CNCs. Comparing to the thermogram of CNCs powder (hydrolyzed from sulfuric acid of cotton) observed by Camarero-Espinosa (2015), CNCs start to degrade at about 200°C. The residual weight of PEC film at above 450°C is about 5% and CNC content in the film are about 20, 22 and 24 wt% for 5, 10 and 20% CNC-PEC film, respectively. Even though the CNC-PEC film start to degrade at lower temperature compare to the film without CNC and thermal degradation decrease with increasing the CNC content, these films utilize at the temperature below the degradation temperature of films, so, this limitation does not concern (Shamoun, 2012).

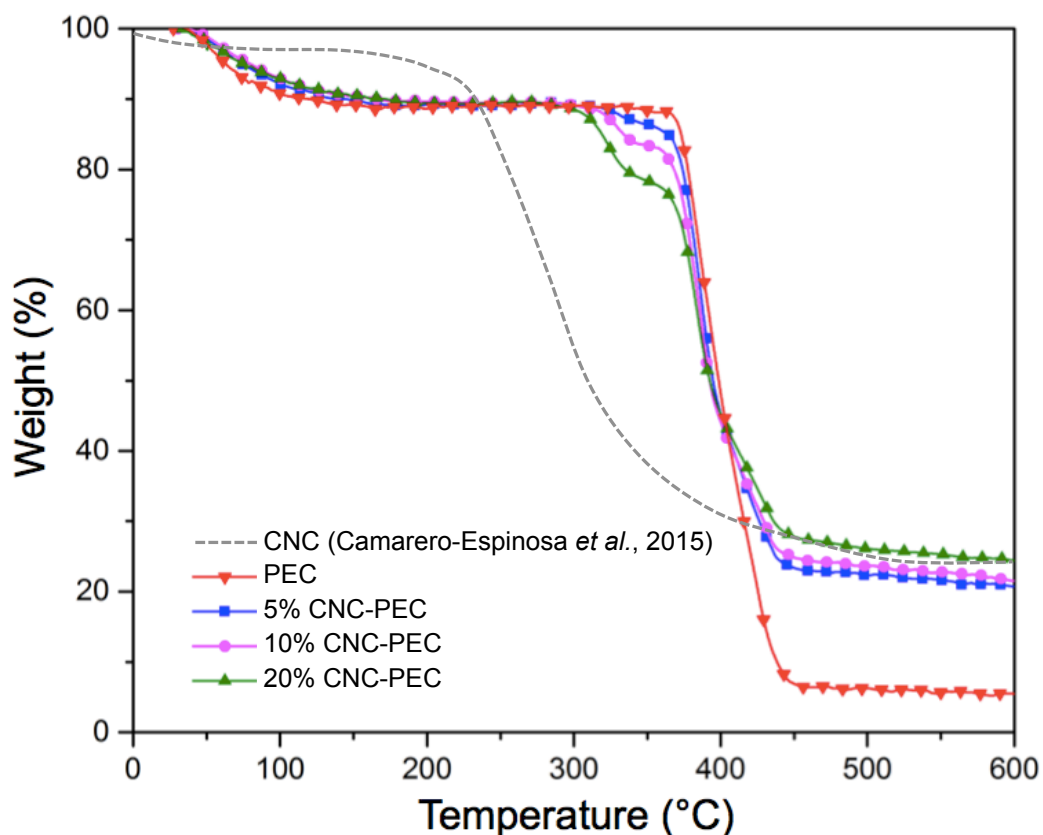


Figure 6.7 TGA thermogram of salt-free CNC-PEC films after soaked in water overnight (Dried at 60°C for 2 days) with heating rate 10°C/min.

A summary of T_g s determined of PEC films for high salt concentrations during complexation (from Chapter 5) and CNC reinforcement are shown in Figure 6.8. The E' of PEC film can be enhanced by both added salt and CNCs, which can confirm by the increasing of T_g near room temperature (24.3°C) of PEC(0) to 39.6 and 40.5°C of PEC(1.5) and 10%CNC-PEC film, respectively. It can be seen at 37°C that CNC-PEC film provides higher in E' modulus of 16 ± 2 MPa than that of neat PEC film (4.2 ± 2 MPa). In term of increasing [NaCl] during mixing, it can enhance the E' by increase chain mobility and entanglement lead to the conversion of extrinsic to intrinsic polymer pairs. However, the film prepared at high salt provides low E' at high temperature due to the relaxation of chains. Adding CNC into PEC film not only obstruct the chains movement but also create hydrogen bonding network of CNCs and electrostatic interaction with PDADMAC/PSS matrix.

In CNC-PEC films, high crystallinity CNCs can reinforce the PEC film at all range of accessible temperatures by both effects of dehydration and mechanical reinforcement.

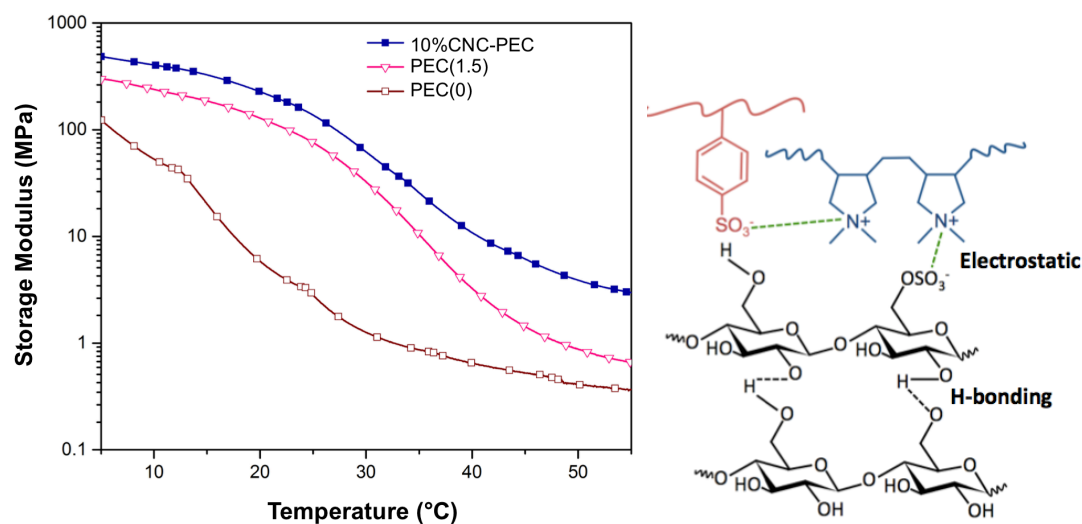


Figure 6.8 Thermal transitions of hydrated films of PDADMAC/PSS and CNC-PDADMAC/PSS from DMA with submersion clamp (Rate 0.5°C/min).

6.3.2 Improving the Mechanical Properties of LbL Assembled Free-Standing PEM Thin Films by Reinforcement with CNCs

The aim of this work is to investigate the LbL self-assembled free-standing films prepared from the PDADMAC and PSS multilayers as a matrix reinforcement with CNCs. The free-standing film was characterized by Fourier transform infrared (FTIR) spectroscopy while the films thickness was measured by ellipsometry. Morphology of film was investigated by atomic force microscopy (AFM).

6.3.2.1 Fabrication of Free-standing PEM films

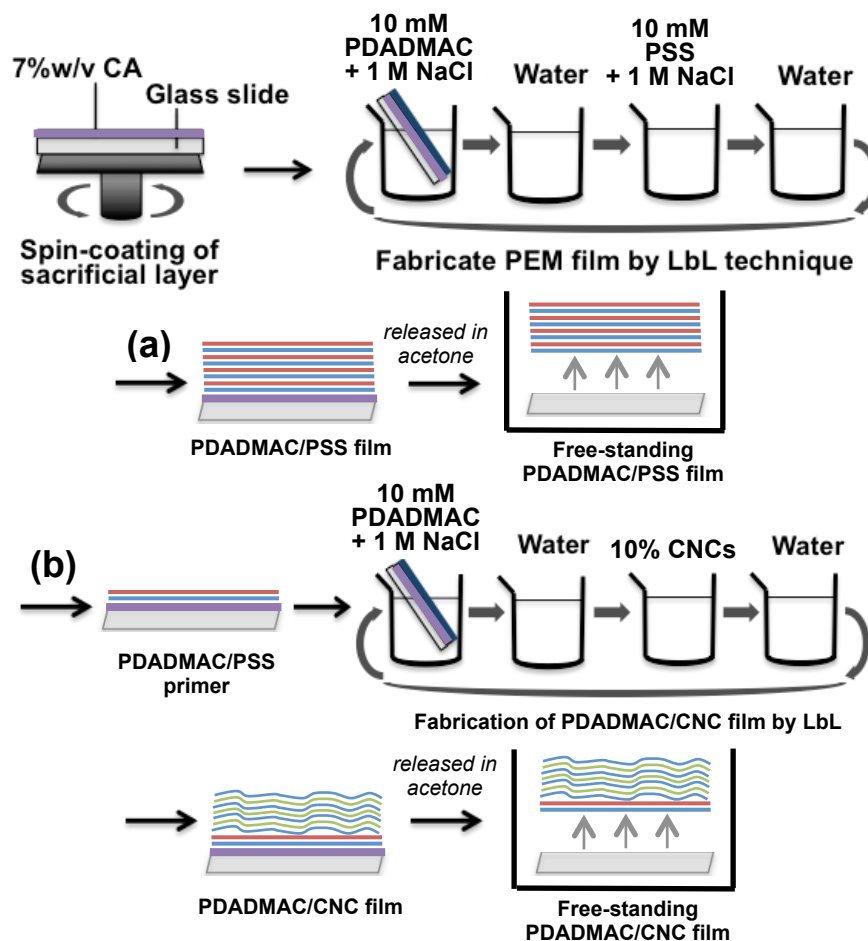


Figure 6.9 Procedure for fabrication of PDADMAC/PSS (a) and PDADMAC/CNC (b) free-standing nanofilm.

The LbL PEM were built on glass slides pre-treated with fresh piranha solution (3:1 v/v of 70% H_2SO_4 and 30% H_2O_2) for 1 hr (Warning! Piranha solution is a strong oxidizer and should be carefully when handled), it can remove organic impurities from substrates and make glass slides completely hydrophilic (Jian, 2013). This is followed by rinsing with DI water and finally drying with air. The procedure for fabricating the free-standing PEM film is schematically shown in Figure 6.9(a). First of all, the multilayer film with 10 mM PDADMAC/PSS was assembled LbL on a pre-treated glass slide, on which acetone-soluble CA was spin-

casted. Specifically, the CA-coated glass slide was immersed in PDADMAC solution for 30 mins. This is to ensure that PDADMAC saturates the surface before doing the LbL assembly. Then it was immersed in PSS solution for 1 min to build-up the second negative layer. The excess positive charge on PSS layer surface plays a role to induce the next PDADMAC layer. Then, remove the excess polyelectrolyte on surface of film by rinse with DI water for 1 min before immersing the film into the next solution and finally, dry in air. When the desired number of layers was achieved, the sacrificial layer was dissolved in acetone. The PEM gradually separated from the edges of the substrate withing a few minutes of immersion in acetone.

6.3.2.2 Characterizations of Free-standing PEM films

The infrared spectra were acquired by using Digilab FTS 7000 equipped with HgCdTe detector from 4000 to 600 cm^{-1} in Attenuated Total Reflectancy (ATR) mode. The nominal spectral resolution is 4 cm^{-1} . The ATR-IR spectroscopy was used to study by the changes in the intensity of characteristic peaks of PDADMAC/PSS multilayer deposited on the CA-modified glass slides by comparing between the characteristic peaks among the CA, PDADMAC, PSS and the PDADMAC/PSS film increasing the layers.

The ATR-IR spectra of the increasing number of layers of PEM on CA is shown in Figure 6.10 Spectrum for 7%w/v CA as a sacrificial layer spin-casted on glass slide, identified characteristic peak for acetate group of CA at 1738 cm^{-1} from C-O stretching vibration and its absorbance is going to drop with increasing number of layers of PEM. Also, intensity at 1430 cm^{-1} , which is attributed to the CH_3 asymmetric deformation, decreases because fo the increasing number of PEM layers from 5 to 20-bilayer. Likewise, the absorbance at 1220 cm^{-1} assigned to C-C-O acetate stretching decrease in the distance between the top of the PEM and the CA sacrificial layer (Maculi, 2006). The new peak around 1010 cm^{-1} , which is first observed when reach the 10-bilayer, is attributed to the S=O symmetric stretching vibration of the sulfonate (SO_3^-) group. In the same way, the peak at 1125 cm^{-1} , which is designated to the SO_3^- asymmetric stretching vibration and aromatic C-H in-plane bending, increases (Li, 2006). This confirms the increasing amount of PSS on the PEM. The amine (NH_4^+) group symmetric deformation peak (1650 cm^{-1})

derived from the PDADMAC were absent in form of NR_4^+Cl^- . Moreover, a small broad peak increases with increasing the deposit layer at around 2885 cm^{-1} related to NH_4^+ asymmetric deformation (Bragaru, 2012). The increasing absorbance of the characteristic peaks of PDADMAC and PSS proves the growth of the PEM films as a function of the number of layers. Furthermore, a broad peak at $3390 - 3450\text{ cm}^{-1}$, corresponding to the O-H stretching vibration of water, is observed and is result of the increasing hydrophilicity of the PEM film. Table 6.3 summarizes the ATR-IR spectra result, identified the characterized peak of PDADMAC/PSS film on glass slide spun with CA.

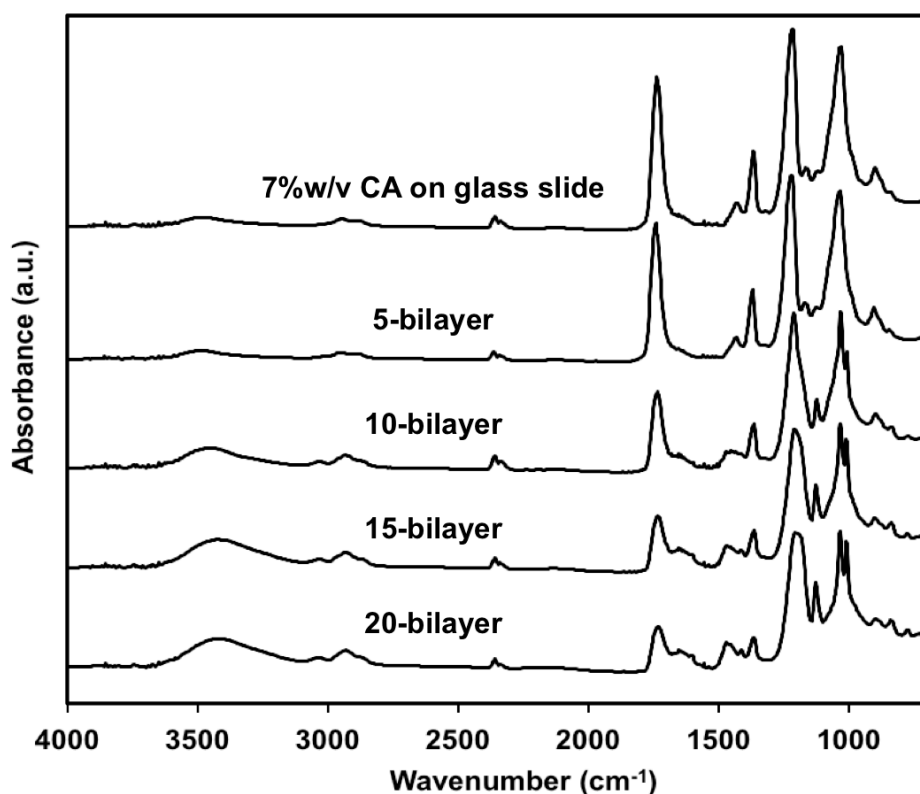


Figure 6.10 ATR-IR spectra 10 mM PDADMAC/PSS with 1M NaCl on CA-modified glass slide.

Table 6.3 Peak assignments for PDADMAC/PSS multilayer on the CA-coated glass slide

Identification peaks of CA	
Wavenumber (cm ⁻¹)	Indication results
1738	C-O stretching
1430	CH ₃ asymmetric deformation
1220	C-C-O acetate stretching
Identification peaks of PDADMAC/PSS multilayer	
Wavenumber (cm ⁻¹)	Indication results
1010	SO ₃ ⁻ symmetric stretching
1125	SO ₃ ⁻ asymmetric stretching
1650	NH ₄ ⁺ symmetric deformation

The growth of the PEM free-standing film was studied by measuring the absorbance of characteristic peaks at the number of layers increases (Figure 6.11). The absorbance at 1738 cm⁻¹ (characteristic peak for CA) decreases by as much as three times when PDADMAC and PSS were deposited on it. Additionally, the peak at 1125 cm⁻¹ (corresponding to the SO₃⁻ asymmetric stretching of PSS) (Wang, 2009) and the peak at 1650 cm⁻¹ (corresponding to the NH₄⁺ asymmetric deformation peak of PDADMAC) were found to slightly increase with the number of layers. The changes in the absorbance of the PEM characteristic peaks when the number of deposited bilayers is increased means that the films become thicker as a function of the number of PDADMAC/PSS bilayers.

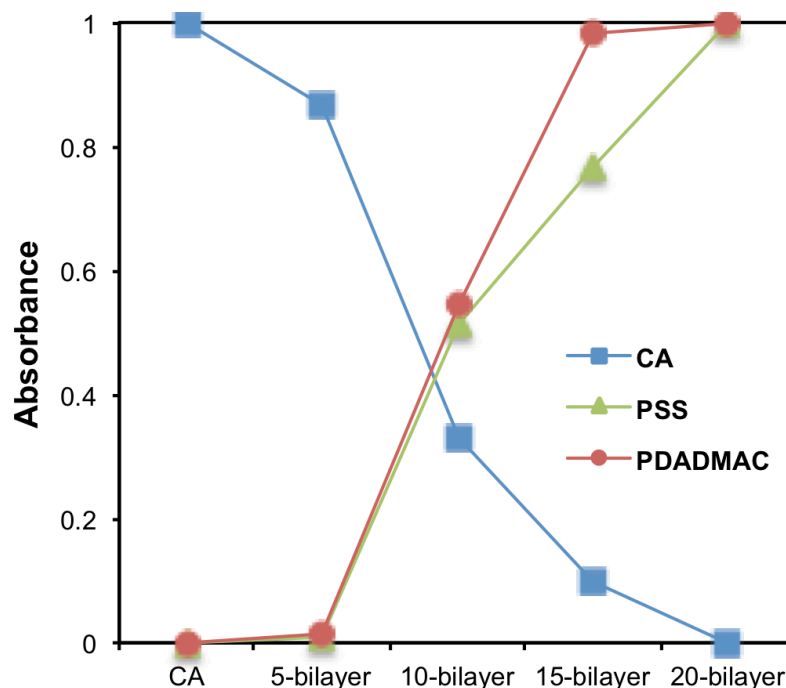


Figure 6.11 The absorbance for CA (1738 cm^{-1}), PSS (1125 cm^{-1}) and PDADMAC (1650 cm^{-1}) as a function of the number of PEM layers.

To measure the thickness of the PEM film, a parallel experiment was done on pre-treated silicon wafer. The PEM film was fabricated on a silicon wafer pre-treated with piranha solution followed by immersion in a hot ammonia solution. The thickness of the LbL film fabricated on the silicon wafer was measured by using a null-ellipsometer operating in polarizer-compensator-sample-analyzer (Multiskop, Optrel Berlin) mode. As a light source, a He-Ne laser ($\lambda = 632.8\text{ nm}$) was used, and the angle of incidence was set to 60 degree. A multilayer flat film model was used to calculate the thicknesses of the layered film from the experimentally measured ellipsometric angles, Δ and Ψ , assuming refractive indices of $n = 1.5$ for the polymer film. The thicknesses of the PEM as a function of the number of bilayers are shown in Figure 6.12(a). Odd layers represent PDADMAC layer, while even layers represent PSS layer. The measured thicknesses were 12.34, 45.87, 92.64 and 157.64 nm for 2, 4, 6, and 8 bilayers of PDADMAC and PSS, respectively. As expected, the thickness of the PEM film increases with increasing linearly after 4 PDADMAC/PSS bilayers, signifying that the thickness increases by

approximately 9.85 nm per layer. The values thickness of film calculated from ellipsometry measurement are 197.06, 295.58 and 394.11 nm for 10, 15 and 20 bilayers film, respectively. The average thickness of a single bilayer film was found to be 19.71 nm. The result was in agreement to the thickness of films for a 10 mM PDADMAC/PSS film with 1 M NaCl measure by ellipsometry by Dubas et al. (1999).

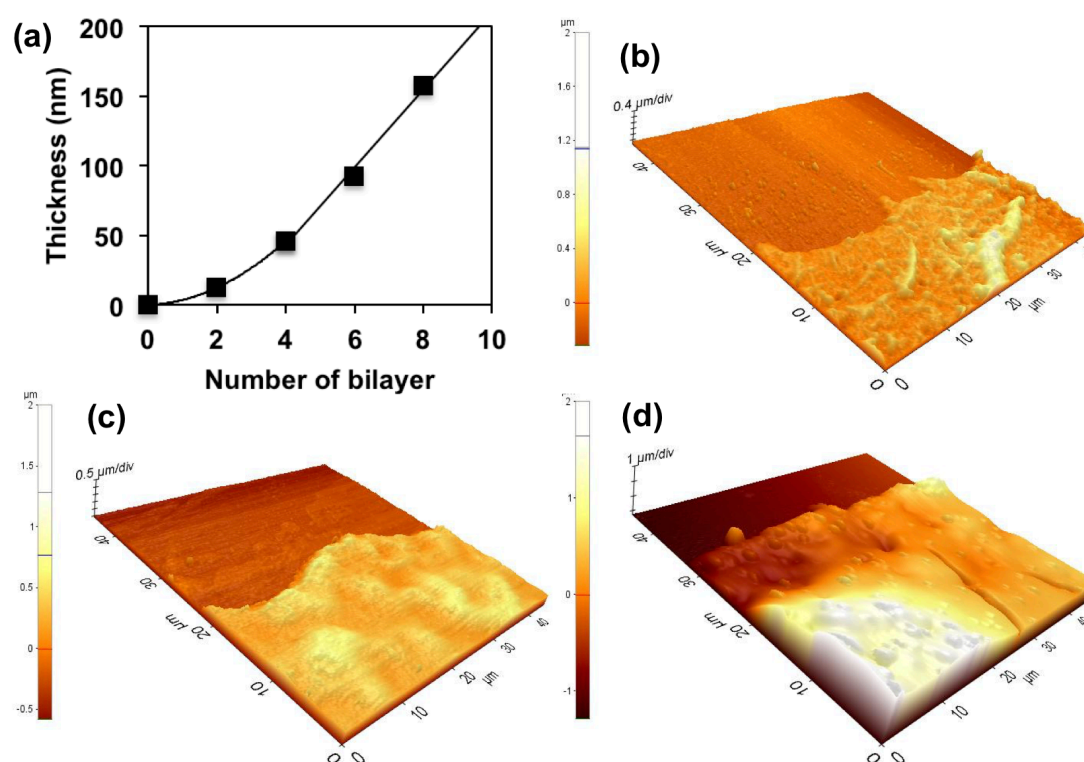


Figure 6.12 (a) The thickness of free-standing films with various number of bilayers measured from ellipsometry, AFM images of (b) 10-bilayer (c) 15-bilayer (d) 20-bilayer free-standing film on mica substrate.

To verify the thickness of free-standing film, the film was fabricated on the glass slide pre-coated with CA by the same condition as used as in ellipsometry analysis. Then, the film was released from the glass slide by immersing it in acetone. The released film was transferred to mica substrate. A floating film was put on a mica substrate for AFM. AFM used to study the surface morphology and roughness of free-standing PDADMAC/PSS film. All AFM images were recorded

using Park AFM system in Tapping Mode (Park Systems) with 45x45 μm scanner and scan rate 0.5 Hz. The AFM topographic images indicate the surface morphology of free-standing film after the deposition of 10, 15 and 20 PDADMAC/PSS bilayers after releasing in acetone are depicted in Figure 6.12(b)-(d), respectively. It was found that the surface of free-standing film was rough and not as flat as the mica surface. The root mean square (rms) roughness of the films was measured to be 189, 346 and 1325 nm for 10, 15, and 20 bilayers. The surface analysis of film showed a significant difference in the film thickness as a function of number of bilayer. With increasing the number of assembly layer, 10, 15, and 20 bilayers, thickness values of each film are 285, 664 and 746 nm, respectively. The increment for PDADMAC/PSS from 10 to 20 bilayers is almost 4 times higher. This demonstrates the importance role of the number of bilayer on the free-standing film thickness. Additionally, to compare the thickness of PDADMAC/PSS multilayer film between different characterization methods, it shows in Table 6.4. The thicknesses of free-standing film were found to double higher than the thickness of film calculated from ellipsometry technique, because the films floating in acetone lead to twisting the shape and not good attach with mica surface.

Table 6.4 Root mean square (rms) roughness and the thickness of PDADMAC/PSS multilayer film measure from AFM analysis and ellipsometry calculation

Number of bilayer	Thickness (nm)		Rms roughness (nm) from AFM
	from ellipsometry	from AFM	
10	197.06	285.0	189.0
15	295.58	664.0	346.0
20	394.11	746.0	1325.0

A 20-bilayer free-standing PDADMAC/PSS film was observed in a little bit opaque than a few layer film (Figure 6.13). The film was released from substrate by slowly drop of acetone onto the film. In order to transfer this film, which floats in acetone, without twisting the shape, we chose a PDMS as a flexible substrate to scoop the film in acetone.

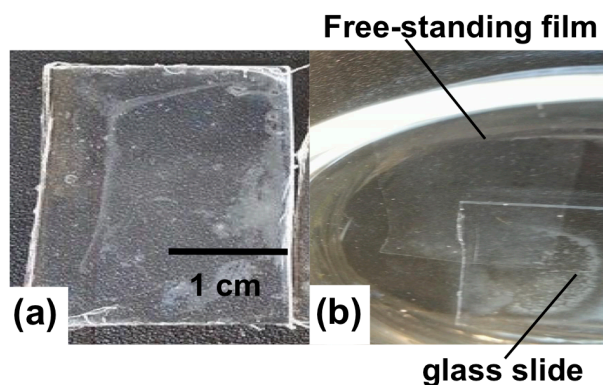


Figure 6.13 Photographic images for a 20-bilayer of free-standing PDADMAC/PSS film on glass slide (1.9x2.5 cm) (a) and film released from substrate in acetone (b).

6.2.2.3 Free-standing PEM films reinforcement with CNCs

However, the free-standing PDADMAC/PSS film is hard to manipulate and remove out from the solution. To improve the mechanical properties of these films, the anionic CNCs were used to replace with PSS and fabricate the LbL films. 5-layer PDADMAC/PSS primer was coated on the CA-treated glass slide and then LbL with PDADMAC/CNC containing 1 M NaCl. The free-standing film was released from the substrate by soaking in acetone. As seen in Figure 6.14 when increase the multilayers of PDADMAC/CNC film, the films display more opaque confirming the growth of PDADMAC/CNC film on the substrate.

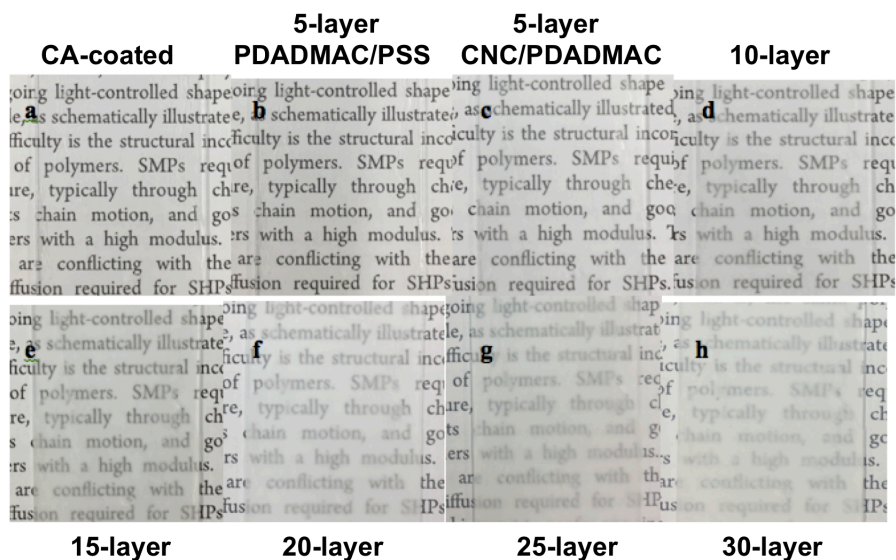


Figure 6.14 CA-coated on glass slide, LbL of 5-layer PDADMAC/PSS primer and PDADMAC/CNC film with increasing the number of layer from 5 to 30.

Figure 6.15 depicts the releasing of 20-layer PDADMAC/CNC film in acetone. The film was completely released out from a substrate within 10 min. The CNC film is easier to manipulate with half of the number of layers used to fabricate the neat PDADMAC/PSS films. The free-standing film reinforcement with CNCs is a potential way to improve the mechanical properties of film that can be applied to many applications.

PEM thin film fabricated from PDADMAC and PSS polyelectrolytes were used as a matrix for incorporating CUR to create a nanoadhesive patch. It can be conclude that the free-standing film based biocompatible PEM films can used as a patch for biomedical applications. The CUR patch is self-adhesive film with high flexibility and strong adhesion on the skin. The advantages of having a very thin patch are transparent which can see through the patch and can stick on the wound with any shape. Additionally, the PDADMAC/PSS free-standing films will have further study for in vitro applications such as tissue engineering, surgical application, and biosensing.

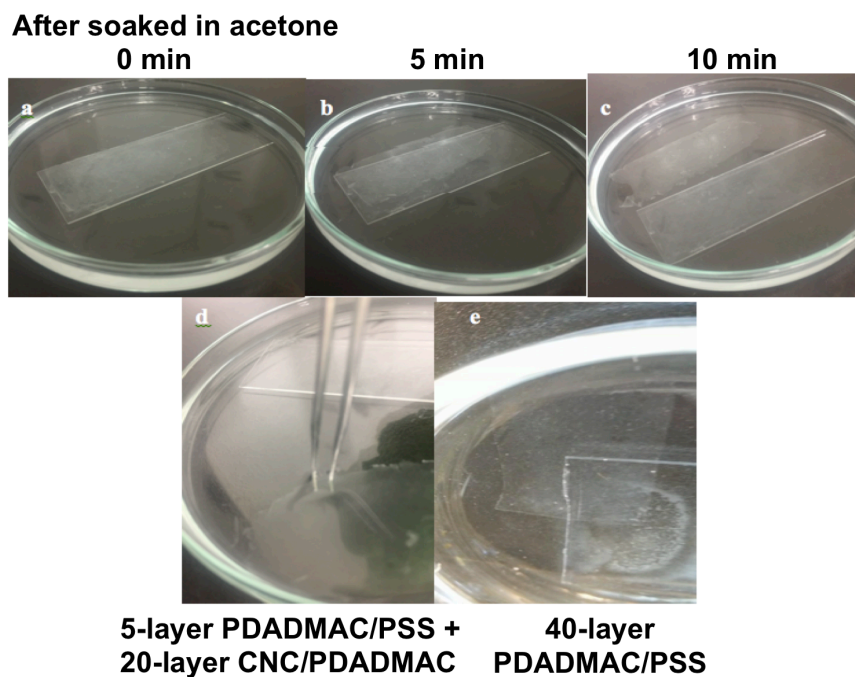


Figure 6.15 Free-standing film of 20-layer CNC/PDADMAC with 1 M NaCl after soaked in acetone. The film is easy to manipulate compare to 40-layer PDADMAC/PSS free-standing film.

6.5 Conclusion

The advantages of preparing composite polyelectrolytes by solution-mixing method and LbL deposition are required low temperature that prevent the degradation of CNCs or preserve the activity of additive molecules, short-time processing and can performed under aqueous solution. The CNCs provided more hydrophobicity that prevents the plasticizing effect from water absorption and creates strong hydrogen bonding inside the bulk film lead to not only a rise of the T_g up to 40°C but also improvement of E' at high temperature. It can be suggested that to prevent the aggregation of CNCs, which lead to the decrease in E' values, the system should perform without or low salt content and the amount of CNC ought to be at the percolation point. For PEM system, a new strategy to provide an improvement of the mechanical properties in free-standing nano-multilayer films has been presented. The PDADMAC/CNC floating film fabricated from LbL self-assembly provides more

ability to handle than a neat PDADMAC/PSS film. There are many potential applications of these composite PEMs and PECs blended with CNCs could then be applied for the drug delivery, sensors, fuel cell membrane or electrode for energy storage devices.

6.6 Acknowledgement

This work has been financially supported by the Petroleum and Petrochemical College, Grant for International Research Integration: Chula-Research Scholar, Ratchadaphiseksompot Endowment Fund and the Center of Excellence on Petrochemical and Materials Technology, Chulalongkorn University and the Development and Promotion of Science and Technology Talents (DPST) Project. The authors also acknowledge funding from the Adolphe Merkle Foundation, the Swiss National Science Foundation (Ambizione Grant no. PZ00P2_167900 to J.Z.) and the Swiss Confederation (doctoral scholarship to W.M.).

6.7 References

- Bragaru, A., Kusko, M., Radoi, A., Danila, M., Simion, M., Craciunoiu, F., Rascu, R., Mihalache, I., Ignat, T. (2012) Microstructures and growth characteristics of polyelectrolytes on silicon using layer-by-layer assembly. Cent. Eur. J. Chem., 11 (2), 205-214.
- Camarero-Espinosa, S., Boday, D. J., Weder, C., Foster, E. J. (2015) Cellulose nanocrystal driven crystallization of poly(D,L-lactide) and improvement of the thermomechanical properties. J. Appl. Polym. Sci., DOI: 10.1002/APP.41607.
- Dubas, S. T., Schlenoff, J. B. (1999) Factors Controlling the Growth of Polyelectrolyte Multilayers. Macromolecules, 32, 8153-8160.
- Hariri, H. H., Schlenoff, J. B. (2010) Saloplastic macroporous polyelectrolyte complexes: cartilage mimics. Macromolecules, 43, 8656-8663.

- Hubbe, M. A., Ferrer, A., Tyagi, P., Yin, Y., Salas, C., Pal, L., Rojas, O.J. (2017) Nanocellulose in thin films, coatings, and plies for packaging applications: A review. BioResources, 12(1), 2143-2233.
- Jaber, J. A., Schlenoff, J. B. (2006) Mechanical properties of reversibly cross-linked ultrathin polyelectrolyte complexes. Journal of American Chemical Society, 128, 2940- 2947.
- Jian, W., Xu, S., Wang, J., Feng, S. (2013) Layer-by-Layer assembly of poly(allylamine hydrochloride)/polyurethane and its loading and release behavior for methylene orange. J. Appl. Polym. Sci., 129 (4), doi: 10.1002/app.38921.
- Li, L., Ma, R., Iyi, N., Ebina, Y., Takada, K., Sasaki, T. (2006) Hollow nanoshells of layered double hydroxide. Chem. Commun., 3125-3127.
- Köhler, K., Shchukin, D. G., Möhwald, H., Sukhorukov, G. B. (2005) Thermal behavior of polyelectrolyte multilayer microcapsules. 1. The effect of odd and even layer number. Journal of Physical Chemistry B, 109, 18250-18259.
- Ogawa, T., Ding, B., Sone, Y., Shiratori, S. (2007) Super-hydrophobic surfaces of layer-by-layer structured film-coated electrospun nanofibrous membranes. Nanotechnology, 18, 165607.
- Qi, W., Xu, H. N., Zhang, L. (2015) The aggregation behavior of cellulose micro/nanoparticles in aqueous media. RSC Advances, 5, 8770.
- Shamoun, R. F., Reisch, A., Schlenoff, J. B. (2012) Extruded saloplastic polyelectrolyte complexes. Advanced Functional Materials, 22, 1923-1931.
- Volodkin, D., von Klitzing, R. (2014) Competing mechanisms in polyelectrolyte multilayer formation and swelling: Polycation-polyanion pairing vs. polyelectrolyte-ion pairing. Current Opinion in Colloid & Interface Science, 19, 25-31.
- Wang, Q., Hauser, P. J. (2009) New characterization of layer-by-layer self-assembly deposition of polyelectrolytes on cotton fabric. Cellulose, 16 (6), 1123-1131.

- Zhang, Y., Batys, P., O'Neal, J. T., Sammalkorpi, M., Lutkenhaus, J. L. (2018) Molecular origin of the glass transition in polyelectrolyte assemblies. ACS Central Science, 4, 638-644.
- Zhu, Y., Hu, J., Luo, H., Young, R. J., Deng, L., Zhang, S., Fan, Y., Ye, G. (2012) Rapidly switchable water-sensitive shape-memory cellulose/elastomer nano-composites. Soft Matter, 8, 2509-2517.

CHAPTER VII

CONCLUSION AND RECOMMENDATIONS

Throughout these chapters, it has been demonstrated that the assembly of two characteristic polyelectrolytes that are PDADMAC and PSS into either multilayer thin films (PEM) or complex membranes (PEC) is a versatile method to produce active films over a wide range of thicknesses and functionalities. The layer-by-layer (LbL) approach to fabricate nano-scale coatings is a mature process which can produce films with tunable properties but requires a solid support and can only be used as coating. In order to obtain stand-alone membrane, an increase in thickness from nano- to micro-scale films is necessary and can be achieved through PEC precipitates using the solution-mixing approach followed by compression molding. One of the main interest of using these PEC is their tunable stoichiometry which can infer either a cationic or anionic character to the membrane. Most of the work presented in these chapter related to the thermo-mechanical behaviors and sensing of these films which are sensitive to solvent, temperature, salt content during fabrication, and polymer molar ratio of cationic[P⁺]:anionic[P]. Another interesting feature of these polyelectrolyte membranes is their fabrication and processing simplicity making the process transferable to the industry since it is fairly inexpensive and based on non-toxic chemical soluble in water.

Based on the electrostatic nature of the PEM or PEC, it is well known that hydrophilic molecules can easily be embedded in the films, yet in Chapter 3 it was shown that even hydrophobic molecules such as curcumin (Cur) could also be incorporated. Between Chapter 3 and 4 an interesting parallel has been done between the tunable PEM top layer charges with the tunable PEC overall charge. Excess cationic or anionic character can be attributed to either the PEM or the PEC leading to the interesting applications of Cur in pH and ammonia sensors to be used in the food industry.

A big part of this work (Chapter 5) has been devoted to the understanding of the effect of salt on the thermo-mechanical both the glass transition temperature (T_g) and storage modulus (E') properties of these films. The salt was found to improve the E' and T_g of PEC films leading to the improvement of the shape memory effect.

The fact that PEM or PEC can be doped with molecules or nanoparticles can be used to modify or improve the properties of the pristine material. Lastly in Chapter 6, cotton cellulose nanocrystals (CNCs) isolated from sulfuric hydrolysis were used as reinforcing agent in each PDADMAC/PSS matrix. The unexpected shape memory, the modulus as well as the T_g shift in salt-free film has open a new way of fabricating PEC films that can produce films with tunable ion conductivity (σ) and are being developed in Fuel cells and in Super Capacitors.

REFERENCES

- Ajaykumar, T. M. (2014) Nanotechnology: Emerging tool in food sector. Research Journal of Biotechnology, 9, 12-24.
- Ariga, K., Yamauchi, Y., Rydzek, G., Ji, Q., Yonamine, Y., Wu, K.C.W., Hill, J.P. (2014) Layer-by-layer nanoarchitectonics: invention, innovation, and evolution. Chem. Lett., 43, 36-68.
- Azeredo, H. M. C., Rosa, M. F., Mattoso, L. H. C. (2016) Nanocellulose in bio-based food packaging applications. Ind. Crops Prod.
- Baxamusa, S. H., Stadermann, M., Aracne-Ruddle, C., Nelson, A. J., Chea, M., Li, S., Youngblood, K., Suratwala, T. I. (2014) Enhanced Delamination of ultrathin free-standing polymer films via self-limiting surface modification. Langmuir, 30, 5126-5132.
- Bertrand, P., Jonas, A., Laschewsky, A., Legras, R. (1999) Ultrathin polymer coatings by complexation of polyelectrolytes at interfaces: suitable materials, structure and properties. Macromol. Rapid Commun., 21, 319-348.
- Carvalho, D. M., Takeuchi, K. P., Grealine, R. M., Moura, C. J., Torres, M. C. L. (2015) Production, solubility and antioxidant activity of curcumin nanosuspension. Food Science and Technology, 31(1), 115-119.
- Correa, E. C., Jimenez-Ariza, T., Diaz-Barcos, V., Barreiro, P., Diezma, B., Oteros, R., Echeverri, C., Arranz, F. J., Ruiz-Altisent, M. (2014) Advanced characterisation of a coffee fermenting tank by multi-distributed wireless sensors: Spatial interpolation and phase space graphs. Food and Bioprocess Technology, 7, 3166-3174.
- Crespilho, F.N., Zucolotto, V., Oliveira Jr.O.N., Nart, F.C. (2006) Electrochemistry of Layer-by-Layer films: a review. Int. J. Electrochem. Sci., 194-214.
- Dautzenberg, H. (1997) Polyelectrolyte complex formation in highly aggregating systems. 1. Effect of salt: Polyelectrolyte complex formation in the presence of NaCl. Macromolecules, 30, 7810-7815.
- Decher, G. (1997) Fuzzy nanoassemblies: Toward layered polymeric multicomposites. Science, 277(5330), 1232-1237.

- Decher, G., Hong, J.D., Schmitt, J. (1992) Buildup of ultrathin multilayer films by a self-assembly process: III. Consecutively alternating adsorption of anionic and cationic polyelectrolytes on charged surface. Thin Solid Films, 210/211, 831-835.
- Decher, G., Schmitt, J. (1992) Fine-tuning of the film thickness of ultrathin of ultrathin multilayer films composed of consecutively alternating layers of anionic and cationic polyelectrolytes. Progress in Colloid and Polymer Science, 89, 160-164.
- Detsri, E., Popanyasak, J. (2015) Fabrication of silver nanoparticles/polyaniline composite thin films using Layer-by-Layer self-assembly technique for ammonia sensing. Colloids and Surfaces A: Physicochem. Eng. Aspects, 467, 57-65.
- Dobrynin, A.V. (2008) Theory and simulations of charged polymers: From solution properties to polymeric nanomaterials. Current Opinion in Colloid & Interface Science, 13, 376-388.
- Donath, E., Sukhorukov, G. B., Caruso, F., Davis, S. A., Möhwald, H. (1998) Novel hollow polymer shells by colloid-templated assembly of polyelectrolytes. Angewandte Chemie International Edition, 37(16), 2201-2205.
- Dubas, S.T., Schlenoff, J.B. (1999) Factors controlling the growth of PEMs. Macromolecules, 32, 8153-8160.
- Dubas, S.T., Schlenoff, J.B. (2001) Swelling and smoothing of PEMs by salt. Langmuir, 17, 7725-7727.
- Espinosa, S. C., Kuhnt, T., Foster, E. J., Weder, C. (2013) Isolation of thermally stable cellulose nanocrystals by phosphoric acid hydrolysis. Biomacromolecules, 14, 1223-1230.
- Estillore, N. C., Advincula, R. C. (2011) Stimuli-Responsive Binary Mixed Polymer Brushes and Free-Standing Films by LbL-SIP. Langmuir, 27(10), 5997-6008.
- Fu, J., Abbett, R. L., Rares, H. M., Schlenoff, J. B. (2017) Water and the glass transition temperature in a polyelectrolyte complex. ACS Macro Letters, 1114-1118.

- Fu, J., Wang, Q., Schlenoff, J.B. (2015) Extruded superparamagnetic saloplastic polyelectrolyte nanocomposites. *ACS Appl. Mater. Interfaces*, 7, 895-901.
- Fujie, T., Okamura, Y., Takeoka, S. (2007) Ubiquitous Transference of a Free-Standing Polysaccharide Nanosheet with the Development of a Nano-Adhesive Plaster. *Adv. Mater.*, 19, 3549-3553.
- Fujie, T., Park, J. Y., Murata, A., Estillore, N. C., Tria, M. C. R., Takeoka, S., Advincula, R. C. (2009) Hydrodynamic Transformation of a Freestanding Polymer Nanosheet Induced by a Thermoresponsive Surface. *Materials and Interfaces*, 1(7), 1404-1413.
- Gai, M., Frueh, J., Kudryavtseva, V.L., Mao, R., Kiryukhin, M.V., Sukhorukov, G.B. (2016) Patterned microstructure fabrication: polyelectrolyte complexes vs polyelectrolyte multilayers. *Sci. Rep.*, 6, 37000.
- Ge, A., Matsusaki, M., Qiao, L., Akashi, M., Ye, S. (2016) Salt effects on surface structures of PEMs investigated by vibrational sum frequency generation spectroscopy. *Langmuir*, 32, 3803-3810.
- Gelves, G. A., Lin, B., Sundararaj, U., Haber, J. A. (2006) Low electrical percolation threshold of silver and copper nanowires in polystyrene composites *Adv. Funct. Mater.*, 16, 2423-2430.
- Gentile, P., Carmagnola, I., Nardo, T., Chiono, V. (2015) Layer-by-Layer assembly for biomedical applications in the last decade. *Nanotechnology*, 26, 422001.
- Ghostine, R.A., Markarian, M.Z., Schlenoff, J.B. (2013) Asymmetric growth in polyelectrolyte multilayers. *Journal of the American chemical society*, 135, 7636-7646.
- Ghostine, R.A., Shanoun, R.F., Schlenoff, J.B. (2013) Doping and diffusion in an extruded saloplastic polyelectrolyte complex. *Macromolecules*, 46, 4089-4094.
- Goel, A., Kunnumakkara, A. B., Aggarwal, B. B. (2008) Curcumin as “curcumin”: From kitchen to clinic. *Biochemical Pharmacology*, 75, 787-809.
- Golmohammadi, H., Morales-Narváez, E., Naghdi, T., Merkoçi, A. (2017) Nanocellulose in sensing and biosensing. *Chem. Mater.*, 29, 5426-5446.

- Gong, X., Han, L., Yue, Y., Gao, J., Gao, C. (2011) Influence of assembly pH on compression and silver nanoparticle synthesis of polyelectrolyte multilayers. Journal of Colloid and Interface Science, 355, 368-373.
- Gucht, J.V.D., Spruijt, E., Lemmers, M., Stuart, M.A.C. (2011) Polyelectrolyte complexes: Bulk phases and colloidal systems. Journal of Colloid and Interface Science, 407-422.
- Hariri, H.H., Lehaf, A.M., Schlenoff, J.B. (2012) Mechanical properties of osmotically stressed polyelectrolyte complexes and multilayers: water as a plasticizer. Macromolecules, 45, 9364-9372.
- Hariri, H.H., Schlenoff, J.B. (2010) Saloplastic macroporous polyelectrolyte complexes: Cartilage mimics. Macromolecules, 43(20), 8656-8663.
- Hasan, S. A., Rigueur, J. L., Dickerson, J. H. (2010) Transferable graphene oxide films with tunable microstructures. ACS NANO, 4(12), 7367-7372.
- Hasan, S. A., Kavich, D. W., Dickerson, J. H. (2009) Sacrificial layer electrophoretic deposition of free-standing multilayered nanoparticle films. Chem. Commun., 3723-3725.
- Hazra, M. K., Roy, S., Bagchi, B. (2014) Hydrophobic hydration driven self-assembly of curcumin in water: similarities to nucleation and growth under large metastability, and an analysis of water dynamics at heterogeneous surface. Journal of Chemical Physics, 141, 18C501
- Huang, X., Bolen, M.J., Zacharia, N.S. (2014) Silver aided self-healing of polyelectrolyte multilayers. Phys. Chem. Chem. Phys., 16, 10267-10273.
- Hubbe, M. A., Ferrer, A., Tyagi, P., Yin, Y., Salas, C., Pal, L., Rojas, O.J. (2017) Nanocellulose in thin films, coatings, and plies for packaging applications: A review. BioResources, 12(1), 2143-2233.
- Jaber, J. A., Schlenoff, J. B. (2006) Mechanical properties of reversibly cross-linked ultrathin polyelectrolyte complexes. Journal of American Chemical Society, 128, 2940-2947.
- Jaber, J. A., Schlenoff, J. B. (2006) Recent developments in the properties and applications of polyelectrolyte multilayers. Current Opinion in Colloid & Interface Science 11, 324-329.

- Jagannathan, R., Abraham, P.M., Poddar, P. (2012) Temperature-dependent spectroscopic evidences of curcumin in aqueous medium: a mechanistic study of its solubility and stability. *J. Phys. Chem. B*, 116, 14533-14540.
- Jian, W., Xu, S., Wang, J., Feng, S. (2013) Layer-by-layer assembly of poly(allylamine hydrochloride)/polyurethane and its loading and release behavior for methylene orange. *Journal of Applied Polymer Science*. 129, 2070-2075.
- Jiang, C., Markutsya, S., Tsukruk, V.V. (2004) Compliant, robust, and truly nanoscale free-standing multilayer films fabricated using spin-assisted Layer-by-Layer assembly. *Advanced Materials*, 16(2), 157-161.
- Joe, B., Vijaykumar, M., Lokesh, B. R. (2004) Biological properties of curcumin-cellular and molecular mechanisms of action. *Crit. Rev. Food Sci. Nutr.*, 44, 97-111.
- Karibyants, N., Dautzenberg, H., Colfen, H. (1997) Characterization of PSS/PDADMAC-co-AA polyelectrolyte complexes and their stoichiometry using analytical ultracentrifugation. *Macromolecules*, 30, 7803-7809.
- Kelly, K.D., Schlenoff, J.B. (2015) Spin-coated polyelectrolyte coacervate films. *ACS Appl. Mater. Interfaces*, 7, 13980-13986.
- Kittitheeranun, P., Sanchavanakit, N., Sajomsang, W., Dubas, S.T. (2010) Loading of curcumin in polyelectrolyte multilayers. *Langmuir*, 26(10), 6869-6873.
- Köhler, K., Shchukin, D. G., Möhwald, H., Sukhorukov, G. B. (2005) Thermal behavior of polyelectrolyte multilayer microcapsules. 1. The effect of odd and even layer number. *Journal of Physical Chemistry B*, 109, 18250-18259.
- Köhler, R., Donch, I., Ott, P., Laschewsky, A., Fery, A., Krastev, R. (2009) Neutron reflectometry study of swelling of polyelectrolyte multilayers in water vapors: Influence of charge density of the polycation. *Langmuir*, 25(19), 11576-11585.
- Kuswandi, B., Jayus, Larasati, T. S., Abdullah, A., Heng, L. Y. (2012) Real-time monitoring of shrimp spoilage using on-package sticker sensor based on natural dye of curcumin. *Food Analytical Methods*, 5, 881-889.

- Kwon, H., Samain, F., Kool, E. T. (2012) Fluorescent DNAs printed on paper: sensing food spoilage and ripening in the vapor phase. Chemical Science, 3, 2542-2549.
- Lankalapalli, S., Kolapalli, V.R.M. (2009) Polyelectrolyte complexes: A review of their applicability in drug delivery technology. Indian Journal of Pharmaceutical Sciences, 71(5), 481-487.
- Lee, K. Y., Aitomäki, Y., Berglund, L. A., Oksman, K., Bismarck, A. (2014) On the use of nanocellulose as reinforcement in polymer matrix composites. Compos. Sci. Technol., 105, 15-27.
- Lee, W. H., Loo, C. Y., Debawy, M., Luk, F., Mason, R. S., Rohanizadeh, R. (2013) Curcumin and its derivatives: their application in neuropharmacology and neuroscience in the 21st century. Current Neuropharmacology, 11, 338-378.
- Li, G., Lee-Sullivan, P., Thring, R. W. (2000) Determination of activation energy for glass transition of an epoxy adhesive using dynamic mechanical analysis. Journal of Thermal Analysis and Calorimetry, 60, 377-390.
- Li, S. K., Zhang, L., Huang, F. Z., Yu, X. R., Xie, A. J. (2011) AuCl₄⁻ ion-assisted fabrication of bimetallic {Poly(ethylenimine)-Ag/Au} multilayer polyelectrolyte film and application in electrocatalysis. Thin Solid Films, 519, 5609-5615.
- Limsavarn, L., Sritaveesinsub, V., Dubas, S.T. (2007) Polyelectrolyte assisted silver nanoparticles synthesis and thin film formation. Materials Letters, 61, 3048-3051.
- Lin, C. L., Lin, J. K. (2008) Curcumin: a potential cancer chemopreventive agent through suppressing NF-κB signaling. Journal of Cancer Molecules, 4(1), 11-16.
- Lin, N., Dufresne, A. (2014) Nanocellulose in biomedicine: Current status and future prospect. Eur. Polym. J., 59, 302-325.
- Lynge, M.E., Laursen, M.B., Hosta-Rigau, L., Jensen, B.E.B., Ogaki, R., Smith, A.A.A., Zelikin, A.N., Stadler, B. (2013) Liposomes as drug deposits in multilayered polymer films. ACS Appl. Mater. Interfaces, 5, 2967-2975.

- Ma, Y., Sun, J., Shen, J. (2007) Ion-triggered exfoliation of layer-by-layer assembled poly(acrylic acid)/poly(allylamine hydrochloride) films from substrates: A facile way to prepare free-standing multilayer films. Chem. Mater., 19, 5058-5062.
- Maheshwari, R. K., Singh, A. K., Gaddipati, J., Srimal, R. C. (2006) Multiple biological activities of curcumin: A short review. Life Sciences, 78, 2081-2087.
- Mahmood, K., Zia, K. M., Zuber, M., Salman, M., Anjum, M. M. (2015) Recent developments in curcumin and curcumin based polymeric materials for biomedical applications: A review. International Journal of Biological Macromolecules, 81, 877-890.
- Mermut, O., Lefebvre, J., Gray, D.G., Berrett. (2003) Structure and mechanical properties of polyelectrolyte multilayer films studied by AFM. Macromolecules, 36, 8819-8824.
- Mertz, G., Bour, J., Toniazzo, V., Ruch, D., Ball, V. (2013) Deposition of polyelectrolyte multilayer films made from PDADMAC and PSS: Influence of NaCl concentration for film obtained by alternated spraying and alternated dipping. Colloids and Surfaces A: Physicochem. Eng. Aspects, 415, 77-85.
- Michaels, A. (1965) Polyelectrolyte complexes. Industrial and Engineering Chemistry, 57(10), 32-40.
- Michaels, A.S., Miekka, R.G. (1961) Polycation-polyanion complexes: preparation and properties of poly-(vinylbenzyltrimethylammonium) poly-(styrenesulfonate). J. Phys. Chem., 1765-1773.
- Ng, L.Y., Mohammad, A.W., Ng, C.Y., Leo, C.P., Rohani, R. (2014) Development of nanofiltration membrane with high salt selectivity and performance stability using polyelectrolyte multilayers. Desalination, 351, 19-26.
- Pandey, A., Gupta, R. K., Srivastava, R. (2011) Curcumin-the yellow magic. Asian J. Applied Sci., 4 (4), 343-354.
- Patel, R., Singh, S. K., Sheth, N. R., Gendle, R. (2009) Development and characterization of curcumin loaded transfersome for transdermal delivery. J. Pharm. Sci. & Res., 1 (4), 71-80.

- Porcel, C.H., Schlenoff, J.B. (2009) Compact polyelectrolyte complexes: “Saloplastic” candidates for biomaterials. Biomacromolecules, 10, 2968-2975.
- Pothukuchi, S., Li, Y., Wong, C.P. (2004) Development of a novel polymer-metal nanocomposite obtained through the route of in situ reduction for integral capacitor application. Journal of Applied Polymer Science, 93, 1531-1538.
- Potter, K. A., Jorfi, M., Householder, K. T., Foster, E. J., Weder, C. (2014) Curcumin- releasing mechacially adaptive intracortical implants improve the proximal neuronal density and blood-brain barrier stability. Acta Biomaterialia, 10, 2209-2222.
- Pourreza, N., Golmohammadi, H. (2015) Application of curcumin nanoparticles in a lab-on-paper device as a simple and green pH probe. Talanta, 131, 136-141.
- Prasad, S., Gupta, S. C., Tyagi, A. K., Aggarwal, B. B. (2014) Curcumin, a component of golden spice: From bedside to bench and back. Biotechnology Advances, 32, 1053-1064.
- Reisch, A., Roger, E., Phoeung, T., Antheaume, C., Orthlieb, C., Boulmedais, R., Lavalle, P., Schlenoff, J.B., Frisch, B., Schaaf, P. (2014) On the benefits of rubbing salt in the cut: Self-healing of saloplastic PAA/PAH compact polyelectrolyte complexes. Adv. Mater., 26, 2547-2551.
- Richardson, J.J., Cui, J., Björmalm, M., Braunger, J.A., Ejima, H., Caruso, F. (2016) Innovation in layer-by-layer assembly. Chemical Reviews, 116, 14828-14867.
- Richert, L., Lavalle, P., Payan, E., Shu, X. Z., Prestwich, G. D., Stoltz, J. F., Schaaf, P., Voel, J. C., Picart, C. (2004) Layer by layer buildup of polysaccharide films: Physical chemistry and cellular adhesion aspects. Langmuir, 20, 448-450.
- Rydzek, G., Ji, Q., Li, M., Schaaf, P., Hill, J.P., Boulmedais, F., Ariga, K. (2015) Electrochemical nanoarchitectonics and Layer-by-Layer assembly: From basics to future. Nano Today, 10, 138-167.
- Saikaew, R., Bijaisoradat, O., Netcharoensirisuk, P., Dubas, S. T. (2016) Improved pH sensing of curcumin loaded polyelectrolyte multilayers thin films. Sensor Letters, 14(6), 572-576.

- Schaaf, P., Schlenoff, J.B. (2015) Saloplastics: Processing compact polyelectrolyte complexes. *Adv. Mater.*, 27, 2420-2432.
- Schlenoff, J.B. Charge balance and transport in ion-paired polyelectrolyte multilayers. (2012) Multilayer thin films: Sequential assembly of nanocomposite materials, second edition. Edited by Decher, G. and Schlenoff, J.B. *Wiley-VCH Verlag GmbH & Co. KGaA*, 281-282.
- Schlenoff, J.B., Dubas, S.T., Farhat, T. (2000) Sprayed polyelectrolyte multilayers. *Langmuir*, 16, 9968-9969.
- Shamoun, R.F., Hariri, H.H., Ghostine, R.A., Schlenoff, J.B. (2012) Thermal transformations in extruded saloplastic polyelectrolyte complexes. *Macromolecules*, 45, 9759-9767.
- Shamoun, R.F., Reisch, A., Schlenoff, J.B. (2012) Extruded saloplastic polyelectrolyte complexes. *Advanced Functional Materials*, 22, 1923-1931.
- Shehzad, A., Rehman, G., Lee, Y. S. (2012) Curcumin in inflammatory diseases. *BioFactors*, 39(1), 69-77.
- Sidhu, G. S., Singh, A. K., Thaloor, D., Banaudha, K. K., Patnaik, G. K., Srimal, R. C., Maheshwari, R. K. (1998) Enhancement of wound healing by curcumin in animals. *Wound Repair Regen.*, 6(2), 167-177.
- Sim, M. Y. M., Shya, T. J., Ahmad, M. N., Shakaff, A. Y. M., Othman, A. R., Hitam, M. S. (2003) Monitoring of milk quality with disposable taste sensor. *Sensors*, 3, 340-349.
- Steitz, R., Jaeger, W., Klitzing, R.V. (2001) Influence of charge density and ionic strength on the polyelectrolyte multilayer formation of strong polyelectrolytes. *Langmuir*, 17, 4471-4474.
- Tang, J., Sisler, J., Grishkewich, N., Tam, K. C. (2017) Functionalization of cellulose nanocrystals for advanced applications. *J. Colloid Interface Sci.*, 494, 397-409.
- Tang, Z., Wang, Y., Podsiadlo, P., Kotov, N. A. (2006) Biomedical Applications of layer-by-layer assembly: from biomimetics to tissue engineering. *Advanced Materials*, 18, 3203-3224.
- Thunemann, A.F., Muller, M., Dautzenberg, H., Joanny, J.F., Lowen, H. (2004) Polyelectrolyte complexes. *Adv. Polym. Sci.*, 166, 113-171.

- Trache, D., Hussin, M. H., Haafiz, M. K. M., Thakur, V. K. (2017) Recent progress in cellulose nanocrystals: sources and production. Nanoscale, 9, 1763-1786.
- Villiers, M. M., Otto, D. P., Strydom, S. J., Lvov, Y. M. (2011) Introduction to nanocoatings produced by layer-by-layer (LbL) self-assembly. Advanced Drug Delivery Reviews, 63, 701-715.
- Volodkin, D., Klitzing, R.V. (2014) Competing mechanisms in PEM formation and swelling: polycation-polyanion pairing vs. polyelectrolyte-ion pairing. Current Opinion in Colloid & Interface Science, 19, 25-31.
- Wang, L., Wang, X., Xu, M., Chen, D., Sun, J. (2008) Layer-by-layer assembled microgel films with high loading capacity: reversible loading and release of dyes and nanoparticles. Langmuir, 24, 1902-1909.
- Wang, Q., Schlenoff, J.B. (2014) The polyelectrolyte complex/coacervate continuum. Macromolecules, 47, 3108-3116.
- Wang, Q., Schlenoff, J.B. (2014) Tough strained fibers of a polyelectrolyte complex: pretensioned polymers. RSC Adv., 4, 46675-46679.
- Wong, S. Y., Moskowitz, J. S., Veselinovic, J., Rosario, R. A., Timachova, K., Blaisse, M. R., Fuller, R. C., Klibanov, A. M., Hammond, P. T. (2010) Dual functional polyelectrolyte multilayer coatings for implants: Permanent microbicidal base with controlled release of therapeutic agents. Journal of American Chemical Society, 132, 17840-17848.
- Xu, X., Liu, F., Jiang, L., Zhu, J. Y., Haagenson, D., Wiesenborn, D. P. (2013) Cellulose nanocrystals vs. cellulose nanofibrils: A comparative study on their microstructures and effects as polymer reinforcing agents. ACS Appl. Mater. Interfaces.
- Yildirim, E., Zhang, Y., Lutkenhaus, J.L., Sammalkorpi, M. (2015) Thermal transitions in polyelectrolyte assemblies occur via a dehydration mechanism. ACS Macro Lett., 4, 1017-1021.
- Zhao, Q., An, Q.F., Ji, Y., Qian, J., Gao, C. (2011) Polyelectrolyte complex membranes for pervaporation, nanofiltration and fuel cell applications. Journal of Membrane Science, 379,19-45.

CURRICULUM VITAE

Name: Ms. Rateeya Saikaew

Date of Birth: March 19, 1990

Nationality: Thai

University Education:

2008–2012 Bachelor Degree of Science (Chemistry), Faculty of Science, Chiang Mai University, Chiang Mai, Thailand

2012–2014 Master Degree in Polymer Science, The Petroleum and Petrochemical College, Chulalongkorn University, Bangkok, Thailand

2014-Now Philosophy of Doctoral Degree in Polymer Science, The Petroleum and Petrochemical College, Chulalongkorn University, Bangkok, Thailand

Publications:

1. Saikaew, R., Bijaisoradat, O., Netcharoensirisuk, P., Dubas, S. T. (2016) Improved pH sensing of curcumin loaded polyelectrolyte multilayer thin films. Sensor Letters, 14(6), 572-576.
2. Saikaew, R., Marsal, P., Grenier, B., Dubas, S. T. (2018) Temperature controlled loading and release of curcumin in polyelectrolyte multilayers thin films. Materials Letters, 215, 38-41.

Presentation:

Poster Presentation

1. Saikaew, R., Dubas, S. T. (2018, December 1-3) Curcumin blended non-stoichiometric polyelectrolyte complex membranes for the optical ammonia vapor sensors. Poster presented at International Conference on Advanced and Applied Petroleum, Petrochemicals, and Polymer ICAPPP 2018, Bangkok, Thailand.